ANALYSIS OF FLAT-PLATE SOLAR COLLECTOR DURABILITY TEST DATA

by

Donald Sean Culkin

Thesis submitted to the Faculty of the

Virginia Polytechnic Institute and State University

in partial fulfillment of the requirements for the degree of

MASTER OF SCIENCE

in

Mechanical Engineering

APPROVED:

William C. Thomas, Chairman

H. L. Moses

R. J. Onega

July, 1982

Blacksburg, Virginia

ACKNOWLEDGMENTS

The author would like to express his appreciation to Dr. William C. Thomas for his guidance and patience in the preparation of this thesis. Thanks are also extended to Dr. Hal C. Moses and Dr. Ronald J. Onega for serving as committee members for this thesis. The National Bureau of Standards is gratefully acknowledged for the financial support of this project.

The author would also like to extend special thanks to his parents for their encouragement and support throughout his education.

TABLE OF CONTENTS

LIST OF FIGURES

Figure Page

LIST OF TABLES

NOMENCLATURE

A_a = transparent frontal area of a flat-plate collector (aperture area), sq m

BL = baseline value (subscript)

C_p = specific heat of the transfer fluid, J/kg-C

F_r = heat removal factor, dimensionless

G = total solar radiation incident on the aperture plane of the collector, W/sq m-C

k = thermal conductivity of the insulation, W/m-C

$\dot{m}$ = mass flow rate of the transfer fluid, kg/s

q''_u = rate of useful energy extraction per unit aperture area of collector, W/sq m

t_a = ambient air temperature, C

t_e = temperature of transfer fluid leaving the collector, C

t_i = temperature of transfer fluid entering the collector, C

t_p = average temperature of the absorber plate, C

T = time, s

U_L = overall heat loss coefficient, W/sq m-C

w_i = measurement uncertainty in variable i, same units as variable i

α = absorptance of the absorber plate for solar radiation, dimensionless

ε = emittance of the absorber plate for long-wave radiation, dimensionless

η = collector efficiency, percent

η_o = diffuse fraction of solar radiation

Θ = incident angle of solar radiation

τ = transmittance of the cover for solar radiation, dimensionless

I. INTRODUCTION

Solar collectors should have long service lives to be economically feasible. There is evidence that significant degradation of the thermal performance of flat-plate collectors can occur as a result of exposure to the environment. There is a need to develop test procedures for predicting the long-term (up to 20 years) performance of the materials used in collectors. The process of designing such tests has been hampered by a lack of data from systems in actual operation. The present investigation is concerned with a detailed analysis of collector performance data obtained over 240 days of exposure to the environment. The purpose of the study is to investigate the feasibility of measuring the durability of collectors which have been exposed to the environment for relatively short periods of time.

A program funded by the Department of Energy has been undertaken by the National Bureau of Standards (NBS) to develop meaningful collector reliability and durability tests for solar collectors [1]. To this end, both laboratory and outdoor aging tests were performed using collectors representative of commonly used materials and configurations. The present investigation is concerned with a detailed analysis of the performance data obtained in the NBS program. The approach will be to identify changes in collector material properties by measuring the collector efficiency at specified exposure times. Collector efficiency is defined as the ratio of the useful energy gain of the collector to the solar energy incident on the collector.

This investigation is concerned only with outdoor test results. Outdoor testing of solar collectors presents some unique problems. The performance of collectors is significantly affected by ambient conditions. The test environment cannot be controlled during an outdoor test. As a result, the test conditions cannot be repeated from one day to another during a series of tests. The problem of uncontrollable test conditions can be avoided through the use of indoor solar simulators. While the use of simulators would greatly simplify the test procedure, it has not been demonstrated that indoor test results accurately predict collector performance in actual field conditions. It is not possible to ensure that the degradation caused by a solar simulator would be equivalent to the degradation caused by the outdoor environment. Also, using solar simulators is much more expensive than running outdoor tests.

Flat-Plate Collector Design

The collectors considered in the investigation are of the liquid-heating, flat-plate type. Five different types of collectors were chosen to give a reasonable representation of commonly used materials and configurations. A typical collector configuration is illustrated in Figure 1. The main features pertaining to the thermal performance of the collectors are the absorber plate coating, absorber plate materials, number of covers, cover materials, type of insulation, and flow configuration (parallel or serptentine).

The purpose of the covers is to reduce convection and radiation losses while transmitting a high fraction of the incident solar

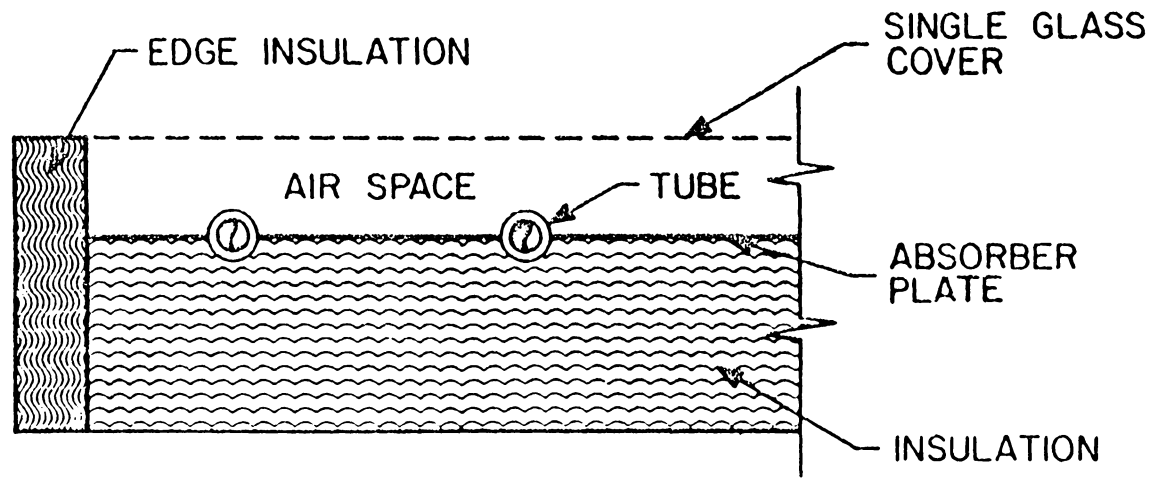

Figure 1 - Typical Flat-Plate Collector Cross Section

radiation. An important factor regarding the reliability of a cover is loss of solar energy transmittance. Another important property of cover materials is the longwave transmittance of infrared radiation emitted by the absorber surface. Dimensional stability and mechanical strength are also essential for cover materials. Excessive expansion or shrinkage can damage the seal between the cover and the collector frame. Such damage could allow dirt and moisture to enter the collector.

Glass is the most commonly used cover material. The properties of glass are well documented. It has a high transmittance for solar energy and low transmittance for longwave radiation. When compared to other materials, glass is highly resistant to deterioration resulting from the thermal and environmental conditions encountered by solar collectors. Glass is susceptible to shattering by thermal shock or impact. Thermal shock can be caused by cold rain striking a hot collector. Shattering as a result of impact can be caused by vandalism or hail.

A number of plastics and glass fiber reinforced plastics are also used as cover plate materials. Compared to glass, these materials are generally lower in cost, lighter in weight, easier to manufacture, and some have higher impact resistance. However, experience has shown that plastics and glass fiber reinforced plastics tend to degrade more rapidly than glass [2]. Discoloration of plastic and fiberglass covers has been observed in operational collectors [3]. This discoloration may indicate a loss of solar transmittance.

An important factor in cover material degradation is elevated temperature caused by the proximity of the hot absorber plate.

Degradation of cover materials is also believed to be caused by solar radiation. Ultraviolet radiation (UV) is believed to be important in the degradation of plastics [2]. The optical properties of cover materials can also be affected by outgassing products from internal sources such as insulation and sealants, dirt deposition on interior surfaces caused by improper sealing, condensation on interior surfaces, and air pollution.

Desirable properties of the absorber plate are high absorptance for solar energy, low emittance for longwave radiation, and high thermal conductivity. The plate material should also be corrosion resistant. The absorber plates used in the program were fabricated from steel, copper, or aluminum.

Absorber plate coatings are of the selective or nonselective type. A selective surface has a high absorptance for solar radiation and a low emittance for longwave radiation. This property takes advantage of the fact that there is little overlap in the spectral ranges between solar radiation and the longwave radiation emitted by the absorber surface. Selective surface technology is a relatively new field. Selective surfaces were first developed in the late fifties and early sixties for space vehicle applications as well as for solar collectors [4, 5, 6,]. The stability of selective surfaces has not yet been demonstrated in actual operating conditions. Color changes in selective surfaces in service for a year or more have been reported [3]. From the available data, it is not possible to determine whether or not the color changes had any effect on the radiation heat transfer properties of coatings.

II. BACKGROUND AND REVIEW OF LITERATURE

Most of the technical literature on solar collectors is concerned with design and performance with little attention to the durability of materials. This investigation is concerned with the available literature in four areas: previous investigations of material degradation in solar collectors, the mechanisms of degradation, the statistical theory behind interpreting accelerated test data, and past experience with outdoor testing of collector performance.

Experience with operational solar systems with documented material properties and environmental conditions is limited. One of the few operational systems which has been monitored for an extended period of time exhibited about a 30 per cent decrease in efficiency after 18 years of use [7]. At the NASA Langley facility, seven types of collectors were exposed under stagnation conditions. These collectors showed 10 percent or greater decreases in thermal efficiency after exposure periods of three to nine weeks [8]. The National Bureau of Standards conducted field inspections of working solar systems to obtain data on the performance of the material used in collectors [3]. Various problems were observed as a result of improper use of materials. The problems included fogging of cover plates caused by outgassing products from sealants and insulation, warping and cracking of certain types of cover plate materials, breakage caused by thermal expansion of glass cover plates, and failure of sealants. These studies give evidence

of material degradation in working solar systems but no previous studies were found where the actual properties of the materials or the environmental conditions were systematically monitored during the exposure period.

Several standard tests exist for predicting the service life of materials used in buildings. Many of these materials are similar to those used in solar collectors. Reference 3 provides an extensive list of standard test methods for a variety of materials used in solar collectors. The problem with these standards is that they were not designed specifically for solar applications. Accelerated test methods building materials are reviewed in references 9 and 10. It is reported in these references that it is difficult to relate accelerated test data quantitatively with in-service performance.

The success of an accelerated test lies in the choice of a model for the variation of material properties with environmental conditions. These models can be classified into two basic types: models derived from an understanding of the physics of the degradation, and models which are basically curve fits correlating material properties to environmental conditions. The most commonly used physical models are based on the concepts of statistical mechanics such as activation energy and reaction rate theories [11]. For example, models based on the Arrhenius and Eyring relations are plausible choices, especially when thermal stresses are involved [12]. Once a number of possible models have been identified, standard statistical methods can be used to select the best models based on the test data [13].

The theoretical basis for analyzing accelerated test data is summarized in reference 11. The methods described in reference 11 are concerned with testing of individual materials. Since collectors are assembled from several different materials, these methods would have to be extended to apply to whole collectors. Reference 12 proposes a methodology for designing accelerated tests of photovoltaic modules. The procedure is intended to be applicable to other devices exposed to the conditions experienced by solar collectors. The reliability of the proposed methodology has not been demonstrated with actual test data.

NBS conducted a round-robin test program to gain experience in performing outdoor tests of solar collectors [14]. Two types of flat-plate liquid-heating collectors were tested at twenty-one test facilities in various parts of the contiguous United States. The tests were run in accordance with ASHRAE Standard 93-77 [15]. This standard has been established as an industry consensus test procedure for determining the thermal performance of collectors. The results from each individual lab were found to be within the predicted measurement uncertainty. However, an unacceptably large spread in measured efficiency was observed when comparing results from one lab to another.

A detailed analysis of the data from approximately half of the round-robin test laboratories was performed to determine the reasons for the wide scatter in the results from different laboratories. Since the effect of varying environmental conditions was suspected as a possible cause of the scatter, an analytical procedure was used to estimate

the effects of the varying conditions. It was found that referring the measurements to a "standard" set of environmental conditions reduced but did not eliminate the scatter. Less than one-third of the scatter was attributed to environmental effects.

While different environmental conditions could have a significant effect on measured results, the overall conclusion from the round-robin program was that the main cause of the scatter was experimental error. Poor experimental procedures, systematic instrumentation calibration errors and mistakes in data reduction were cited as major possible causes of the inconsistencies. Another possible source of error was transient effects during the tests. Specific reasons for the scatter require more detailed investigation.

An analysis of the measurement uncertainty associated with measuring efficiency of collectors using ASHRAE 93-77 is presented in reference 16. This study showed that measurement uncertainties on the order of four per cent can be expected for typical flat-plate collectors even if the standard test procedure is carefully followed. Thus, much of the scatter in outdoor test data is justifiable in terms of instrumentation uncertainty.

In summary, the literature shows a lack of methodical investigations of material degradation in solar collectors. There is also a lack of theoretical investigations concerning the mechanisms of material property changes. The state-of-the-art method for measuring the durability of materials used in collectors appears to be measuring the collector efficiency in order to reveal changes in properties. This approach will be investigated further. The approach is limited in that it can

only reveal the effect of property changes. In general, it is difficult to identify specific property changes from efficiency data. For example, it is difficult to distinguish changes in the conductivity of the insulation from changes in the emittance of the plates.

Scope of the Investigation

An analysis of the collector performance data obtained through 240 days of exposure in the NBS durability/reliability program was carried out. The purpose of the analysis was to identify any changes in collector performance as a result of exposure to the environment. Since significant degradation was not indicated by the test data, the degradation as related to the dominant environmental parameters could not be emphasized. The effects of different test series, varying environmental conditions, and time of year were also considered and found to be insignificant.

The rationale behind the test program is described in the next chapter. The theoretical model for collector performance and the performance method are also outlined in Chapter III. Analytical work is outlined in Chapter IV. The analytical work includes calculating the sensitivity of collector performance to material property changes and the method for calculating the experimental uncertainty associated with the performance tests. The results of the test program are discussed in Chapter V.

III. TEST PROGRAM DESCRIPTION

The purpose of the NBS durability/reliability program was to devise tests which were realistic but which, at the same time, accelerate the degradation of collectors. The planning of the test series, the selection of test specimens and sites, and the procedures used to obtain the results are described in this chapter. The tests were not designed or conducted by the author. The discussion in this chapter is included to help in interpreting results.

Test Specimen Selection

In the NBS durability/reliability program, eight types of commercially available flat-plate collectors were tested. The test results for five of these collector types were considered in this investigation. These collectors give a reasonable representation of commonly used materials and configurations. The eight types of collectors used in the NBS program were designated by the letters A through H [1]. The five collectors considered here are A, B, D, E, and H. The main features of the collectors, including the pertinent optical properties, are summarized in Table 1. Appendix A has a more detailed description.

The distinguishing characteristics of collector A are a selective surface absorber coating and a single glass cover. The absorber plate is steel. The back insulation is fibrous mineral wool and the edge insulation is fiberglass.

Table 1. Test Specimen Material Properties

	Inner Cover		Outer Cover		Absorber			
Collector	Material	Solar Transmittance	Material	Solar Transmittance	Plate Material	Coating	Solar Absorptance (normal beam)	Infrared Emittance
A	Water white glass	0.90	--	--	Steel	Black Nickel	0.87	0.13
B	Low iron glass	0.88	Low iron glass	0.88	Copper	Black Velvet Paint	0.97	0.92
D	Low iron glass	0.88	Low iron glass	0.88	Steel	Black Chrome	0.96	0.06
E	Fiber reinforced plastic	0.85	--	--	Copper	Black Lacquer	0.95	0.86
H	Polytetrafluoroethylene	0.87	Polyester	0.87	Aluminum	Black Polyester Paint	0.96	0.89

Collector B has two covers of a special low-iron glass and a nonselective surface absorber. The absorber plate is copper and the insulation is fiber glass.

Collector D has two low-iron glass covers and a selective surface absorber. The absorber plate is steel and the insulation is fiber glass.

Collector E has a single fiber glass cover and a nonselective surface. This collector is unusual in that it has a relatively elongated configuration compared to the other collectors. The absorber plate is copper and the insulation is made of isocyanurate.

Collector H has two covers. The inner cover is constructed of a thin sheet of polytetrafluoroethylene. The outer cover is made of polyester which has been treated for increased resistance to UV radiation. The absorber is aluminum with a nonselective coating. Collector H is the only collector with a serpentine flow configuration. The other collectors have parallel flow configurations.

Test Series Description

Three test series were considered in this investigation. Each series is characterized by a different set of exposure conditions. The test series were intended to have a duration of 240 days with at least 17,100 kJ/sq m-day of incident solar radiation. Some tests were shortened to less than 240 days because of time constraints.

The NBS test program originally had four test series. Series 4 involved the use of reflectors to augment the radiation incident on

the collectors. This series was discontinued early in the test program because uniform irradience of the collector surface could not be obtained with the reflectors.

Series 1 collectors were exposed to the environment under dry conditions. The collectors were purged with dry air prior to exposure. Performance tests were conducted after 0, 3, 15, 30, 60, 120, and 240 exposure days.

Series 1 tests were intended to show the effects of dry stagnation on the durability of materials. The significance of the 3-day pre-exposure period per ASHRAE 93-77 [15] was investigated by comparing the collector performance after 0 and 3 days of exposure.

Series 2 collectors were filled with water and capped with a pressure-relief cap prior to each exposure period. The collectors were then exposed to the environment and allowed to boil dry. Performance tests were conducted at the same intervals as Series 1 except the 0 day test was deleted. Thermal shock tests per NBSIR 78-1305A [17] were performed after 30 and 120 days exposure. The thermal shock tests involve both spraying the hot collectors with cold water and filling the hot collectors with cold water.

This series was intended to show the effects of no-flow stagnation on the degradation of materials. The thermal shock tests were intended to simulate cold rain striking a hot collector or filling a hot collector with cold fluid.

Series 3 collectors were maintained at 25 per cent standard flow rate during exposure. Standard flow rate is taken to be 0.02 kg/sq m-s unless otherwise specified by the manufacturer of the collector.

Performance tests were conducted at the same intervals as in Series 1 except the 15 day test was deleted.

This series was intended to show the effects of extended exposure under low-flow conditions on collector degradation.

Test Site Description

The NBS program included four test sites. The present investigation will consider the performance data from three of those sites. The test sites were chosen to represent environmental conditions found in various parts of the contiguous U.S. Some of the important environmental conditions considered included level of solar radiation, level of UV radiation, ambient temperatures, humidity, and air pollution.

Test site 1 is characterized by hot, dry conditions accompanied by high solar radiation with high ultraviolet levels. These conditions are found in the southwestern U.S. (Arizona, Nevada, New Mexico). The laboratory chosen for site 1 is located in Phoenix, Arizona.

Test site 2 is characterized by hot, humid conditions accompanied by high solar radiation with low to moderate ultraviolet levels. These conditions are found in Florida and on the Gulf coast of Alabama, Mississippi, Louisiana and Texas. The laboratory chosen for site 2 is located in Cape Canaveral, Florida.

Test site 3 is characterized by moderate temperatures and dry conditions accompanied by high solar radiation with moderate ultraviolet levels. These conditions are found in California. The laboratory for test site 3 is located in Palo Alto, California.

Test Specimen Identification

A three letter identification code will be used for the purposes of this investigation. The first letter indicates the collector; the second character indicates the test site; and the third character indicates the test series. For example, A - 1 - 2 denotes Collector A, Test Site 1, Test Series 2.

All three Test Series were performed at Test Sites 1 and 2. Only Series 1 and 2 were performed at Site 3.

Test Procedures

The collectors were exposed outdoors at the various test labs on exposure stands. The collectors were removed from the exposure stands at the specified time interval and tested on an efficiency test stand. The collectors were then put back on the exposure stand for the next exposure period. In order for a day to be considered a valid exposure day, the total solar radiation for that day must be equal to or greater than 17,100 kJ/sq m-day. When the end of an exposure interval was reached, the collectors were stored inside until performance tests could be conducted.

Daily records of the environmental conditions during the exposure periods were kept by the test laboratories. These records included high and low ambient temperature, high and low relative humidity, total and diffuse solar radiation per day, peak solar radiation, average windspeed and amount of precipitation. Levels of various air pollutants were recorded at test site 3. The maximum daily collector absorber plate temperatures were recorded for each collector.

Collector Performance

The performance of a flat plate collector operating under steady conditions can be described by the following relation [18]:

$$q''_u = G(\tau\alpha) - U_L [t_p - t_a] \qquad [1]$$

The transmittance-absorptance product, $(\tau\alpha)$, is the fraction of the incident solar radiation that is absorbed by the absorber plate. The transmittance-absorptance product accounts for multiple reflections and transmission of the incident solar radiation through the cover-absorber system. Some of the solar radiation is absorbed in the cover, raising the temperature of the cover and reducing the top losses. The heat loss coefficient, U_L, accounts for radiation and convection losses.

Since the mean plate temperature is not known directly, it is convenient to define a collector heat removal factor, F_r, which is defined as [18]:

$$F_r = \frac{\text{actual useful energy gain}}{\text{energy gain if entire collector surface were at inlet fluid temperature}}$$

$$= \frac{\dot{m}C_p[t_e - t_i]}{A_a \{G(\tau\alpha) - U_L[t_i - t_a]\}} \qquad [2]$$

Using the heat removal factor, equation [1] can now be written as:

$$q''_u = F_r\{G(\tau\alpha) - U_L[t_i - t_a]\} \qquad [3]$$

The efficiency of a solar collector is defined as the ratio of the actual energy gain to the solar energy incident on the collector. The collector efficiency is given by

$$\eta = \frac{\dot{m}C_p[t_e - t_i]}{A_a G} \qquad [4]$$

Using equation [4], the efficiency is

$$\eta = F_r(\tau\alpha) - F_r U_L \frac{[t_i - t_a]}{G} \qquad [5]$$

The efficiency is a linear function of $[t_1 - t_a]/G$ if F_r, U_L and $(\tau\alpha)$ are constants. The transmittance-absorptance product, $(\tau\alpha)$, is primarily a function of collector properties. It is a weak function of the incident angle and diffuse fraction of the solar radiation under average operating conditions ($\theta < 30°$ and $\eta_o < 30\%$). The $(\tau\alpha)$ product can be considered constant, i.e., independent of temperature. While the heat loss coefficient, U_L, increases significantly with absorber plate temperature, previous studies [14, 19] have shown that the error resulting from assuming that U_L is independent of temperature is overshadowed by experimental error and variations caused by varying environmental conditions. The heat removal factor, F_r, is a weak function of temperature through the dependence of F_r on U_L. In a later section, it will be shown that a linear relation correlates the measured efficiency to well within experimental uncertainty.

The standard method of depicting the efficiency of a collector is to plot efficiency versus $(t_i - t_a)/G$ as shown in Fig. 2. This

results in a straight line with negative slope equal to F_rU_L and ordinate intercept equal to $F_r(\tau\alpha)$. $F_r(\tau\alpha)$ and F_rU_L are referred to as the performance parameters of a collector.

Efficiency Test Procedure

In order to obtain the efficiency curve for a collector, it is necessary to measure the solar radiation incident on the collector, the fluid mass flow and temperature rise, and the difference between the ambient and inlet temperatures. Reference 15 requires that the test be run under quasi-steady conditions. In order to obtain sufficiently steady conditions, the transfer fluid should be circulated through the collector at the appropriate temperature until the temperature remains constant for fifteen minutes prior to taking readings. The testing standard also requires that the test be run under the weather conditions listed in Table 2.

Reference 15 recommends that four values of t_i be used to determine the collector efficiency curve. In some cases this number was reduced to three for this study. Four data points were taken at each value of t_i, two during the period prior to solar noon and two after solar noon. The specific times were chosen so that the data points would represent times symmetric to solar noon. This requirement is made to reduce any transient effects caused by the movement of the sun. This requirement is not mandatory when using an altazimuth

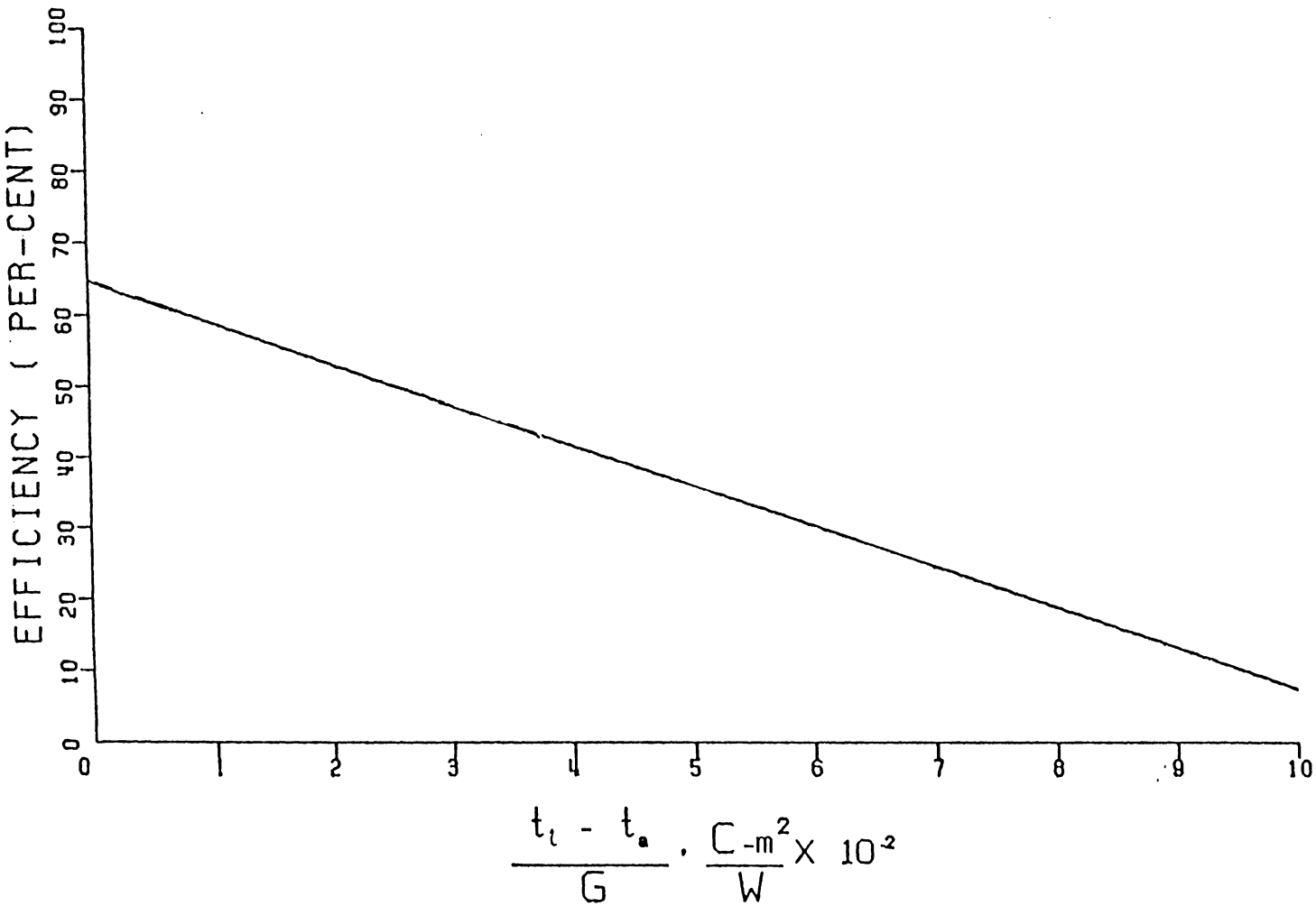

Figure 2 - Standard Collector Efficiency Curve

Table 2. Allowable Weather Conditions

solar radiation	> 630 W/m^2
wind speed	< 4.5 m/s
ambient temperature range	< 30 C

mount which maintains a normal (or fixed non normal) incident angle. Test Sites 1 and 2 used altazimuth mounts.

The efficiency curve for each test was established by data points which represent efficiency values determined by integrating the data over a period equal to the time constant of the collector or five minutes, whichever is larger. With an altazimuth mount, this time is reduced to one-half of the time constant of the collector or five minutes, whichever is larger. The efficiency is calculated by the following equation:

$$\eta = \frac{\dot{m}C_p \int_{T_1}^{T_2} [t_e - t_i]\, dT}{A_a \int_{T_1}^{T_2} G\, dT} \qquad [6]$$

During ASHRAE 93-77 tests, the mass flow rate, $\dot{m}$, is kept constant. Since the test fluid is water, the specific heat varies less than one-half percent over the range of temperature encountered during a test. The mass flow rate and the specific heat are both taken outside the integral in the above expression. Note that the efficiency is based on the aperture area and not the gross area as recommended by ASHRAE 93-77. This convention is consistent with that used in reference 18. The aperture area is used to emphasize the effect of the cover and absorber properties.

IV. ANALYSIS

An analytical model for predicting the steady state collector performance under specified weather conditions has been developed. The model is based on state-of-the-art one-dimensional theory as outlined in Chapter II. It was used in this project to calculate changes in collector performance caused by changes in collector material properties. An algorithm has been developed which uses the collector model to refer the test data to a set of "standard" weather conditions. The method is explained in detail in reference 19. This program was used to investigate the effect of varying environmental conditions on the test data.

Sensitivity of Collector Performance to Material Properties

The performance parameters $F_r(\tau\alpha)$ and F_rU_L are the primary measures of collector performance. Figures 3 through 10 show the theoretical sensitivity of the performance parameters to changes in the important collector material properties. The values were calculated at a "standard" set of weather conditions as shown in Table 3. These weather conditions are approximately the average of those observed for ASHRAE 93-77 tests in the contiguous U.S. over the past several years [19].

Figures 3 through 6 show the range of performance parameters for collector D. Figures 7 through 10 show the performance parameters for collector E. Each curve was calculated at a specific value of $(t_i - t_a)$. Table 1 shows that collector D has two covers and a

Table 3. Recommended Standard Test Conditions

Condition	Value
ambient temperature	20 C
solar irradiance	1000 w/sq m
incident beam angle	15 deg
diffuse fraction of irradiance	0.15
wind speed	3 m/s
test fluid	water
flow rate	0.02 kg/s-sq m
collector slope	45 deg

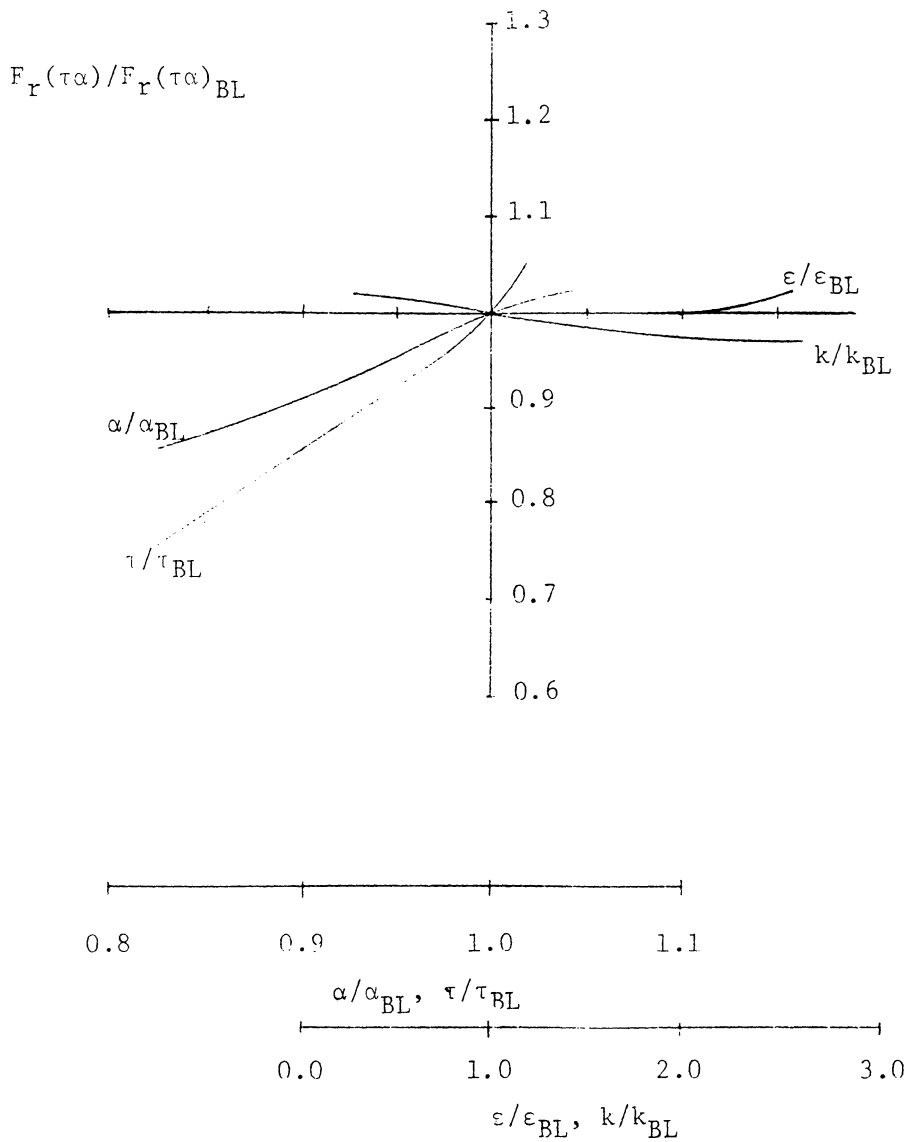

Figure 3 - Theoretical Sensitivity of $F_r(\tau\alpha)$ to Material Property Changes for Collector D ($t_i - t_a$ = 0 C)

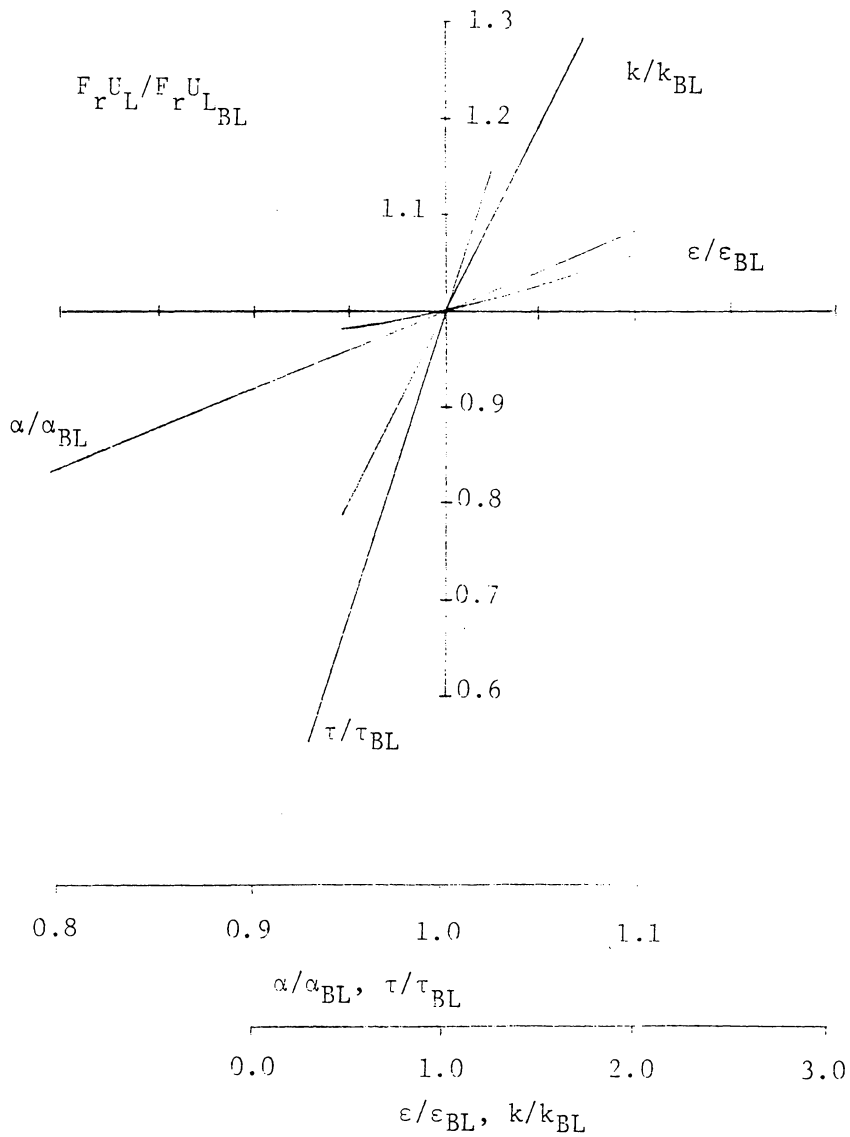

Figure 4 - Theoretical Sensitivity of F_rU_L to Material Property Changes for Collector D ($t_i - t_a = 0$ C)

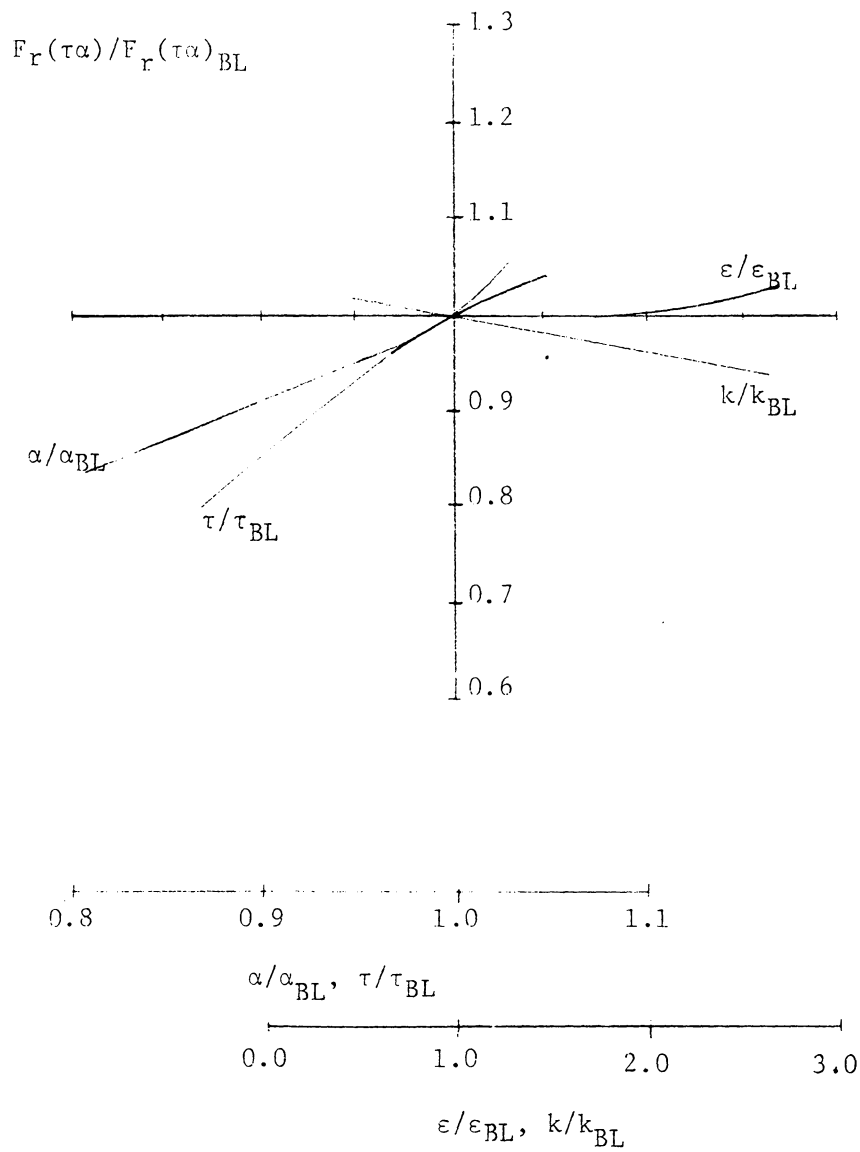

Figure 5 - Theoretical Sensitivity of $F_r(\tau\alpha)$ to Material Property Changes for Collector D ($t_i - t_a$ = 80 C)

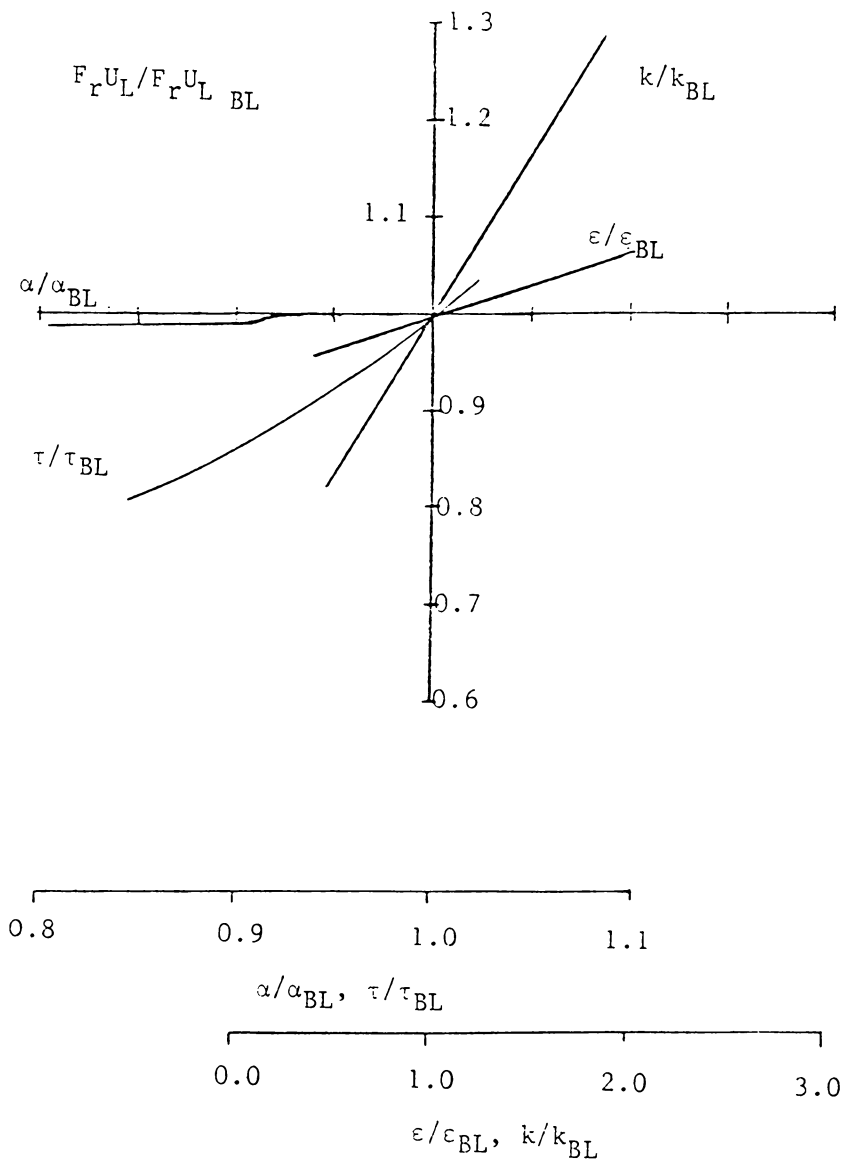

Figure 6 - Theoretical Sensitivity of F_rU_L to Material Property Changes for Collector D ($t_i - t_a$ = 80 C)

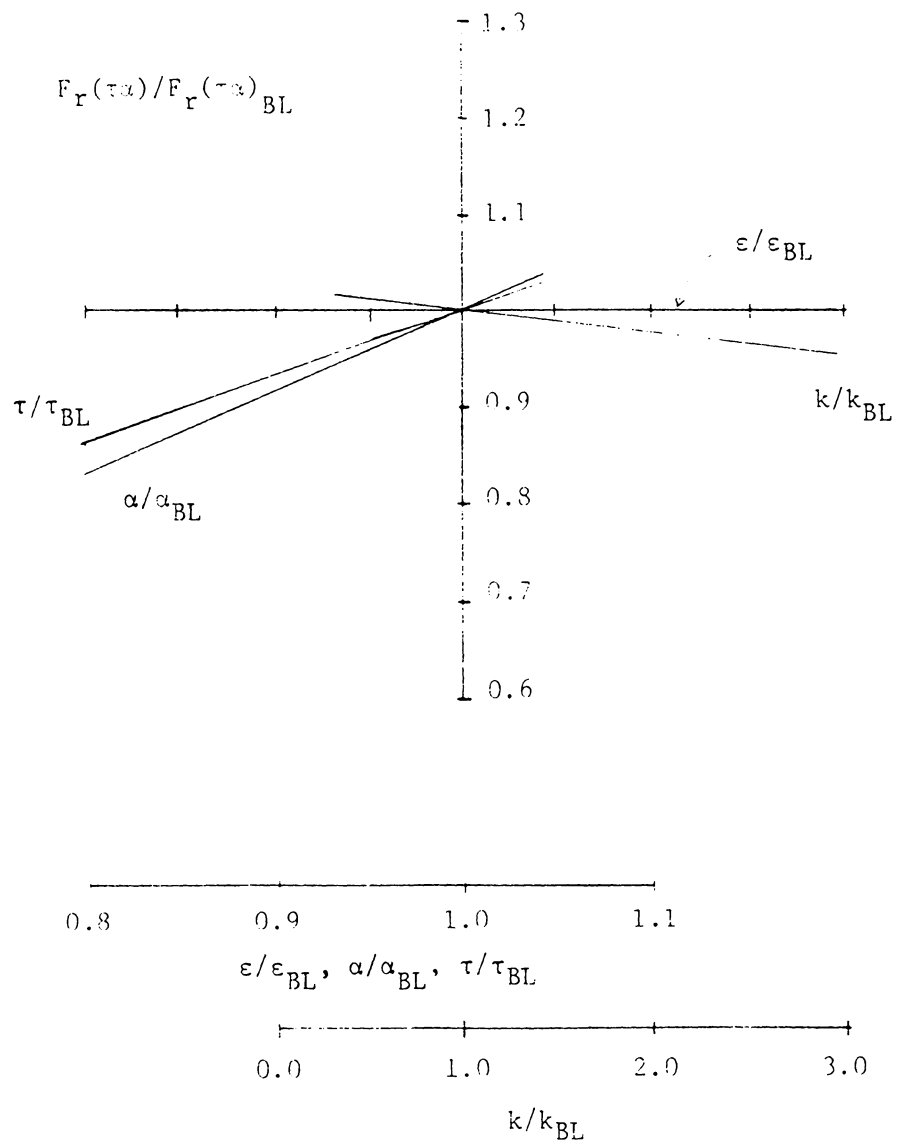

Figure 7 - Theoretical Sensitivity of $F_r(\tau\alpha)$ to Material Property Changes for Collector E ($t_i - t_a = 0$ C)

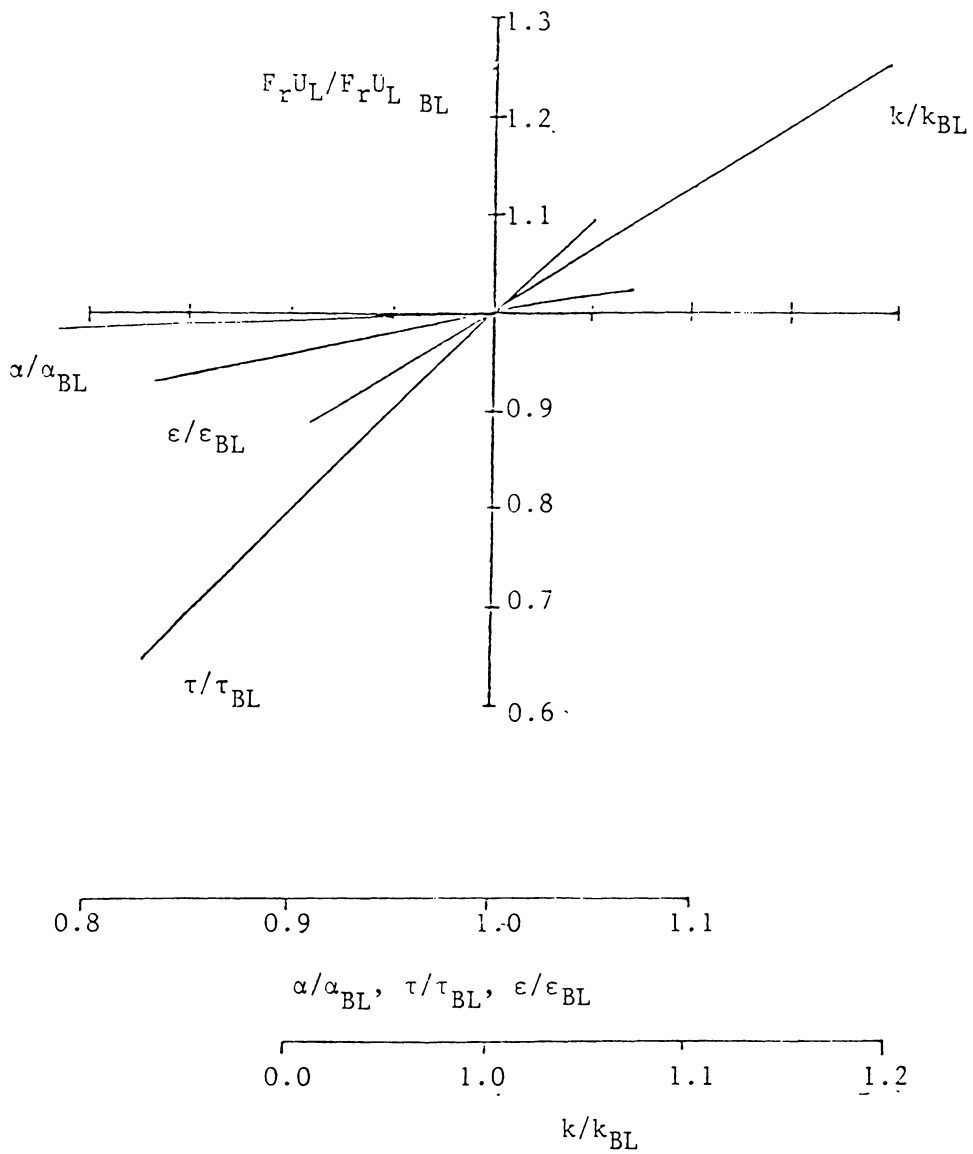

Figure 8 - Theoretical Sensitivity of F_rU_L to Material Property Changes for Collector E ($t_i - t_a = 0$ C)

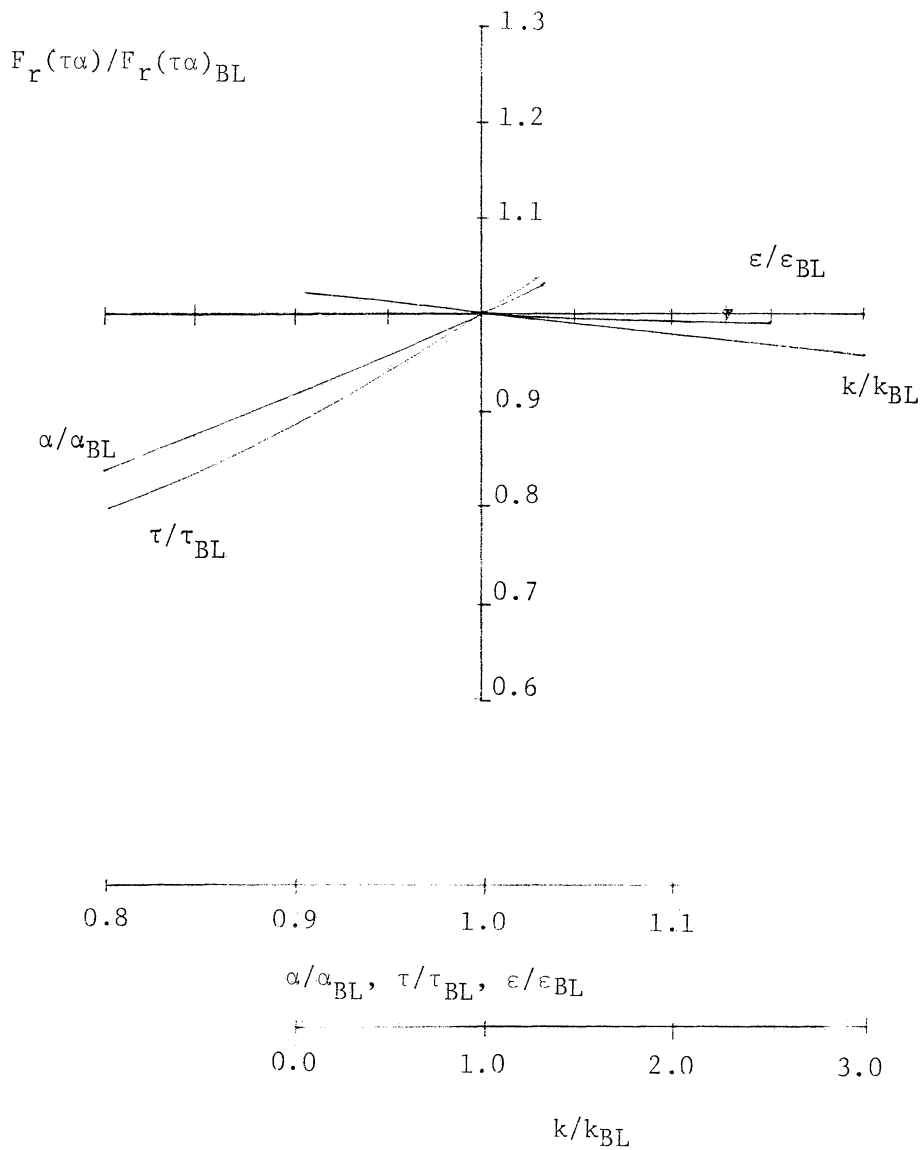

Figure 9 - Theoretical Sensitivity of $F_r(\tau\alpha)$ to Material Property Changes for Collector E ($t_i - t_a$ = 80 C)

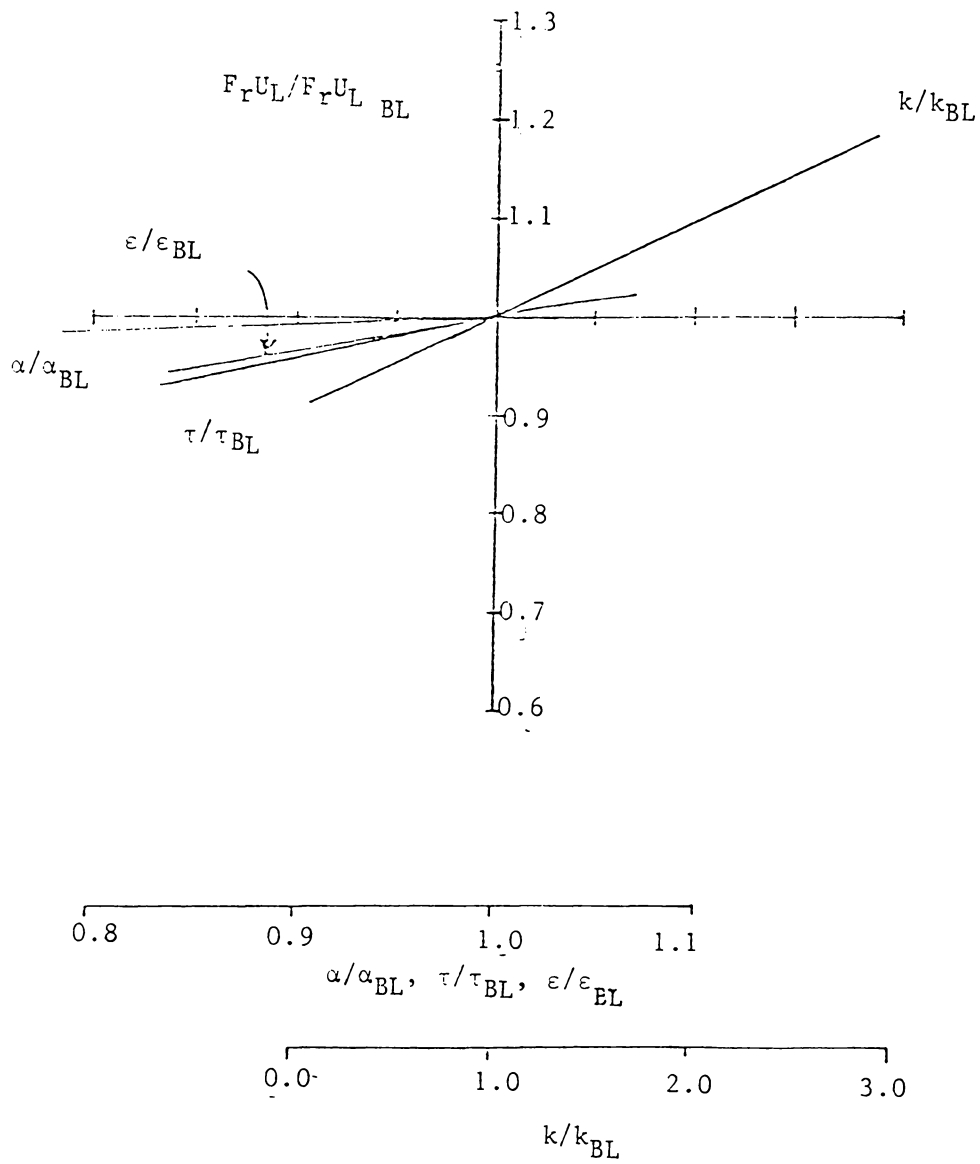

Figure 10 - Theoretical Sensitivity of F_rU_L to Material Property Changes for Collector E ($t_i - t_a$ = 80 C)

selective absorber coating. Collector E has a single cover and a non-selective absorber coating. Collector D should be less sensitive to $(t_i - t_a)$ than collector E. Notice that the range of values of plate emittance for long-wave radiation is different for collector D than for collector E. The emmittance for collector E is about 0.90. A reasonable range for $\varepsilon/\varepsilon_{BL}$ would be from 0.80 to 1.1. Collector D has a selective surface with an emittance of about 0.10. A reasonable range of values for $\varepsilon/\varepsilon_{BL}$ is from 0 to about 2.5.

Figures 3 through 10 show how performance tests can be used to identify changes in collector material properties. For example, a decrease in the solar transmittance of the cover results in a decrease in both $F_r(\tau\alpha)$ and F_rU_L. A change in plate absorptance would have an effect on $F_r(\tau\alpha)$ but little effect on F_rU_L. Insulation conductivity has a significant effect only on F_rU_L. Both performance parameters are relatively insensitive to changes in plate emittance.

It is interesting to note the sensitivity of F_rU_L to the solar transmittance of the cover. The figures show that a decrease in the transmittance of the cover has the favorable effect of decreasing F_rU_L. This effect occurs because when the transmittance decreases, the absorptance of the cover increases (assuming the reflectance remains constant). The increased absorptance results in higher cover temperatures and consequently less heat is lost from the absorber to cover. F_rU_L is especially sensitive to changes in transmittance at low temperature differences. This effect occurs because, at low temperature differences, the overall losses are low and any change

in the top losses will have a greater proportional effect on the overall losses.

Referring the Test Data to Standard Weather Conditions

Reference 19 describes an analytical method for referring or "correcting" performance data to the set of "standard" weather conditions. The method was used to determine the effect of different weather conditions on the performance parameters. Measured efficiencies are corrected to standard conditions by

$$\eta_{corrected}(X, \text{Std. Cond.}) = \eta_{meas}(X, \text{Test Cond.}) + [\eta_{calculated}(X, \text{Std. Cond.}) - \eta_{calculated}(X, \text{Test Cond.})] \quad [7]$$

where $X = (t_i - t_a)/G$ is held constant. The calculated efficiencies are found using the same analytical collector performance model as was used to show the sensitivity of performance to material properties. The model is used only to calculate the difference in measured efficiency caused by "nonstandard" weather conditions. Errors in the model have a smaller effect on corrected efficiency values than on the predicted value of the efficiency.

Uncertainty Analysis

In order to establish the efficiency curve for a collector, it is necessary to measure the mass flow rate, temperature rise in the transfer fluid, incident solar radiation, ambient temperature and

fluid inlet temperature. Each of these measurements has an experimental uncertainty which is specified by reference 15. An analysis is presented for calculating the expected experimental error band of the efficiency curve as a result of instrument uncertainty. The analysis accounts for the uncertainty in both the ordinate and the abscissa values.

The experimental uncertainty, w, in a measured function, f, of n independent variables, x_1, x_2 . . . x_n, is given by [20]:

$$w = \{ [\frac{\partial f}{\partial x_1} w_1]^2 + [\frac{\partial f}{\partial x_2} w_2]^2 + \ldots + [\frac{\partial f}{\partial x_n} w_n]^2 \}^{1/2} \qquad [8]$$

where w_i is the uncertainty in x_i.

The efficiency is given by:

$$\eta = \frac{\dot{m} C_p [t_e - t_i]}{A_a G} \qquad [9]$$

Assuming negligible error in the collector area and fluid specific heat, the uncertainty in the efficiency is given by:

$$w_\eta = \{ [\frac{C_p \Delta t}{A_a G} w_{\dot{m}}]^2 + [\frac{\dot{m} C_p}{A_a G} w_{\Delta t}]^2 + [\frac{-\dot{m} C_p \Delta t}{A_a G^2} w_G]^2 \}^{1/2} \qquad [10]$$

The abscissa value is given by:

$$X = \frac{t_i - t_a}{G} \qquad [11]$$

The uncertainty in the abscissa is given by

$$w_x = \{[\frac{1}{G} w_{t_i}]^2 + [\frac{-1}{G} w_{t_a}]^2 + [\frac{t_a - t_i}{G^2} w_G]^2\}^{1/2} \quad [12]$$

The measurement uncertainties are made up of an uncertainty in the measuring device and an additional uncertainty in the readout device equal to one percent of the measured value. The allowable uncertainties for each measured value are listed in Table 4.

According to equation [8] the uncertainty in the mass flow rate is given by

$$w_m = \{[0.01\ \dot{m}]^2 + [0.01\ \dot{m}]^2\}^{1/2} \quad [13]$$

Similar relationships are written for each measured quantity. By substituting these uncertainties into equations [10] and [12], the uncertainty in the abscissa and ordinate can be found for each data point. The calculated uncertainties can be used to establish an uncertainty rectangle associated with each data point as shown in Fig. 11. The rectangles define an uncertainty region or band for the curve. The uncertainty band is drawn through the corners of the rectangles as shown in Fig. 11.

Figure 12 shows the efficiency curve established by actual test data. As the figure shows, the linear curve fit correlates the collector efficiency to within experimental uncertainty.

The performance parameters, $F_r(\tau\alpha)$ and F_rU_L are found by fitting the test data to a linear least squares fit. Two methods were considered

Table 4. Allowable Measurement Uncertainties

Quantity	Uncertainty
mass flow rate	± 1%
temperature (t_a, t_i)	± 0.5 C
solar irradiance*	± 3%
temperature rise ($t_e - t_i$)	± 0.1 C

* Tolerance for solar irradiance is from manufacturer's data

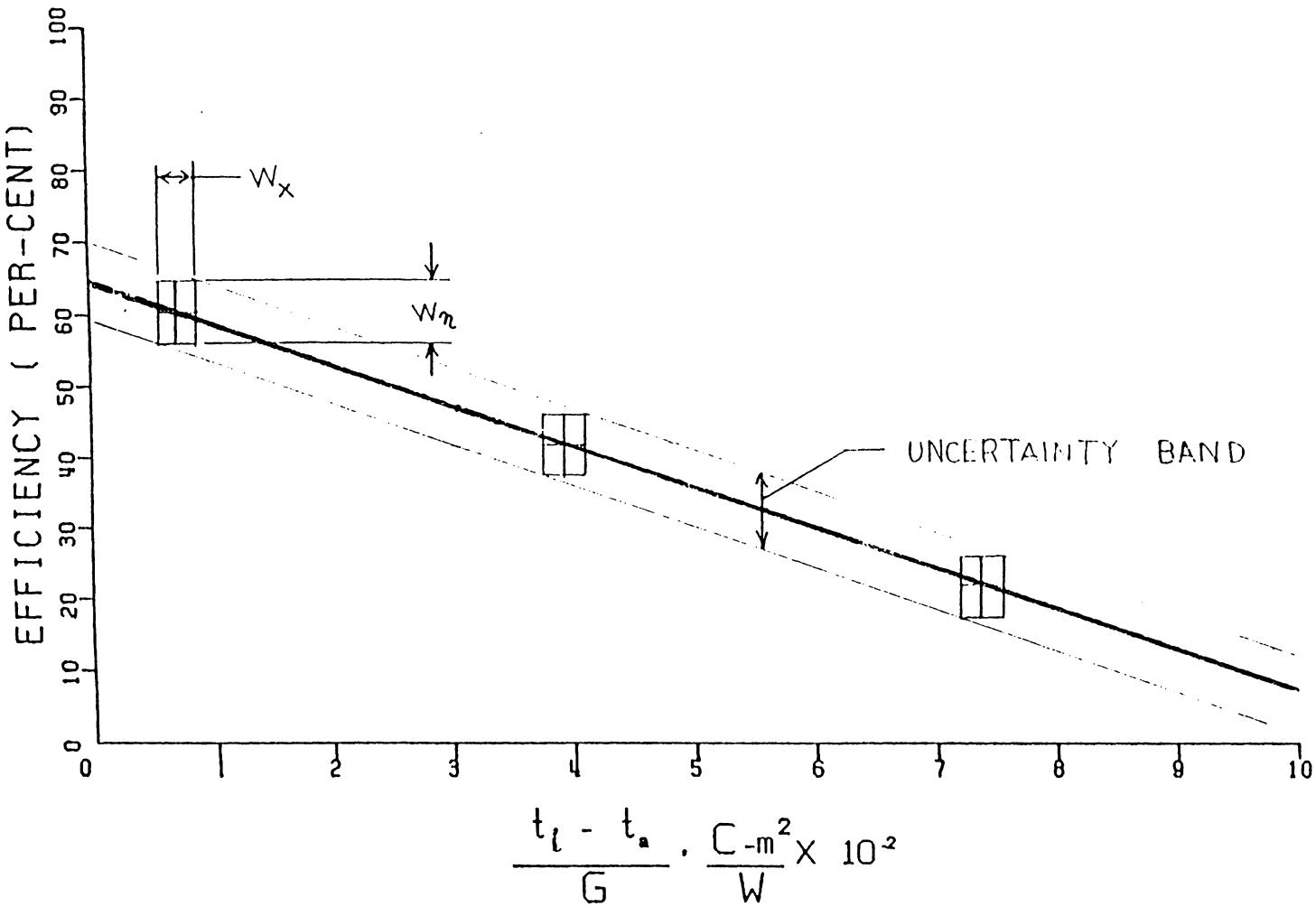

Figure 11 - Uncertainty Band of Measured Efficiency

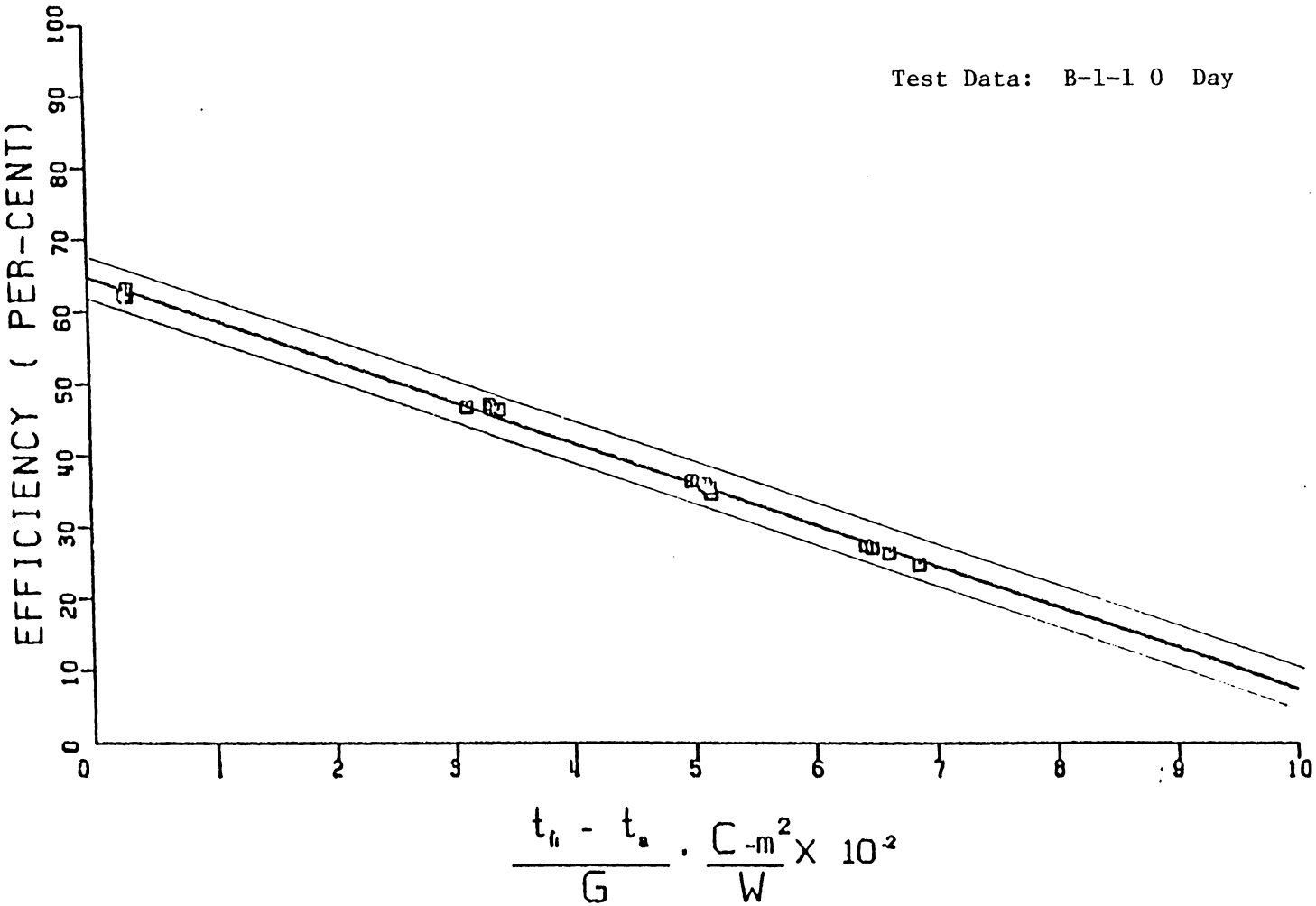

Figure 12 - Measured Efficiency Curve with Uncertainty Band

to estimate the corresponding uncertainty in the measured values of these performance parameters.

A linear least squares curve fit of the form

$$y = a + bx \qquad [14]$$

is used.

The intercept and slope of the line established by m data points are given by [21]:

$$a = \frac{\sum_{i=1}^{m} x_i^2 \sum_{i=1}^{m} y_i - \sum_{i=1}^{m} x_i \sum_{i=1}^{m} x_i y_i}{m \sum_{i=1}^{m} x_i^2 - \left(\sum_{i=1}^{m} x_i\right)^2} \qquad [15]$$

$$b = \frac{m \sum_{i=1}^{m} x_i y_i - \sum x_i \sum y_i}{m \sum_{i=1}^{m} x_i^2 - \left(\sum_{i=1}^{m} x_i\right)^2} \qquad [16]$$

One method for estimating the uncertainties in the slope and intercept of a linear least squares curve fit is presented in reference 21. With this method, the estimated standard deviation of the slope and intercept are expressed as a function of the standard deviation of the measured values of the ordinate of the linear curve fit.

The standard deviation of the intercept and slope of equation [14] are given by

$$\sigma_a = \sigma \sqrt{\frac{\sum_{i=1}^{m} x_i^2}{m \sum_{i=1}^{m} x_i^2 - \left(\sum_{i=1}^{m} x_i\right)^2}} \qquad [17]$$

$$\sigma_b = \sigma \sqrt{\frac{m}{m \sum_{i=1}^{m} x_i^2 = \left(\sum_{i=1}^{m} x_i\right)^2}} \qquad [18]$$

Where σ is the standard deviation in y

$$\sigma = \sqrt{\frac{\sum_{i=1}^{m} [y_i - (a + bx_i)]^2}{m - 1}} \qquad [19]$$

The second method for estimating the uncertainty in the slope and intercept is based on applying equation [8] to the least squares expression for slope and intercept. According to equation [8], the uncertainty in the intercept is given by:

$$w_a = \left[\sum_{i=1}^{m} \frac{\partial a}{\partial x_i} w_{x_i}^{\ 2} + \sum_{i=1}^{m} \frac{\partial a}{\partial y_i} w_{y_i}^{\ 2} \right]^{1/2} \qquad [20]$$

Similarly, the uncertainty in the slope is given by:

$$w_b = \left[\sum_{i=1}^{m} \frac{\partial b}{\partial x_i} w_{x_i}^{\ 2} + \sum_{i=1}^{m} \frac{\partial b}{\partial y_i} w_{y_i}^{\ 2} \right]^{1/2} \qquad [21]$$

The uncertainty in the parameters was calculated using both methods for a variety of environmental conditions. The uncertainty is assumed

to be equal to two standard deviations. It was found that using the first method gave uncertainties which were less than or equal to the uncertainties using the second method. The second method is considered to give a conservative estimate of the uncertainties in the performance parameters since it accounts for uncertainties in the abscissa and ordinate.

It was found that the uncertainty in performance was nearly the same for all collectors. The uncertainty in $F_r(\tau\alpha)$ is approximately 0.01 for all collectors. The uncertainty in F_rU_L is 0.20 W/sq m-C for all collectors except collector D. The uncertainty in F_rU_L for collector D is 0.25 W/sq m-C.

V. RESULTS AND DISCUSSION

The main objective of the durability program was to investigate the thermal degradation of collectors as a function of time for various exposure conditions. In order to show changes that might have occurred in collector performance, graphs were prepared showing the collector performance parameters, $F_r(\tau\alpha)$ and F_rU_L, as a function of exposure time. These plots are included in Appendix B with the mean value and the probable experimental uncertainty shown on the graphs. In the interest of clarity, only typical, or representative results will be presented in this chapter.

In order to show the effects of climatological conditions on collector degradation, performance parameters as a function of exposure time were plotted for series 1-3 for individual test sites for each collector. These plots are shown in Appendix B on Figs. B-1 through B-15. Several overall trends are observed. The scattered in the measured values of the performance parameters is random about mean values. The scatter in $F_r(\tau\alpha)$ values is about what is to be expected from allowable experimental uncertainty. The scatter in F_rU_L values is somewhat larger than justified by experimental uncertainty. A more detailed analysis of the scatter will be presented in a later section.

The results from test site 1 indicate a decrease in $F_r(\tau\alpha)$ at 240 days exposure. This decrease occurs because the pyranometers used at test site 1 were re-calibrated between the 120 day and the 240 day tests. The re-calibration corresponds to an apparent increase in the

measured solar radiation values and, thus, a decrease in $F_r(\tau\alpha)$. The increase in measured radiation does not affect F_rU_L.

One pattern that is noticeable is that the results for series 1 and 2 follow the same local trends. In other words, while there is no overall trend, the parameter values follow the same up and down changes. This pattern is illustrated by Figs. 13 and 14 which show results for collector E from test site 3, where the scatter is relatively large. These figures indicate no consistent trend, but as a group, the performance parameters have the same up and down changes. Figure 15 shows F_rU_L values for collector H from test site 1. This figure shows a clear downward trend in F_rU_L values for series 1 and 2 and a clear upward trend for series 3 from 15 days to 120 days. It is important to note that, at test site 1, the series 1 and 2 tests were run on the same dates while the series 3 tests were run on a different schedule. Series 3 results might differ from series 1 and 2 results because of varying environmental conditions or improper test stand calibration from one test to another. In order to determime the significance of the environmental effect, the series 1 and 3 results shown in Fig. 15 were adjusted to standard weather conditions and plotted in Fig. 16. As this figure shows, environmental effects were not the reason for the difference between series 3 results and series 1 results. Sufficient data were not available to determine the significance of test stand calibration.

In order to show the effects of test series on collector degradation, performance parameters as a function of exposure time were

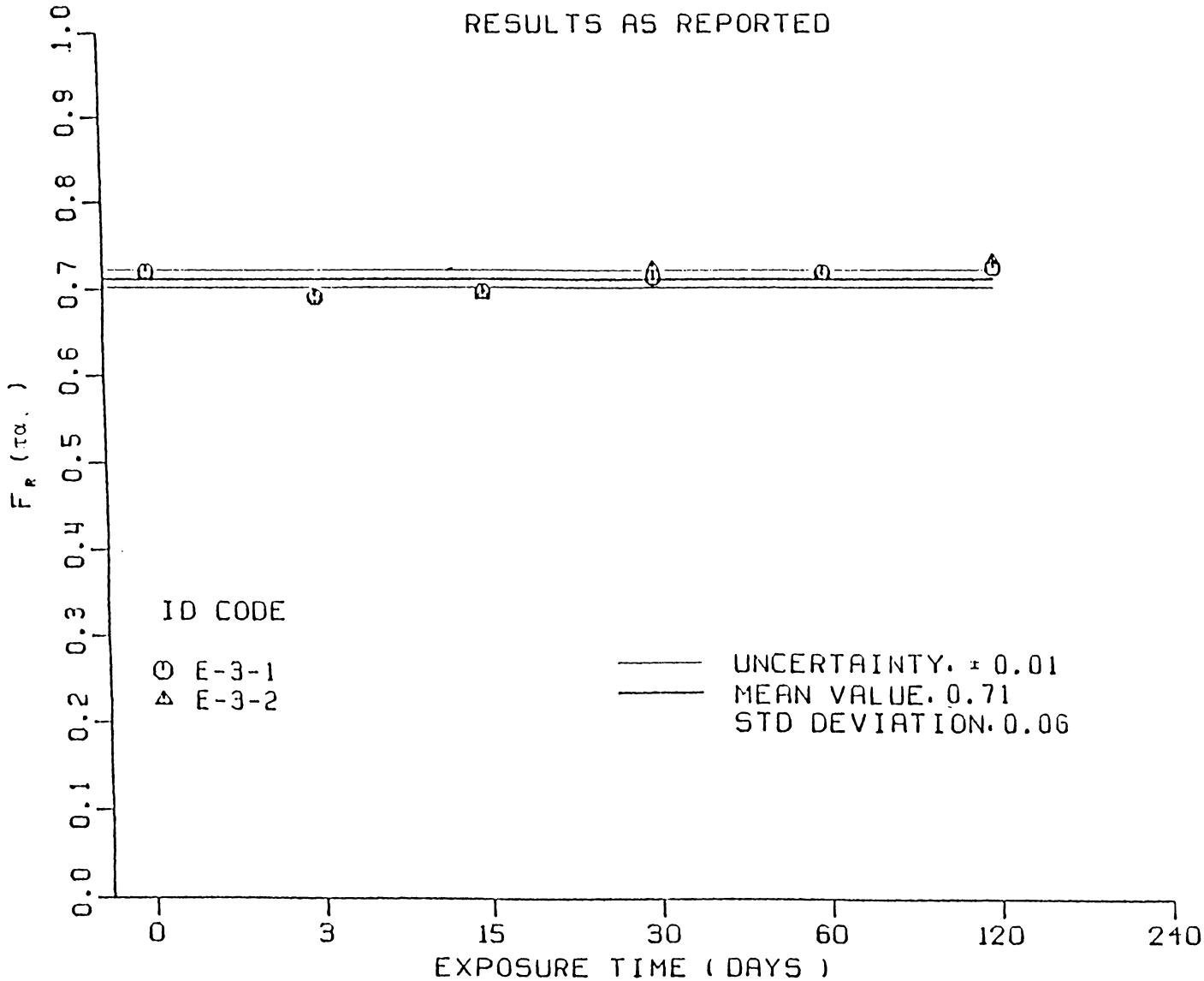

Figure 13 $F_{r(\tau\alpha)}$ versus Exposure Time - Collector E, Test Site 3

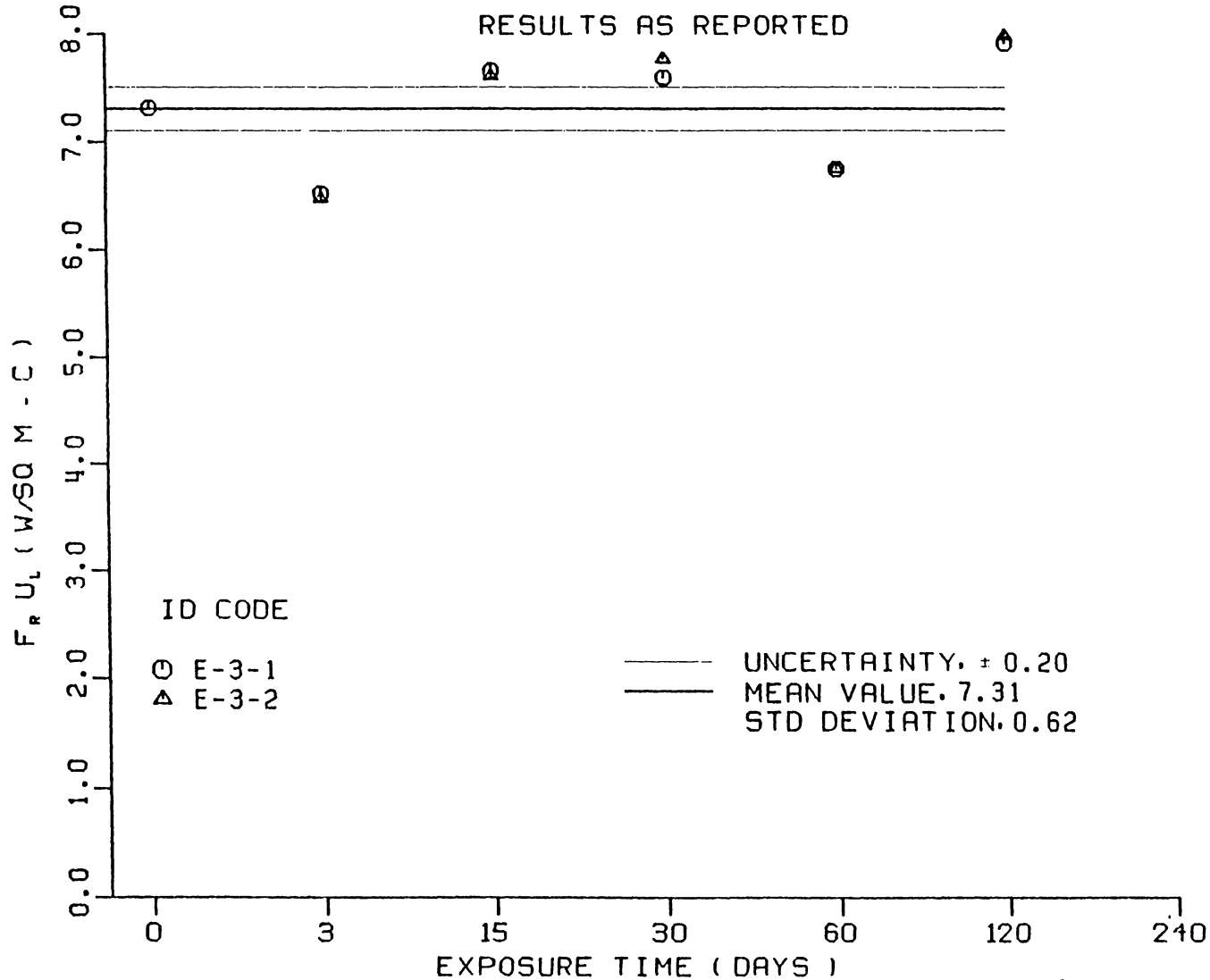

Figure 14 - $F_r U_L$ versus Exposure Time - Collector E, Test Site 3

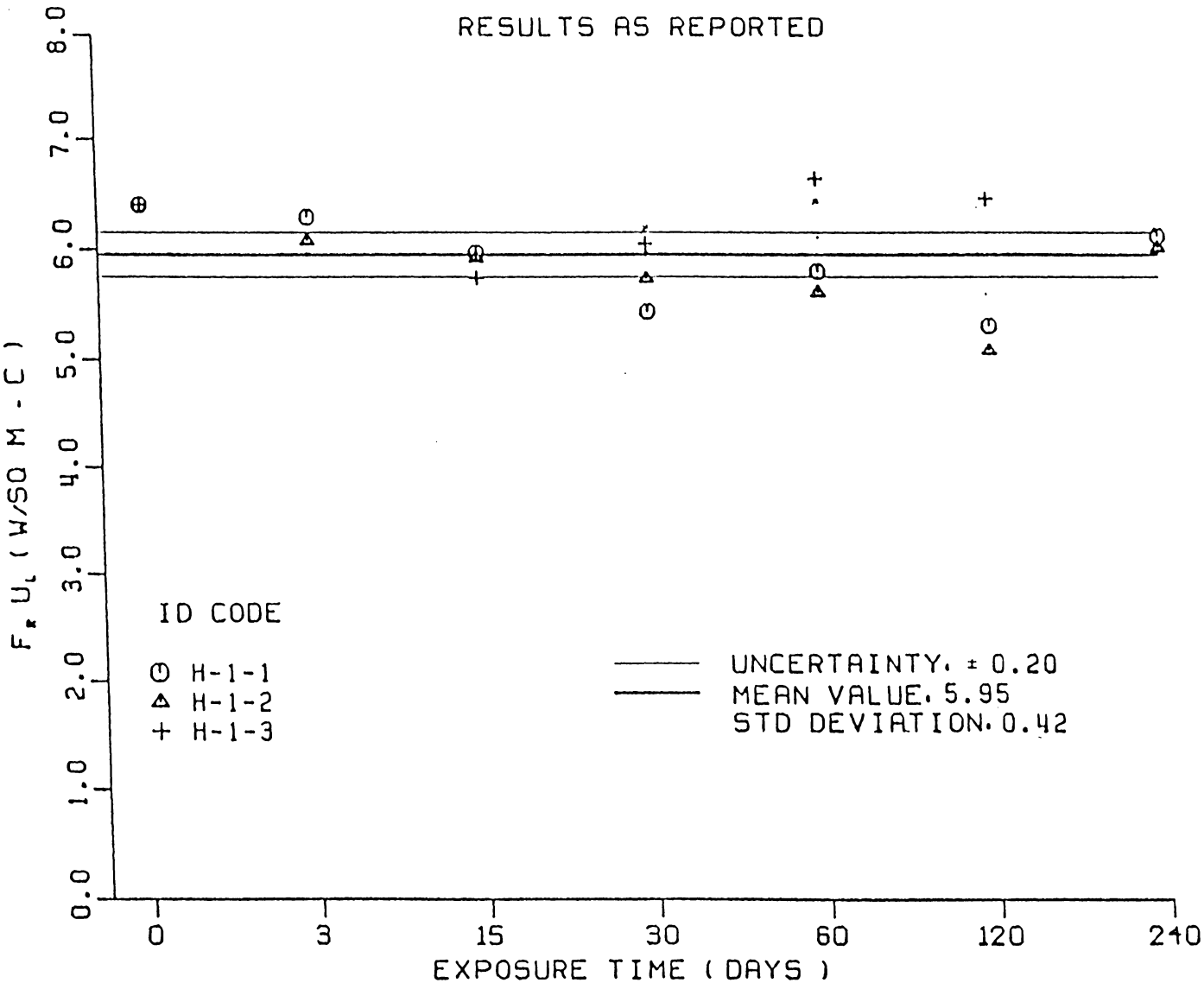

Figure 15 - $F_r U_L$ versus Exposure Time - Collector H, Test Site 1

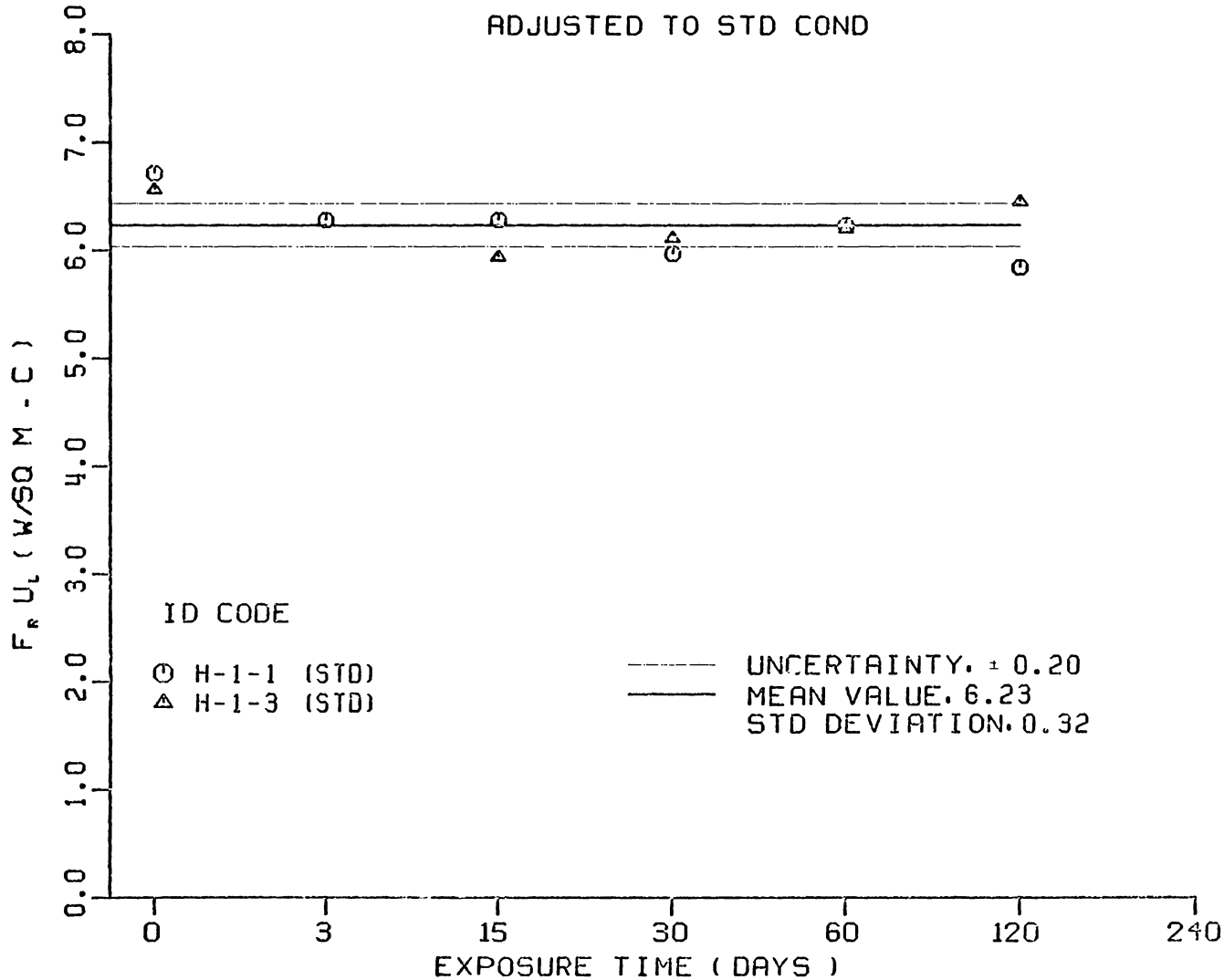

Figure 16 - $F_r U_L$ versus Exposure Time (adjusted to standard weather conditions)--Collector H, Test Site 1.

plotted for test sites 1-3 for individual series for each collector. These plots are Figs. B-16 through B-30 in the Appendix. In general, the test series has no consistent effect on collector degradation. It can be observed that test site 2, more often than not, reported higher values of F_rU_L than the other test sites. Figure 17 shows that, even when adjusted to standard environmental conditions, the F_rU_L values reported by test site 2 for collector B, series 1, are higher than the values from the other test sites. This situation might be caused by improper test stand calibration.

One of the purposes of test series 1 was to investigate the significance of the 3 day pre-exposure per ASHRAE 93-77. The results show that the 3 day pre-exposure has no detectable effect on $F_r(\tau\alpha)$. However, in every case F_rU_L decreased or at least remained constant from 0 days to 3 days exposure time. The effect of the 3 day pre-exposure is illustrated in Appendix B in Figs. B-16 through B-30.

In order to show the effect of environmental conditions on collector degradation, performance parameters were adjusted to standard conditions and plotted as a function of time for collectors B and E for series 1 at test sites 1-3. Collector E is one of the most sensitive collectors to environmental conditions because it has a single cover, nonselective absorber, and a relatively elongated geometry which results in more area for edge losses. Collector B is relatively insensitive to environmental conditions because it has two covers. Figures 18-21 show that adjusting the data to standard conditions does not reduce the scatter in the results or reveal any significant trends.

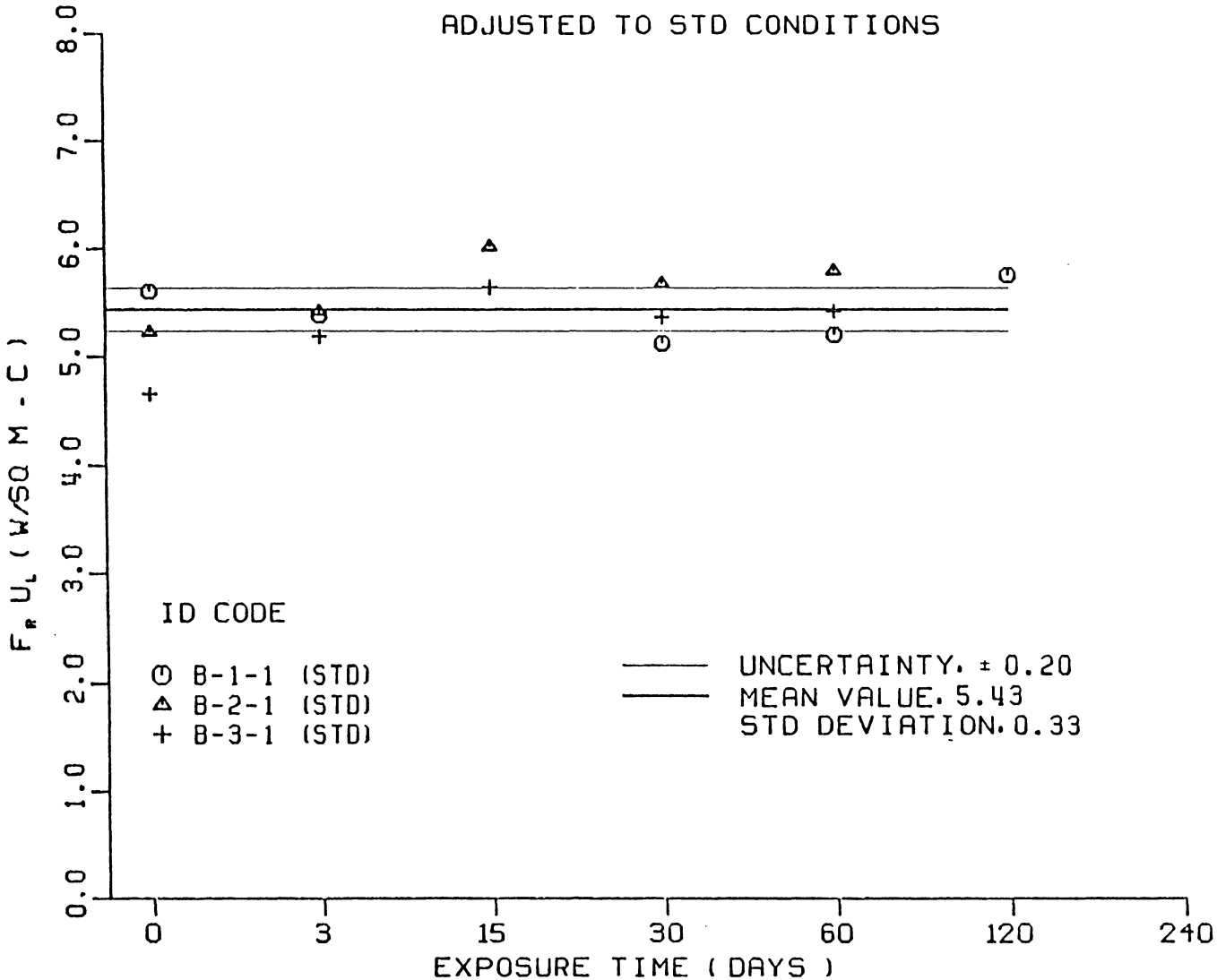

Figure 17 - $F_r U_L$ versus Exposure Time (adjusted to standard weather conditions) - Collector B, Series 1

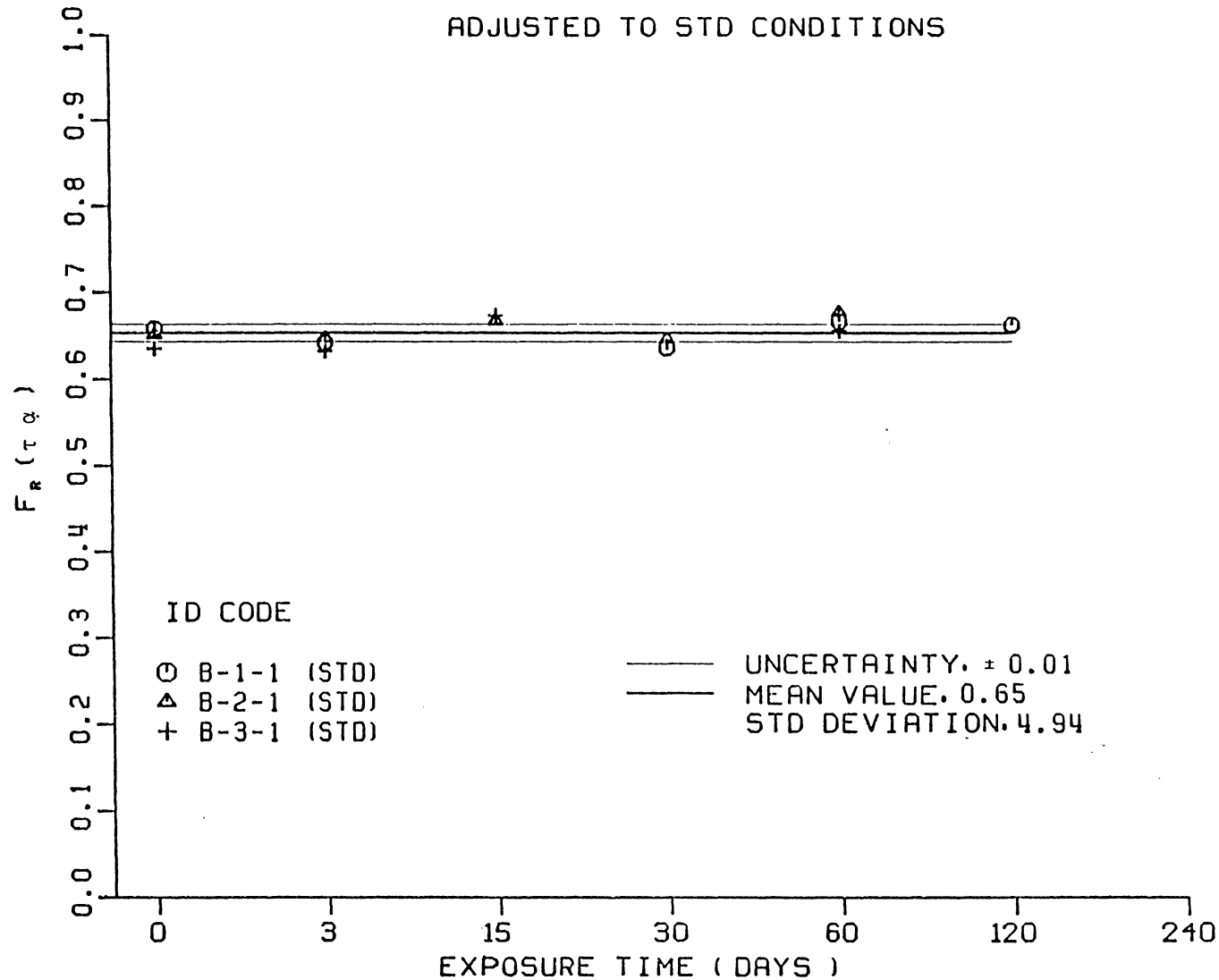

Figure 18 - $F_r(\tau\alpha)$ versus Exposure Time (adjusted to standard weather conditions) - Collector B, Series 1

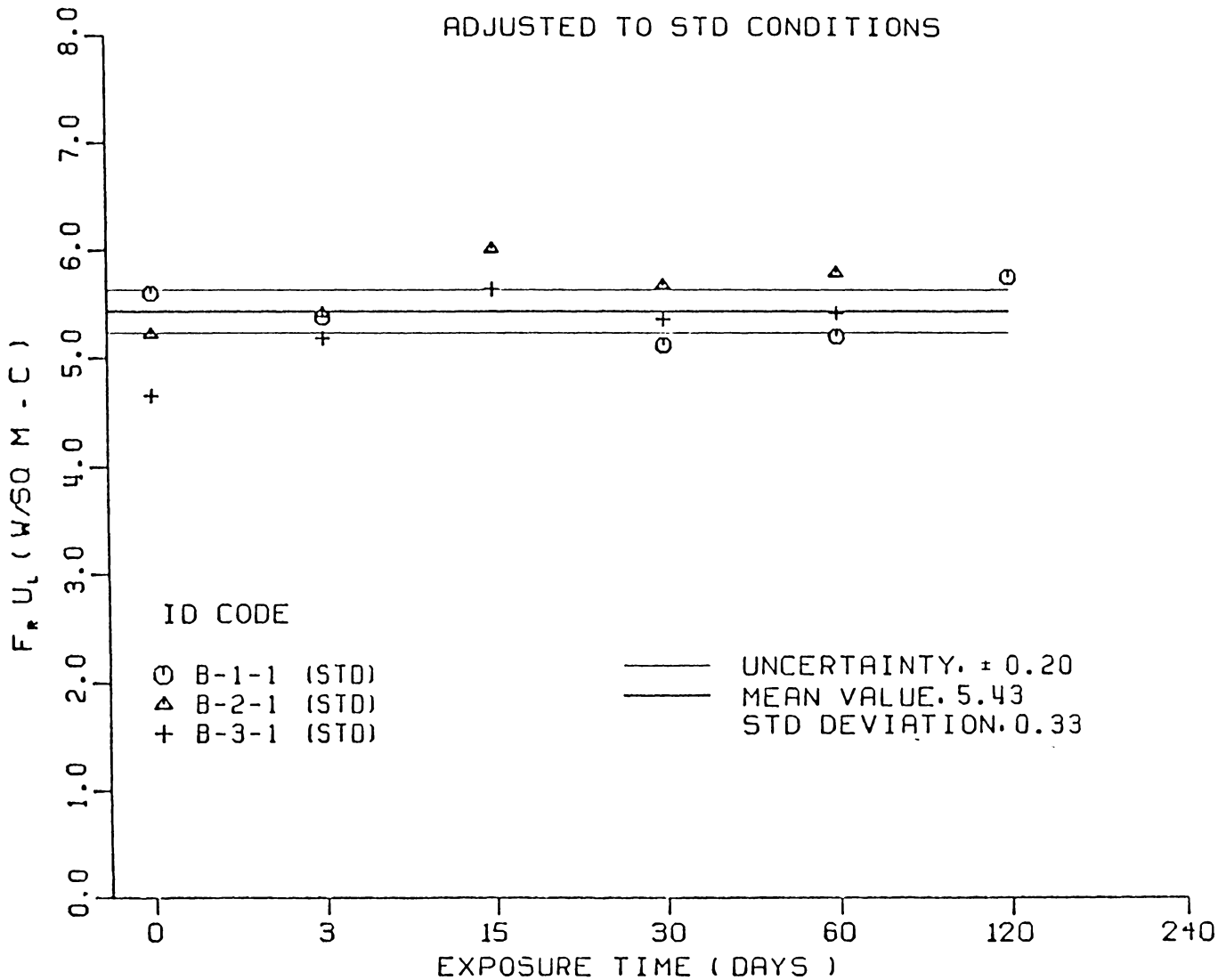

Figure 19 - $F_r U_L$ versus Exposure Time (adjusted to standard weather conditions) - Collector B, Series 1

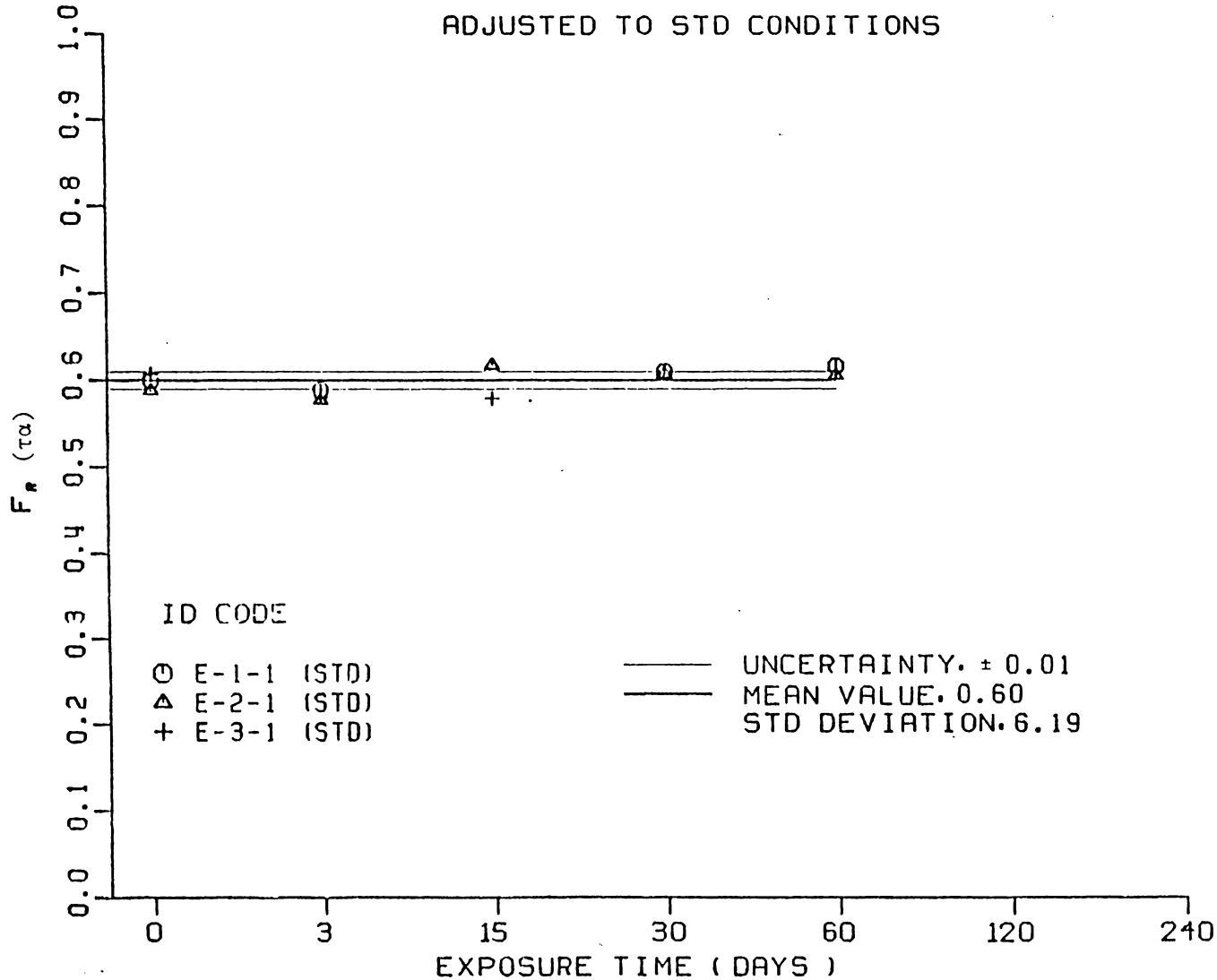

Figure 20 - $F_r(\tau\alpha)$ versus Exposure Time (adjusted to standard weather conditions) - Collector E, Series 1

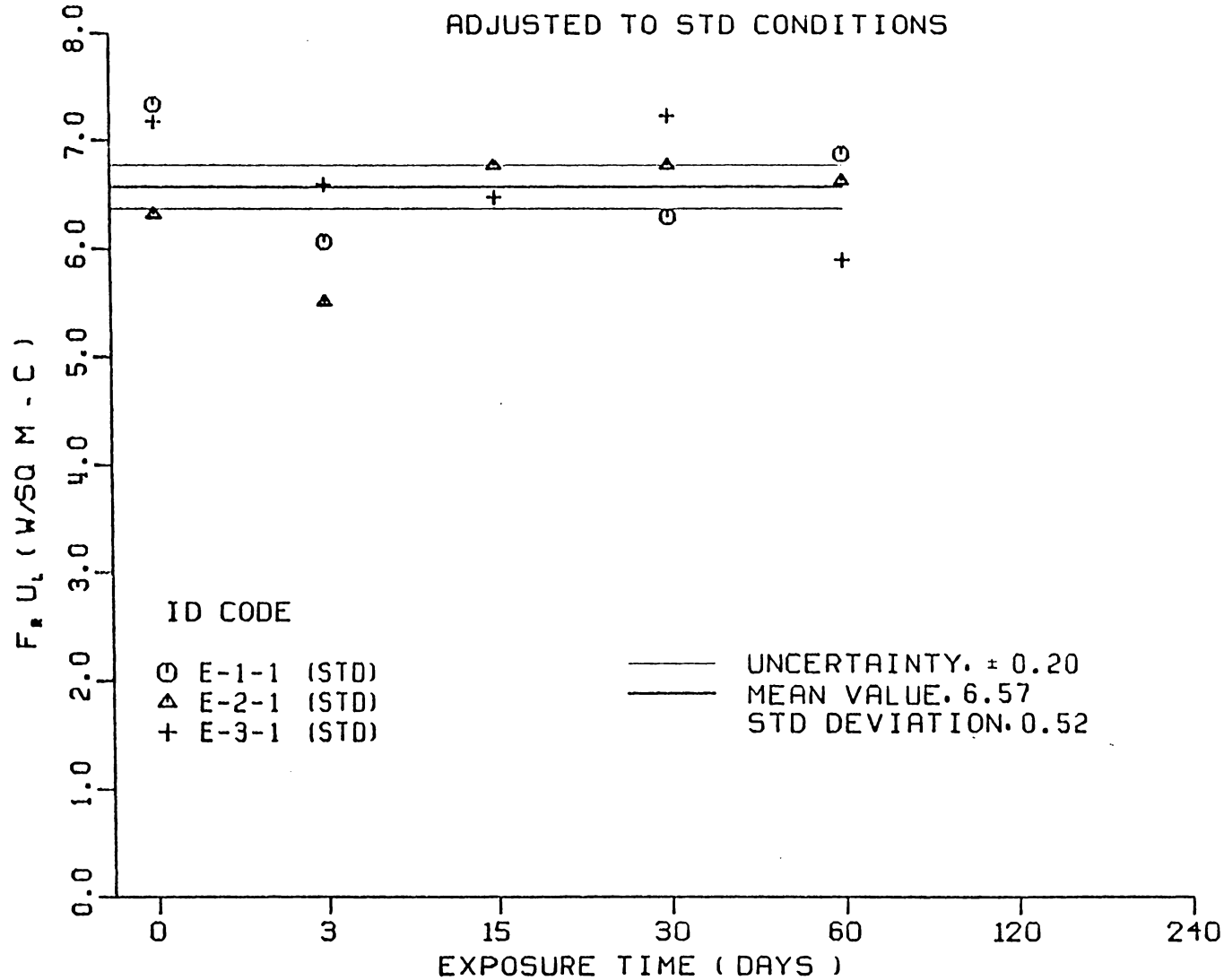

Figure 21 - $F_r U_L$ versus Exposure Time (adjusted to standard weather conditions) - Collector E, Series 1

In order to show the effect of the season during which the performance test was run, performance parameters as a function of season were plotted. These plots are included in Appendix C. The season of the year does not have a strong effect on the performance parameters. F_rU_L does not depend on the season at all. Values of $F_r(\tau\alpha)$ measured during the winter are as high or higher than for the other seasons. However, the effect of season is not strong compared to the effect of experimental uncertainty.

Statistical Analysis

Examination of performance data indicates that no significant property changes have taken place in the collectors. The randomness of the performance parameters indicates that the scatter is a result of a lack of precision in the experimental procedures. In this section, a statistical analysis is performed according to the procedures recommended by ASTM Standard Recommended Practice E177 [22].

Experimental measurements are characterized by accuracy and precision. An investigation of accuracy requires a reference sample for which the correct value of the measured property is known. This discussion will only consider the precision of the experimental method.

The performance parameters of a collector are subject to two sources of variability: the variability between collectors of the same type tested at the same facility and the variability resulting from different test labs. Each source of variability can be characterized by a standard deviation. The former is known as the "within site" standard deviation. The latter is referred to as the "between site"

standard deviation. It is also possible to find the uncertainty of the average value for the performance parameters of each collector. This uncertainty is known as the standard error and is expressed as a standard deviation. The technique for calculating these components of variability is described in detail in reference 23.

Tables 5 and 6 list the average, within and between standard deviations and the standard error for the performance parameters for each collector. There is no apparent relationship between the standard deviations and the corresponding type of collector. The coefficient of variation (standard deviation expressed as a percentage of the average) for $F_r(\tau\alpha)$ is 2.0 percent for within site and 2.7 percent for between site. The within site coefficient for F_rU_L is 9.0 percent and the between site coefficient is 13.0 percent. The variation in results is greater between test sites than within a test site. This result is expected and is consistent with the results from the earlier round-robin test program 14.

The standard error is the uncertainty in the mean value of a measured quantity. The standard error in $F_r(\tau\alpha)$ values was approximately equal to the predicted error. The standard error in F_rU_L values was about twice as large as can be attributed to expected uncertainty.

The test results indicate that 240 days of exposure to the environment are not sufficient to induce significant degradation in the collectors considered in this program. Any degradation which may have occurred was overshadowed by experimental error. NBS is extending the exposure period for some of the collectors to 480 days to see if this is sufficient to induce degradation in the collector performance.

Table 5. Statistical Analysis of $F_r(\tau\alpha)$ Values From All Test Sites

Collector	Mean value of $F_r(\tau\alpha)$	Within site deviation, σ_w		Between site deviation, σ_b		Standard Error	
		--	Percent	--	Percent	--	Percent
A	0.724	0.014	1.9	0.017	2.3	0.011	1.4
B	0.716	0.015	2.1	0.0095	1.3	0.006	0.83
D	0.760	0.013	1.8	0.033	4.4	0.019	2.5
E	0.705	0.015	2.2	0.018	2.6	0.011	1.5
H	0.702	0.016	2.3	0.022	3.1	0.011	1.6

Average σ_w = 2.0 percent

Average σ_b = 2.7 percent

Table 6. Statistical Analysis of F_rU_L Values From All Test Sites

Collector	Mean value of F_rU_L	Within site deviation, σ_w		Between site deviation, σ_b		Standard Error	
		W/sq m·C	Percent	W/sq m·C	Percent	W/sq m·C	Percent
A	5.2	0.78	15	0.89	17	0.50	9.5
B	5.9	0.24	4.0	0.61	10	0.35	6.0
D	3.7	0.48	13	0.39	10	0.24	6.5
E	7.4	0.55	7.4	0.77	10	0.45	6.1
H	6.1	0.34	5.7	0.98	16	0.34	5.5

Average σ_w = 9.0 percent

Average σ_b = 13.0 percent

More data are needed from exposure tests of collectors and materials samples. Particular attention should be given to instrumentation calibration over the course of an extended test program. The effects of transient conditions during tests should also be examined.

VI. CONCLUSIONS

Outdoor testing of solar collector durability will continue to be important in the future. Indoor testing using solar simulators is expensive and the credibility of such tests has not been demonstrated. In order to investigate the feasibility of outdoor durability tests, five different types of flat plate solar collectors were exposed for up to 240 days under various operating and environmental conditions. The exposure conditions were intended to induce degradation in the materials used in the collectors. The durability of the collectors was measured by conducting thermal performance tests at specified intervals.

It is concluded that 240 days of exposure were not sufficient to induce degradation in the performance of the collectors. The test collectors proved to be quite durable, holding up well under conditions much more severe than normal operation. Any degradation that might have occurred was overshadowed by experimental uncertainty in the test procedure for measuring collector efficiency.

The collector performance parameters, $F_r(\tau\alpha)$ and F_rU_L, as functions of time, were scattered in a random fashion about mean values. The scatter in $F_r(\tau\alpha)$ values was approximately equal to the predicted experimental uncertainty. The scatter in F_rU_L values was about twice as large as can be attributed to experimental error. From the available data, it was not possible to identify specific reasons for the excessive scatter in the results. It was shown that referring the test

results to a common set of weather conditions did not reduce the scatter in F_rU_L values. The instrumentation used at the test sites should be studied to identify possible sources of systematic error.

The effect of environmental conditions on collector degradation was investigated by using three test sites in different parts of the contiguous United States. The different environmental conditions had no significant effect on the test results.

Three test series were considered to study the effect of different operating conditions on collector degradation. The test series did not have a significant effect on the test results.

The season of the year during which the tests were run did not have a strong effect on the results.

REFERENCES

[1] Streed, E. R., and D. Waksman, "NBS Solar Collector Durability/ Reliability Program," Durability of Building Materials and Components, ASTM STP 691, P. J. Sereda and G. G. Livtan, Eds., American Society for Testing and Materials, 1980, pp. 239-249.

[2] Clark, E. J., W. E. Roberts, J. W. Grimes, and E. J. Embree, "Solar Energy Systems--Standards for Cover Plates for Flat Plate Solar Collectors," NBS Technical Note 1132, National Bureau of Standards, Washington, D.C., Dec. 1980.

[3] Skada, L. F., and L. W. Masters, "Solar Energy Systems--Survey of Materials Performance," NBSlR 77-1314, National Bureau of Standards, Washington, D.C., Oct. 1977.

[4] Edwards, D. K., K. E. Nelson, R. D. Roddick, and J. T. Gier, "Basic Studies on the Use and Control of Solar Energy," Report No. 60-93, Dept. of Energy, University of California, Oct. 1960.

[5] Martin, D. C., and R. Bell, "The Use of Optical Interference to Obtain Selective Energy Absorption," Proceedings on the Conference on Coatings for the Aerospace Environment, WADD-TR-60-TB, Wright-Patterson Air Development Division, Dayton, Ohio, Nov. 1960.

[6] Schmidt, R. N., K. C. Park, and E. Janssen, "High Temperature Absorber Coatings, Part II," Tech. Doc. Report No. ML-TDR-64-250, Honeywell Research Center, Dept. 1964.

[7] Löf, G. O. G., and J. C. Ward, "Long-term (18 years) Performance of Residential Heating Systems," Solar Energy, Vol. 18, 1976, pp. 301-308.

[8] Knoll, R. H., and S. M. Johnson, "Baseline Performance of Solar Collectors for NASA Langley Solar Building Test Facility," Flat Plate Solar Collector Conference, Orlando, Florida, March 1977.

[9] Masters, L. W., E. J. Clark, G. A. Steater, and A. Hockman, "Durability and Related Tests for Selected Elements and Materials Used in the Exterior Envelope of Buildings," NBSIR 75-955, National Bureau of Standards, Washington, D.C., Nov. 1975.

[10] Masters, L. W., W. C. Wolfe, W. J. Rossiter, and J. R. Shavers, "State of the Art on Durability Testing of Building Components and Materials," NBSIR 73-132, National Bureau of Standards, Washington, D.C., March 1973.

[11] Mann, N. R., R. E. Shafer, and N. D. Singpurwalla, Methods for Statistical Analysis of Reliability and Life Data, John Wiley and Sons, Inc., New York, 1974.

[12] Gaines, G. B., R. E. Thomas, G. C. Derringer, C. W. Kistler, D. M. Bigg, and D. C. Charmichael, "Methodology for Designing Accelerated Aging Tests for Predicting Life of Photovoltaic Arrays," Battelle Columbus Laboratories, Columbus, Ohio, Feb. 1977.

[13] Barlow, R. E., and E. M. Scheuer, "Estimation from Accelerated Life Tests," Technometrics, Vol. 13, No. 1, 1971, pp. 145-149.

[14] Streed, E. R., W. C. Thomas, A. G. Dawson III, B. D. Wood, and J. E. Hill, "Results and Analysis of a Round-Robin Test Program for Liquid-Heating Flat-Plate Solar Collectors," NBS Technical Note 975, National Bureau of Standards, Washington, D.C., Aug. 1978.

[15] "Methods of Testing to Determine the Thermal Performance of Solar Collectors," ASHRAE 93-77 American Society of Heating, Refrigerating and Air-Conditioning Engineers, Inc., New York, 1977.

[16] Adams, R. D., "Measured Efficiency and Analytical Correction of Flat-Plate Collector Thermal Efficiency," M.S. Thesis, Mechanical Engineering Department, Virginia Polytechnic Institute and State University, Blacksburg, Virginia, Aug. 1980.

[17] Waksman, D., E. R. Streed, T. W. Reichard, and L. E. Cattaneo, "Provisional Flat Plate Solar Collector Testing Procedures: First Revision," NBSIR 78-1305A, National Bureau of Standards, Washington, D.C., June 1978.

[18] Duffie, J. A., and W. A. Beckman, Solar Energy Thermal Processes, John Wiley and Sons, Inc., New York, 1974.

[19] Thomas, W. C., "Solar Collector Test Procedures: Development of a Method to Refer Measured Efficiency to Standard Test Conditions," VPI & SU Report VPI-E-80.23, Virginia Polytechnic Institute and State University, Blacksburg, Virginia, Nov. 1980.

[20] Kline, S. J., and F. A. McClintock, "Describing Uncertainties in Single-Sample Experiments," Mechanical Engineering, American Society of Mechanical Engineering, American Society of Mechanical Engineers, New York, Jan. 1953.

[21] Melissinos, A. C., Experiments in Modern Physics, Academic Press, New York, 1966.

[22] Duncan, A. J., "Views of the E-11 Task Group on Statements of the Precision and Accuracy of a Test Method," ASTM Standardization News, American Society of Testing and Materials, New York, Feb. 1977.

[23] Mandel, J., "The Analysis of Interlaboratory Test Data," ASTM Standardization News, American Society of Testing and Materials, New York, Mar. 1977.

APPENDIX A

COLLECTOR PROPERTIES

Properties for Collector A

Absorber Plate

Material: Cold Rolled Mild Steel

Length (flow direction): 1.92 m Width: 0.95 m

Flow Configuration: Parallel No. Tubes: 8

Coating: Tabor Selective

Long-wave Emittance: 0.20

Solar Absorptance: 0.93

Cover Assembly Consisting of 1 Cover

Plate Material: Water White Glass

Solar Beam Transmittance: 0.91

Infrared Transmittance: 0.04

Insulation

Back: 8 cm Fibrous Mineral Wool

Thermal Conductivity: 0.035 W/m-c

Edge: 1 cm Fiber Board

Thermal Conductivity: 0.04 W/m-c

Overall Assembly

Length: 2.0 m Width: 1.1 cm

Depth: 0.13 m

Back Cover: Galvanized Steel

Properties for Collector B

Absorber Plate

Material: Copper

Length (flow direction): 1.91 m Width: 0.84 m

Flow Configuration: Parallel No. Tubes: 6

Coating: Black Velvet Nextel

Long-wave Emittance: 0.89

Solar Absorptance: 0.96

Cover Assembly Consisting of 2 Covers

	Inner	Outer
Plate Material	Low Iron Glass	Low Iron Glass
Solar Bean Transmittance:	0.89	0.89
Infrared Transmittance:	0.04	0.04

Insulation

Back: 7.6 cm Fiberglass

Thermal Conductivity: 0.04 W/m-c

Edge: 2.5 cm Fiberglass

Thermal Conductivity: 0.04 W/m-c

Overall Assembly

Length: 1.96 m Width: 0.89 m

Depth: 0.13 m

Back Cover: Aluminum

Properties for Collector D

Absorber Plate

Material: Steel Plate

Length (flow direction): 1.73 m Width: 0.81 m

Flow Configuration: Parallel No. Tubes: 10

Coating: Black Chrome

Long-wave Emittance: 0.10

Solar Absorptance: 0.94

Cover Assembly Consisting of 2 Covers

	Inner	Outer
Plate Material:	Low Iron Glass	Low Iron Glass
Solar Beam Transmittance:	0.96	0.96
Infrared Transmittance:	0.04	0.04

Insulation

Back: 8.9 cm Semi-Rigid Fiberglass

Thermal Conductivity: 0.04 W/m-c

Edge: 2.5 cm Semi-Rigid Fiberglass

Thermal Conductivity: 0.04 W/m-c

Overall Assembly

Length: 1.82 m Width: 0.91 m

Depth: 0.16 m

Backside Cover: 22 Gage Steel

Properties for Collector E

Absorber Plate

Material: Copper

Length (flow direction): 2.91 m Width: 0.56 m

Flow Configuration: Parallel No. Tubes: 5

Coating: Flat Black Lacquer

Long-wave Emittance: 0.87

Solar Absorptance: 0.95

Cover Assembly Consisting of 1 Cover

Plate Material: Kalwall Sun-Lite Premium II

Solar Beam Transmittance: 0.86

Infrared Transmittance: 0.07

Insulation

Back and Edge: 2.5 cm Isocyanurate

Thermal Conductivity: 0.02 W/m-c

Overall Assembly

Length: 305 m Width: 0.62 m

Depth: 0.09 m

Backside Cover: Aluminum

Properties for Collector H

Absorber Plate

Material: Extruded Aluminum

Length (flow direction): 2.34 m Width: 1.13 m

Flow Configuration: Serptentine No. Passes: 8

Coating: Flat Black Paint

Long-wave Emittance: 0.88

Solar Absorptance: 0.96

Cover Plate Assembly Consisting of 2 Covers

	Inner	Outer
Plate Material:	Teflon Steel	UV Resistant Polyester
Solar Beam Transmittance:	0.96	0.80
Infrared Transmittance:	0.60	0.10

Insulation

Back and Edge: 2.5 cm Isocyanurate

Thermal Conductivity: 0.02 W/m-c

Overall Assembly

Length: 2.43 m Width: 1.21 m

Depth: 0.10 m

Backside Cover: Aluminum

APPENDIX B

PLOTS OF PERFORMANCE PARAMETERS AS A FUNCTION OF EXPOSURE TIME

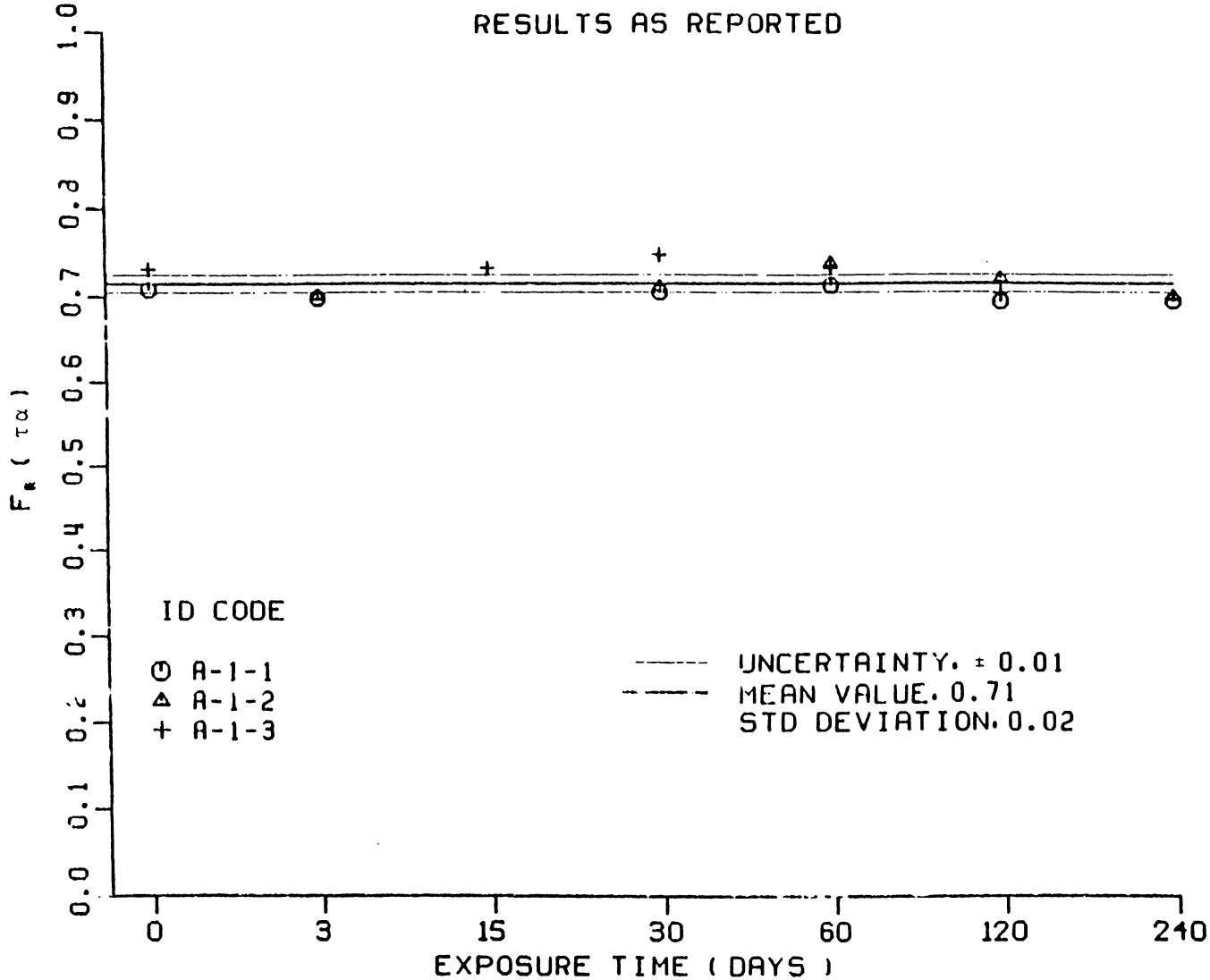

Figure B-1 $F_r(\tau\alpha)$ versus Exposure Time - Collector A, Test Site 1

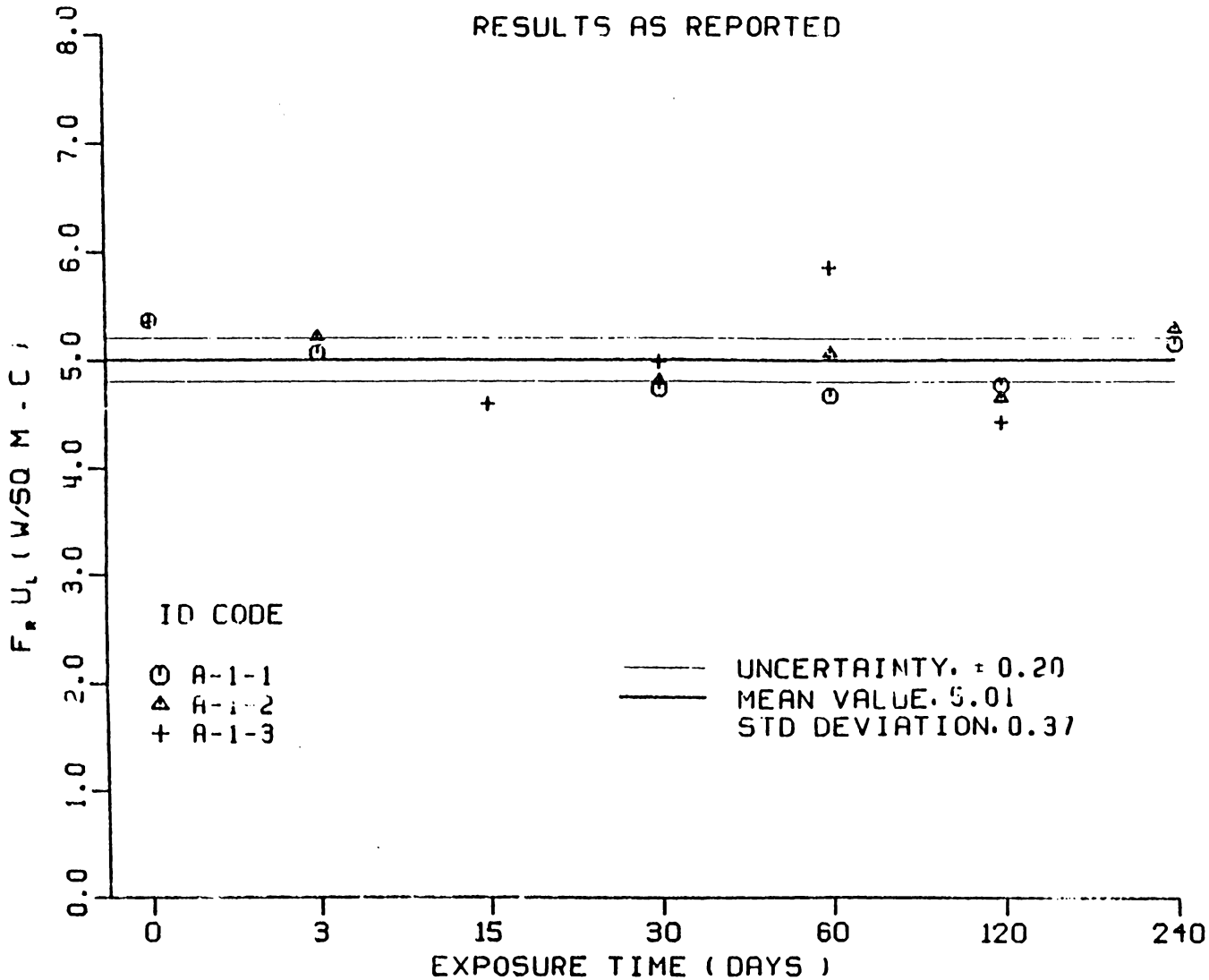

Figure B-2 $F_r U_L$ versus Exposure Time - Collector A, Test Site 1

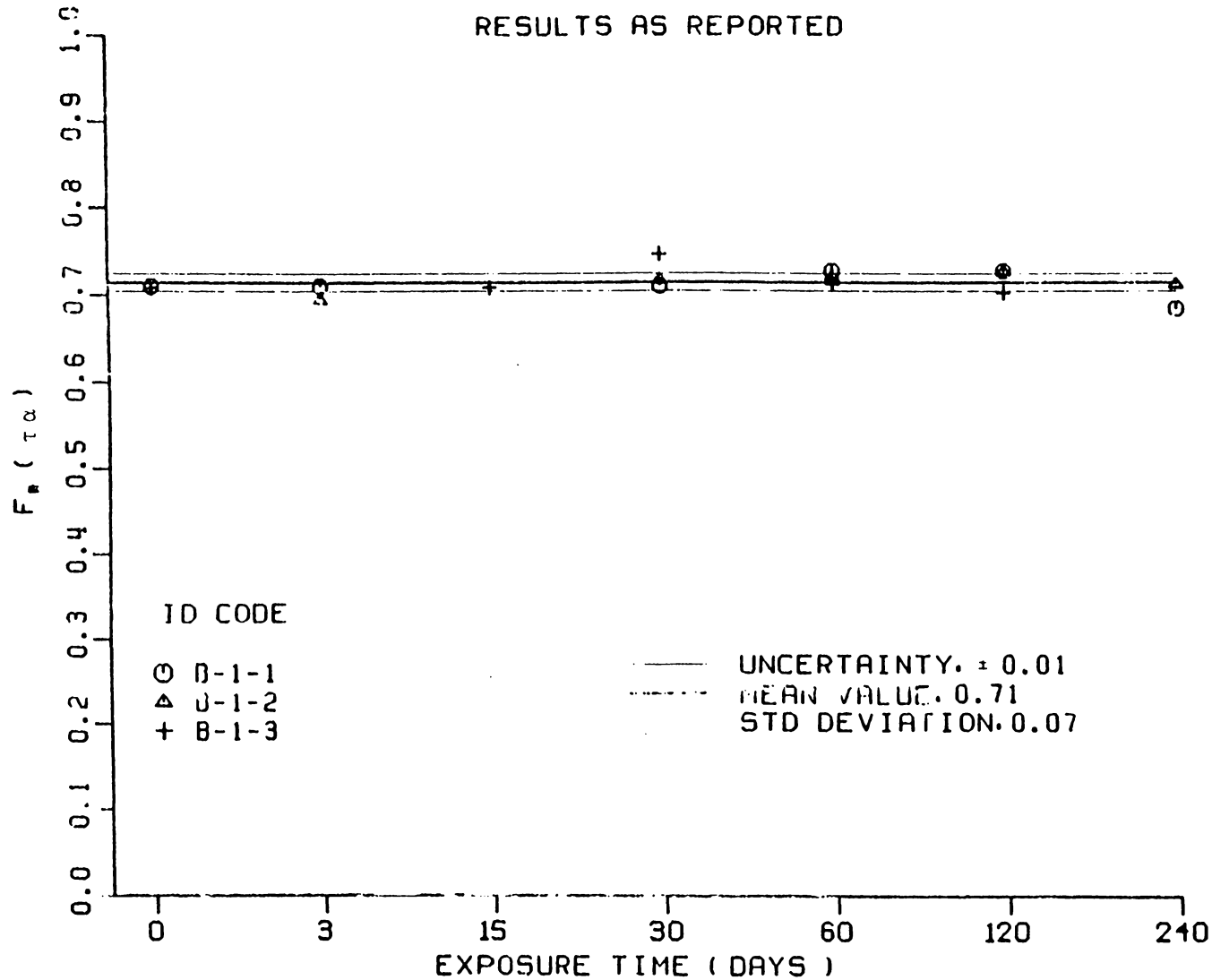

Figure B-3 $F_r(\tau\alpha)$ versus Exposure Time - Collector B, Test Site 1

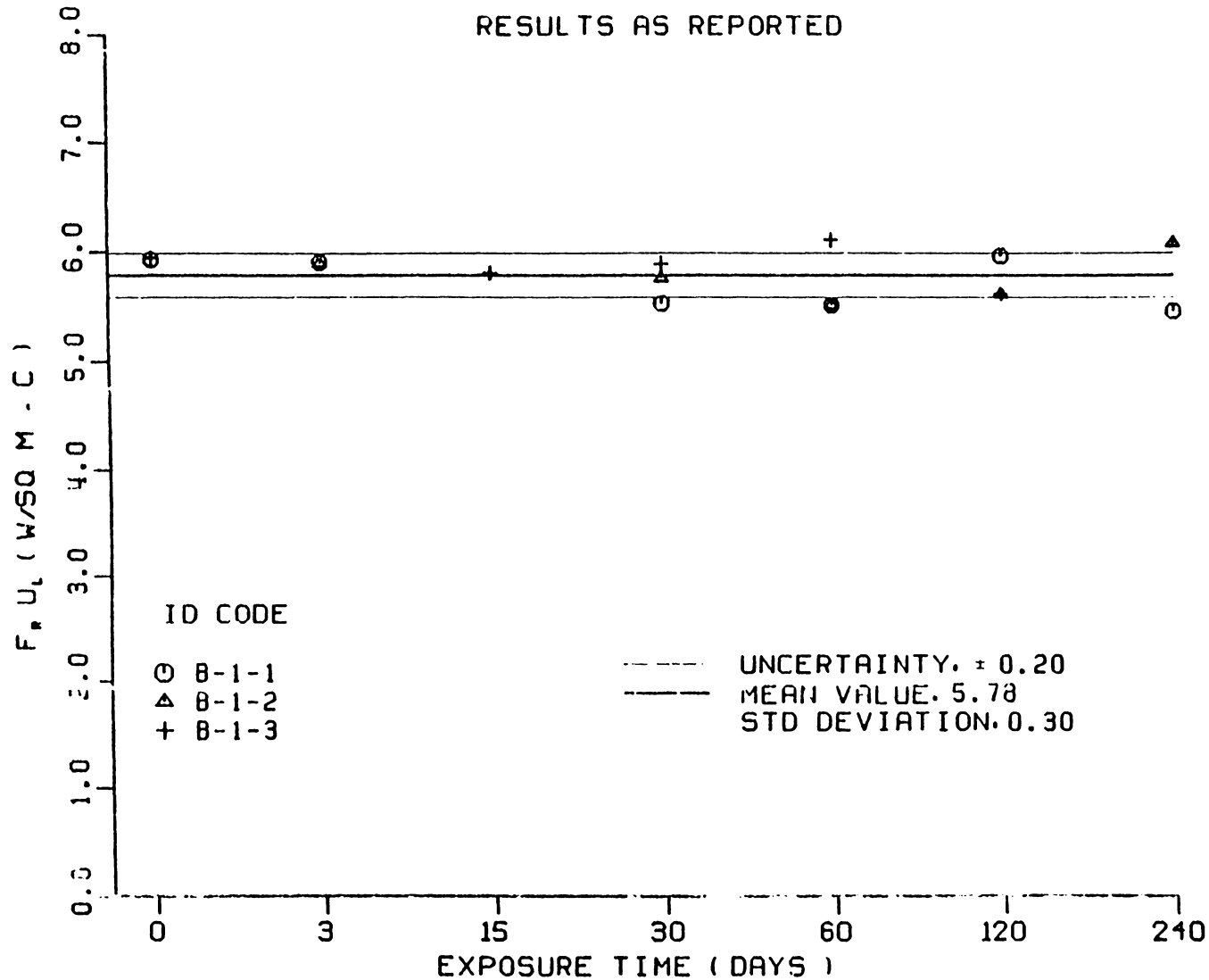

Figure B-4 $F_r U_L$ versus Exposure Time - Collector B, Test Site 1

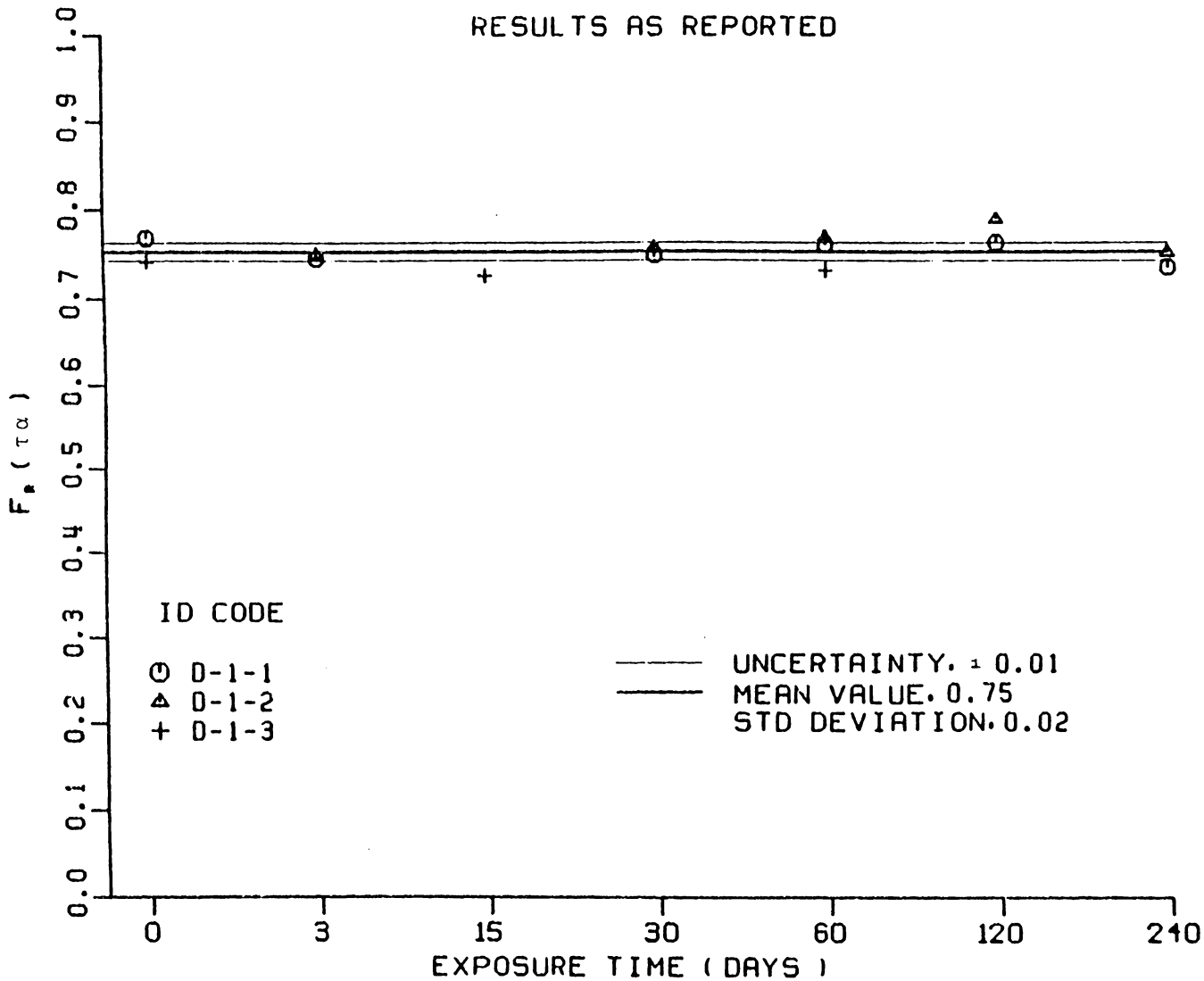

Figure B-5 $F_r(\tau\alpha)$ versus Exposure Time - Collector D, Test Site 1

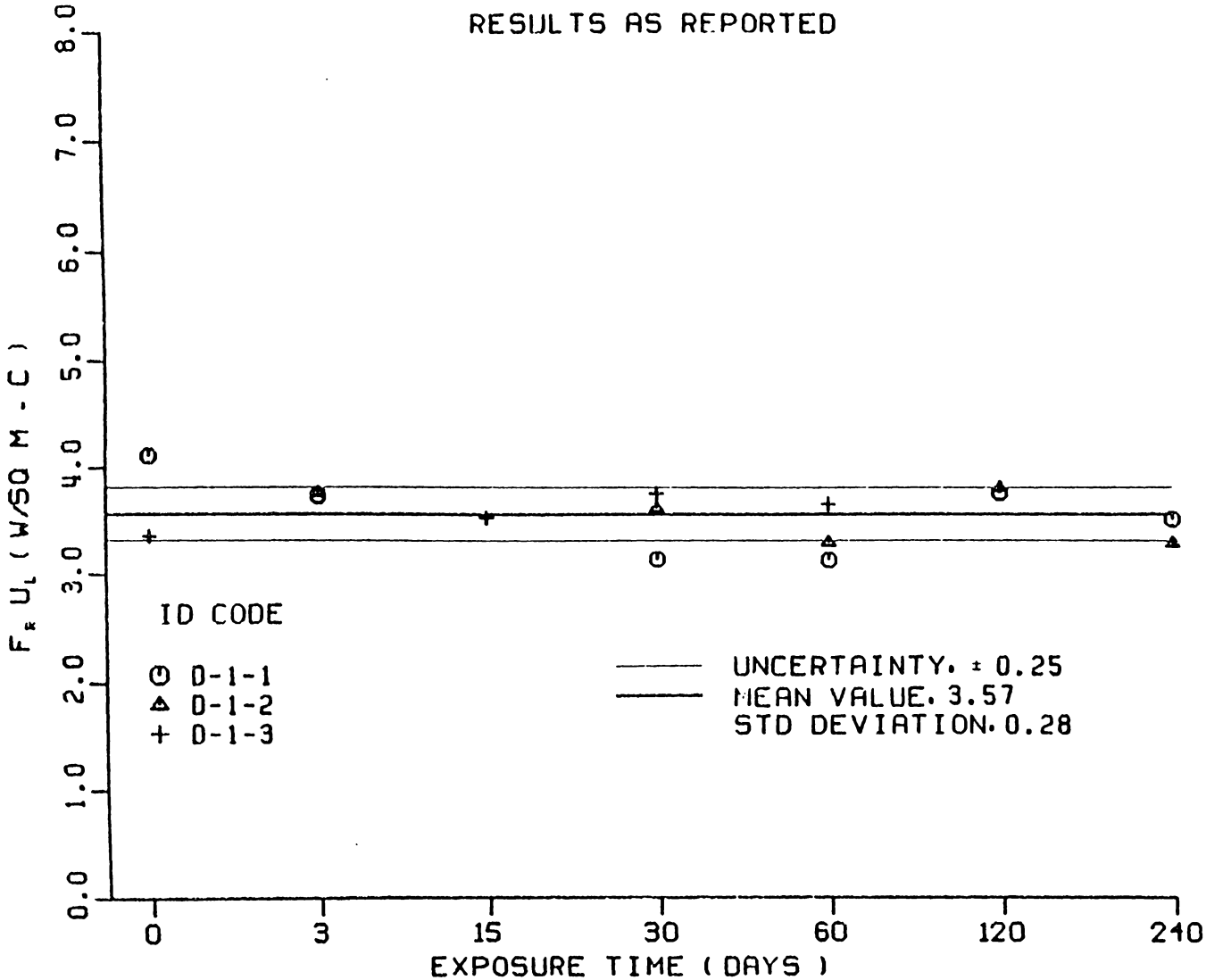

Figure B-6 $F_r U_L$ versus Exposure Time - Collector D, Test Site 1

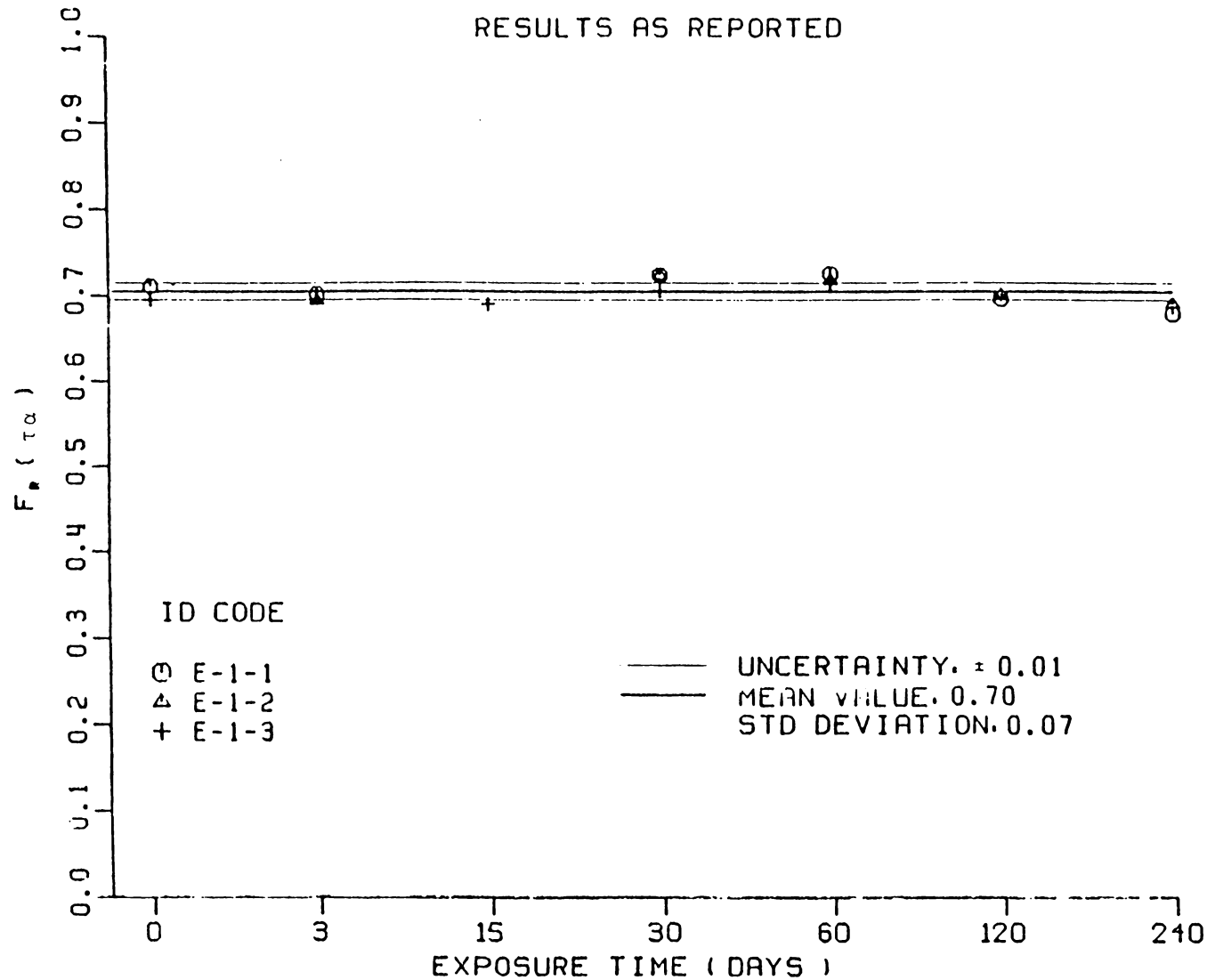

Figure B-7 $F_r(\tau\alpha)$ versus Exposure Time - Collector E, Test Site 1

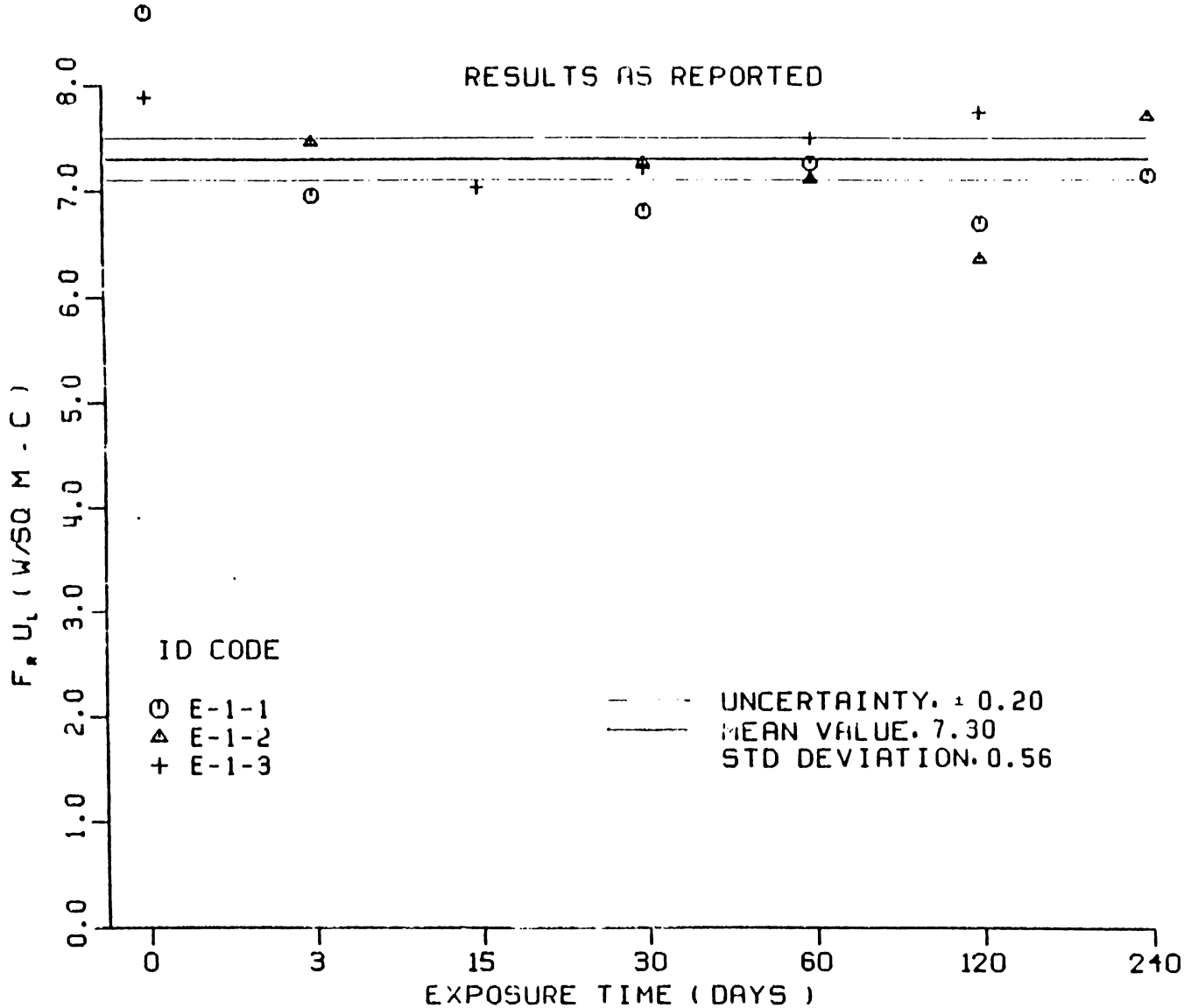

Figure B- 8 $F_r U_L$ versus Exposure Time - Collector E, Test Site 1

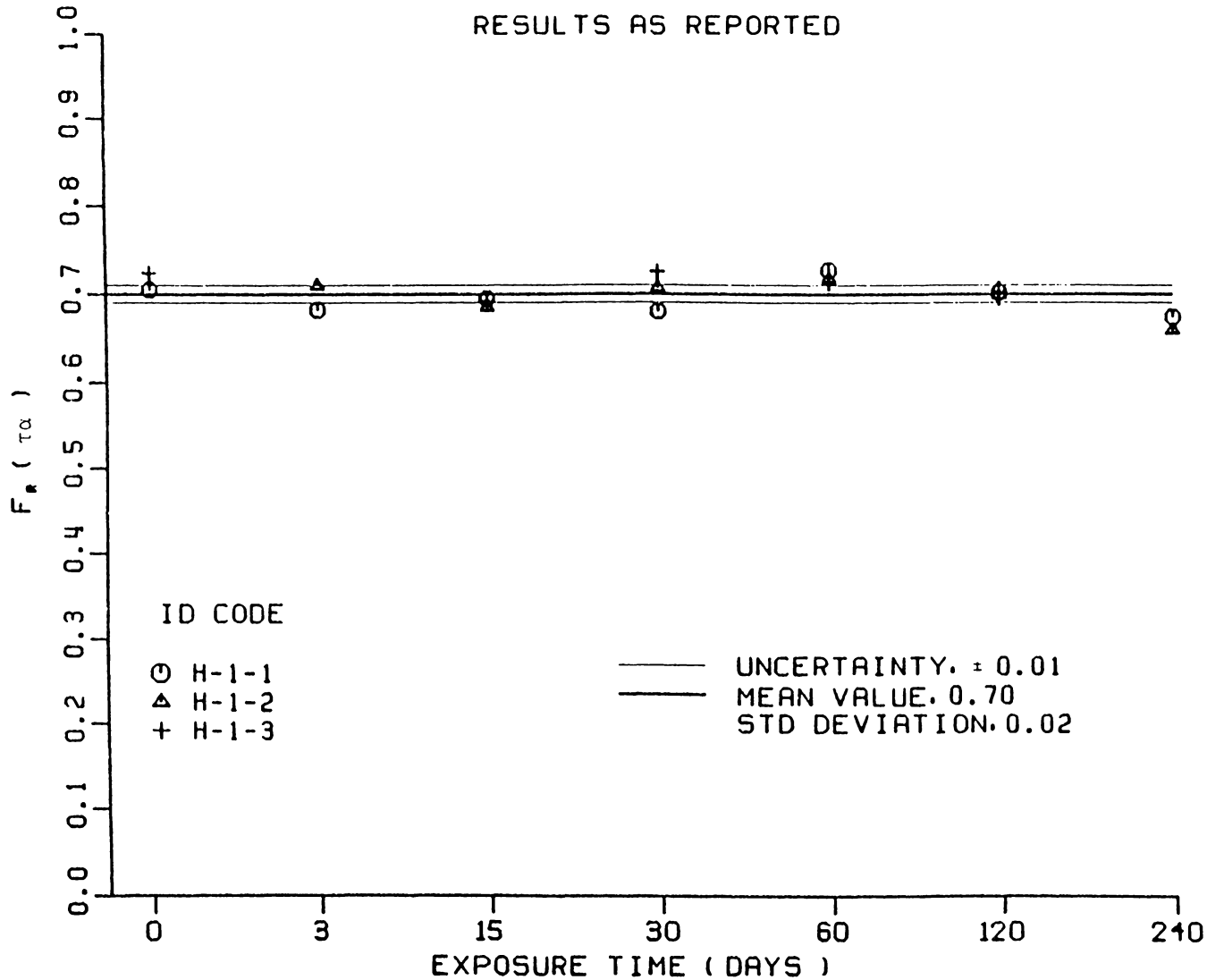

Figure B-9 $F_r(\tau\alpha)$ versus Exposure Time - Collector H, Test Site 1

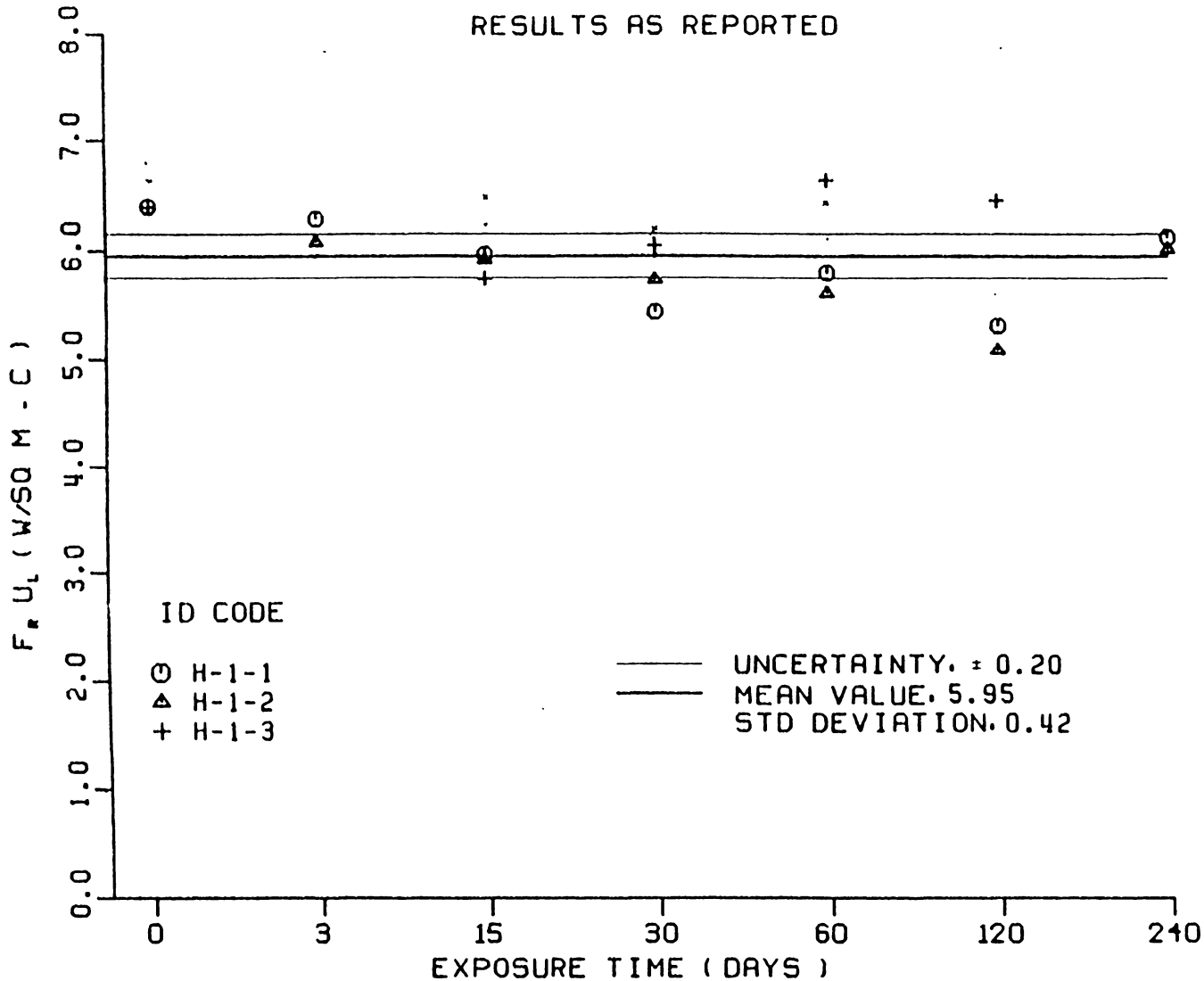

Figure B-10 $F_r U_L$ versus Exposure Time - Collector H, Test Site 1

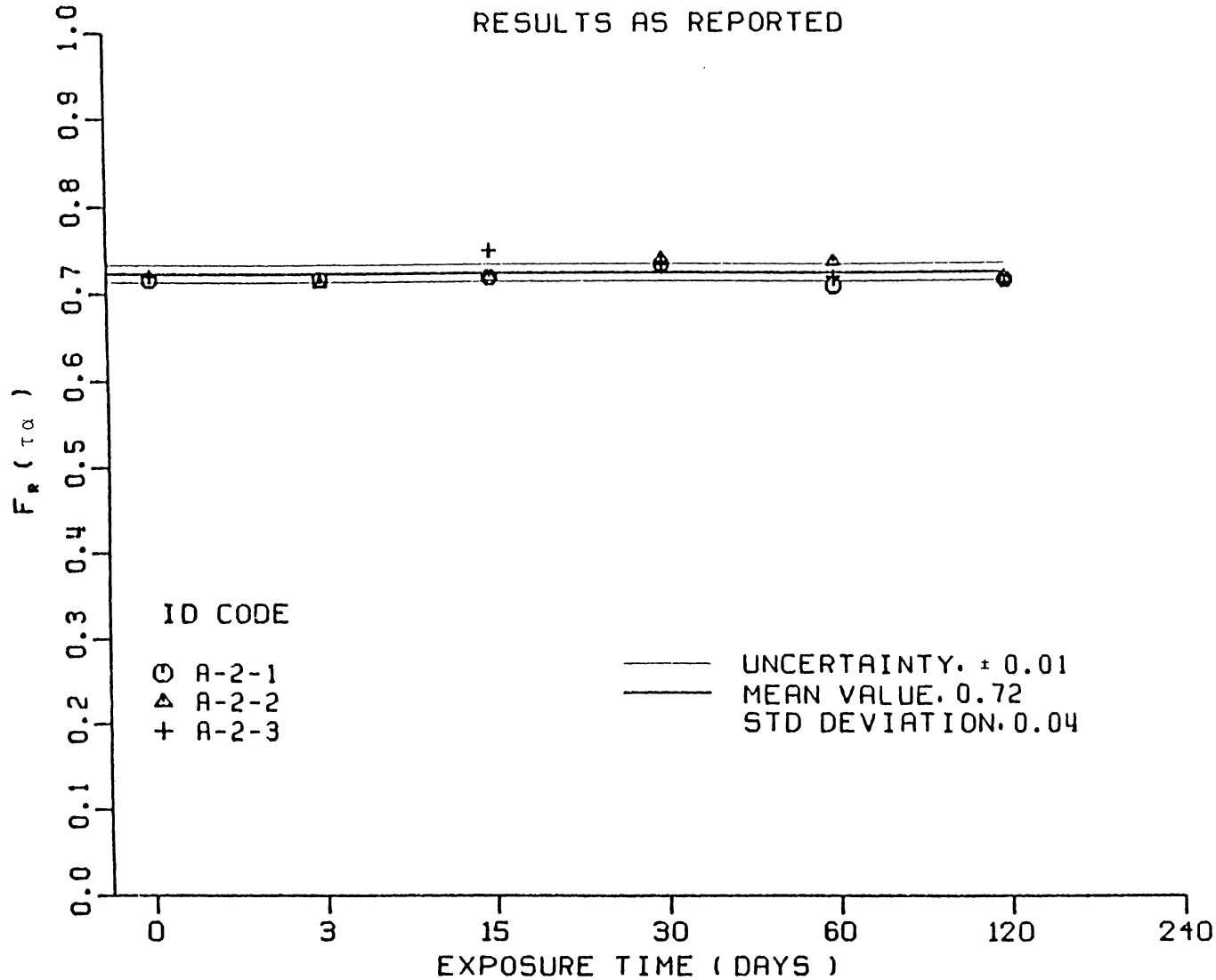

Figure B-11 $F_r(\tau\alpha)$ versus Exposure Time - Collector A, Test Site 2

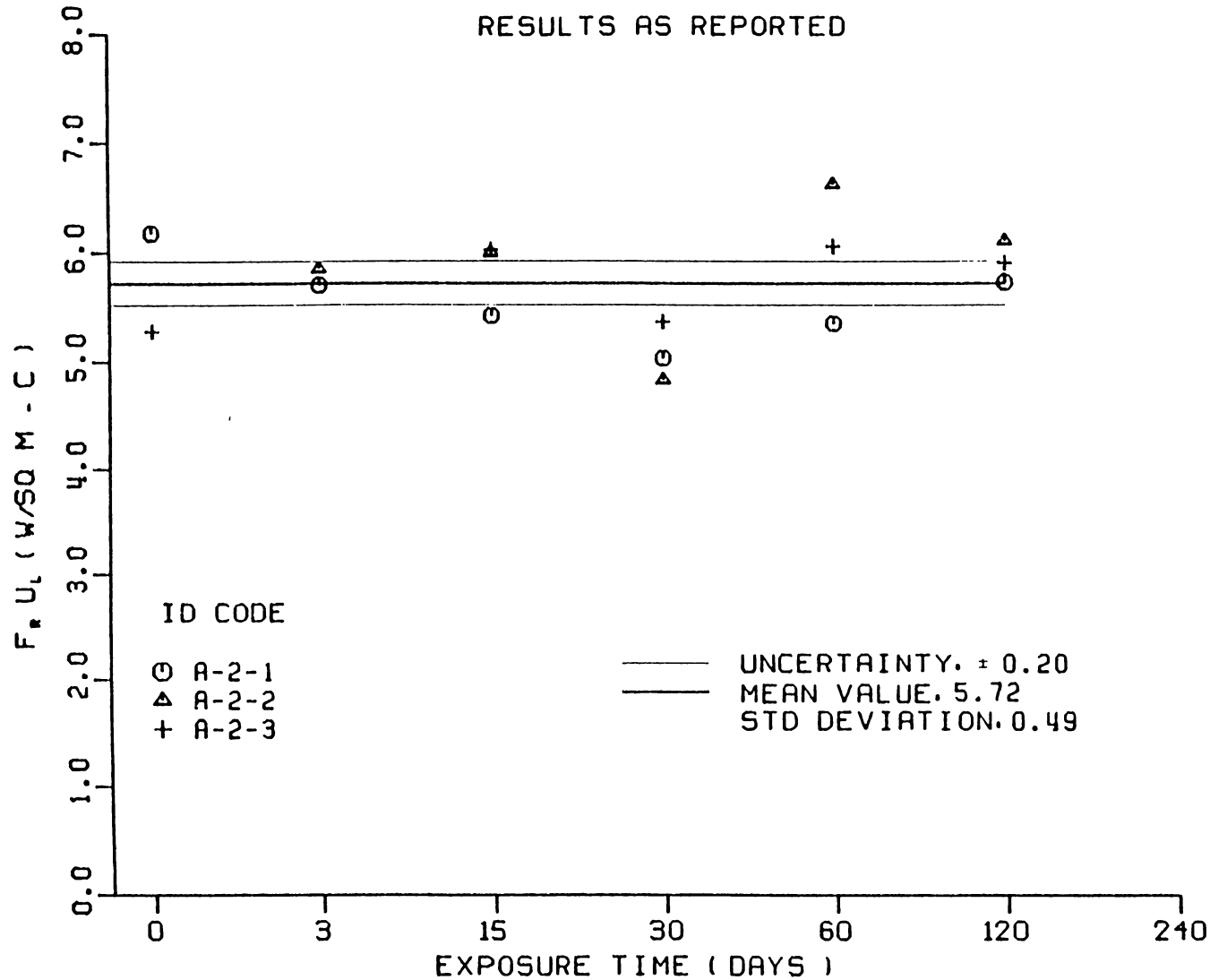

Figure B-12 $F_r U_L$ versus Exposure Time - Collector A, Test Site 2

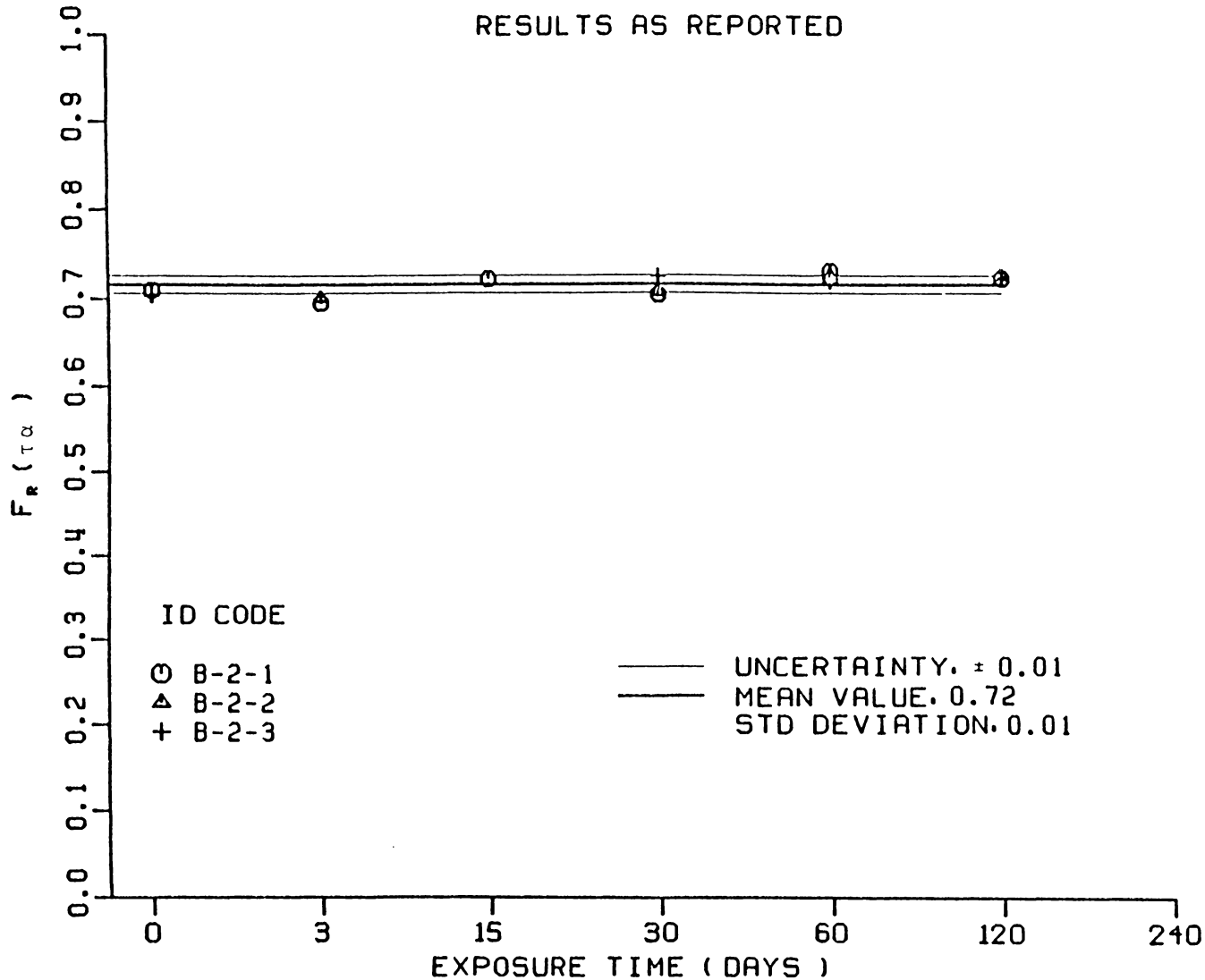

Figure B-13 $F_r(\tau\alpha)$ versus Exposure Time - Collector B, Test Site 2

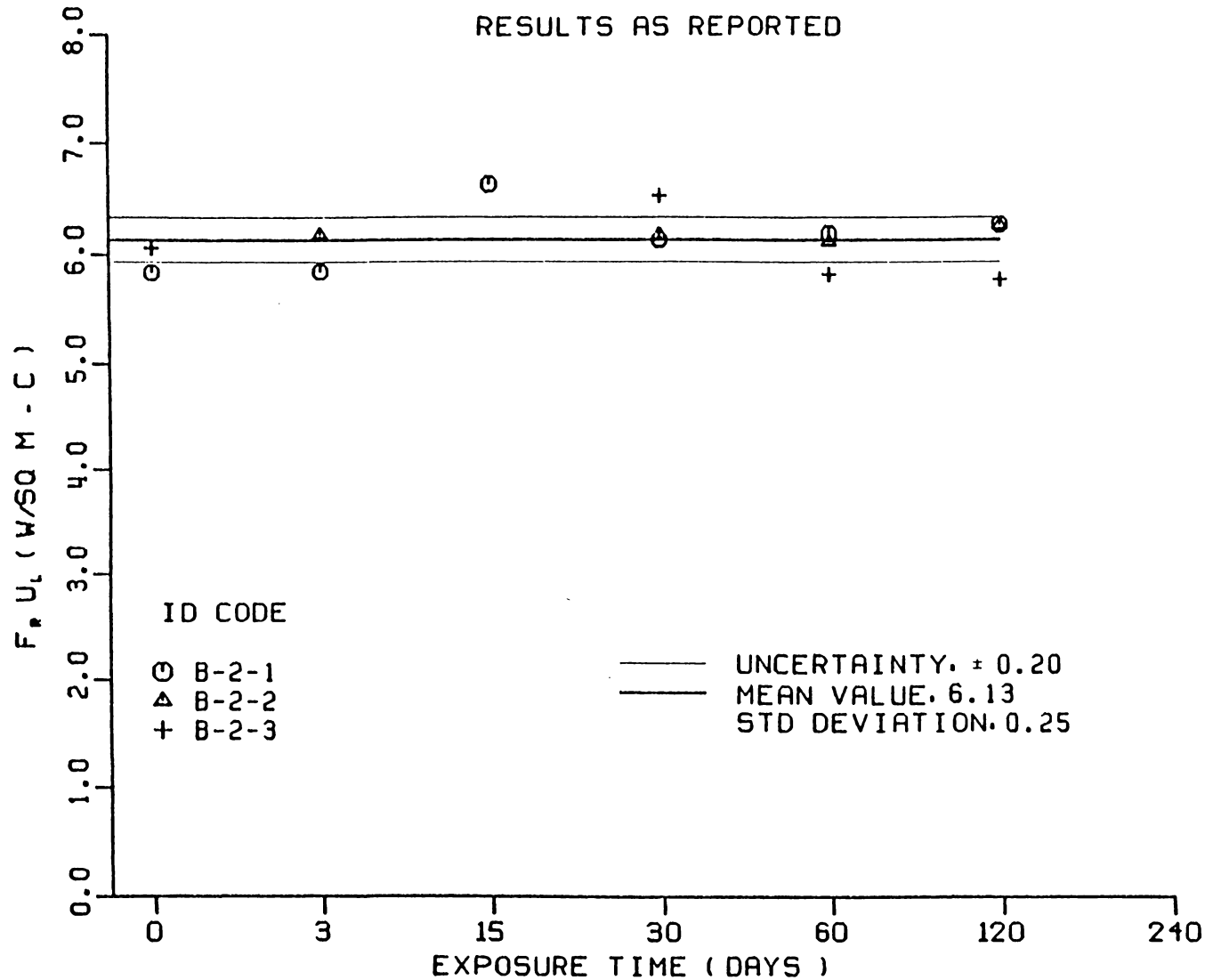

Figure B-14 $F_r U_L$ versus Exposure Time - Collector B, Test Site 2

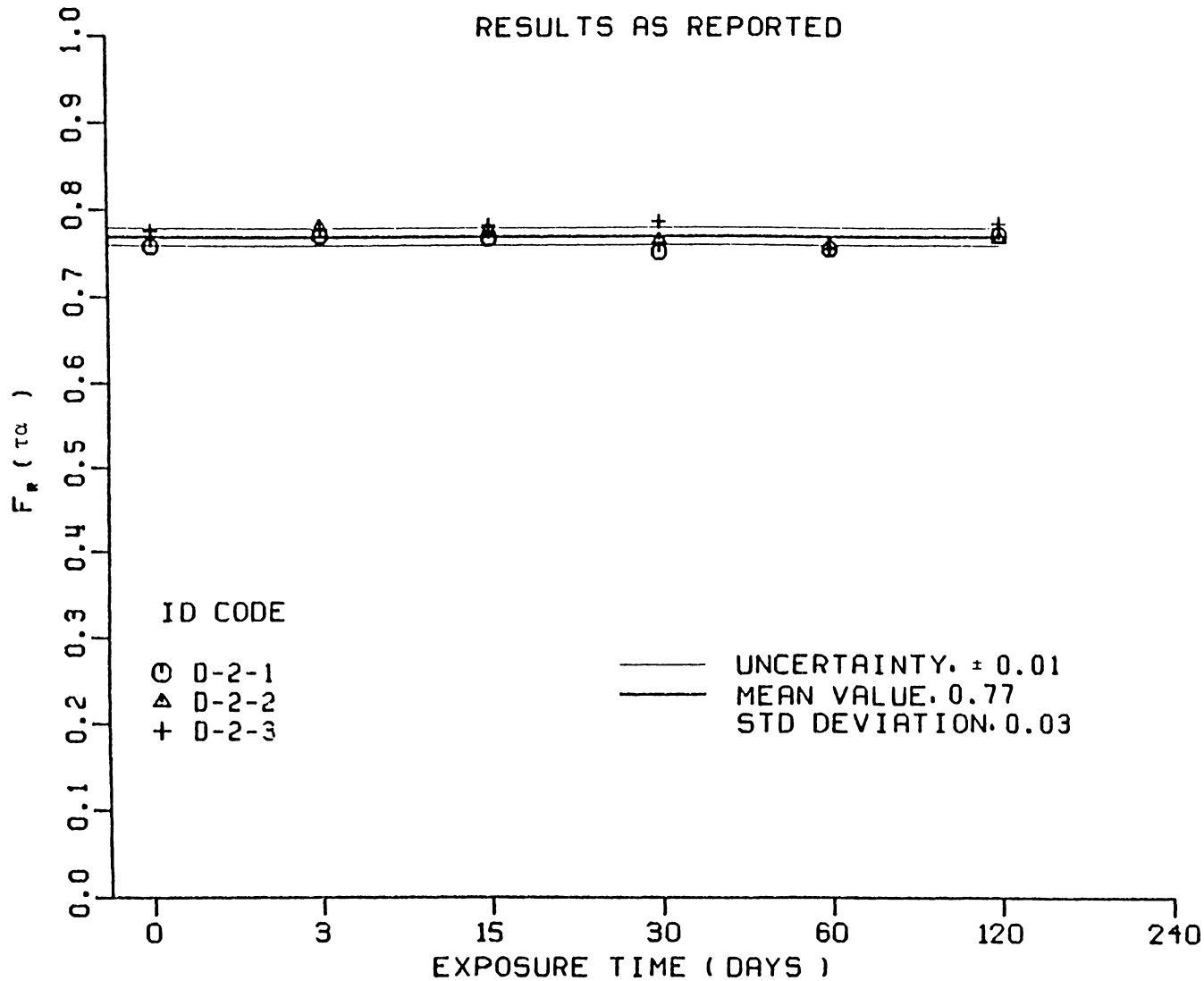

Figure B-15 $F_r(\tau\alpha)$ versus Exposure Time - Collector D, Test Site 2

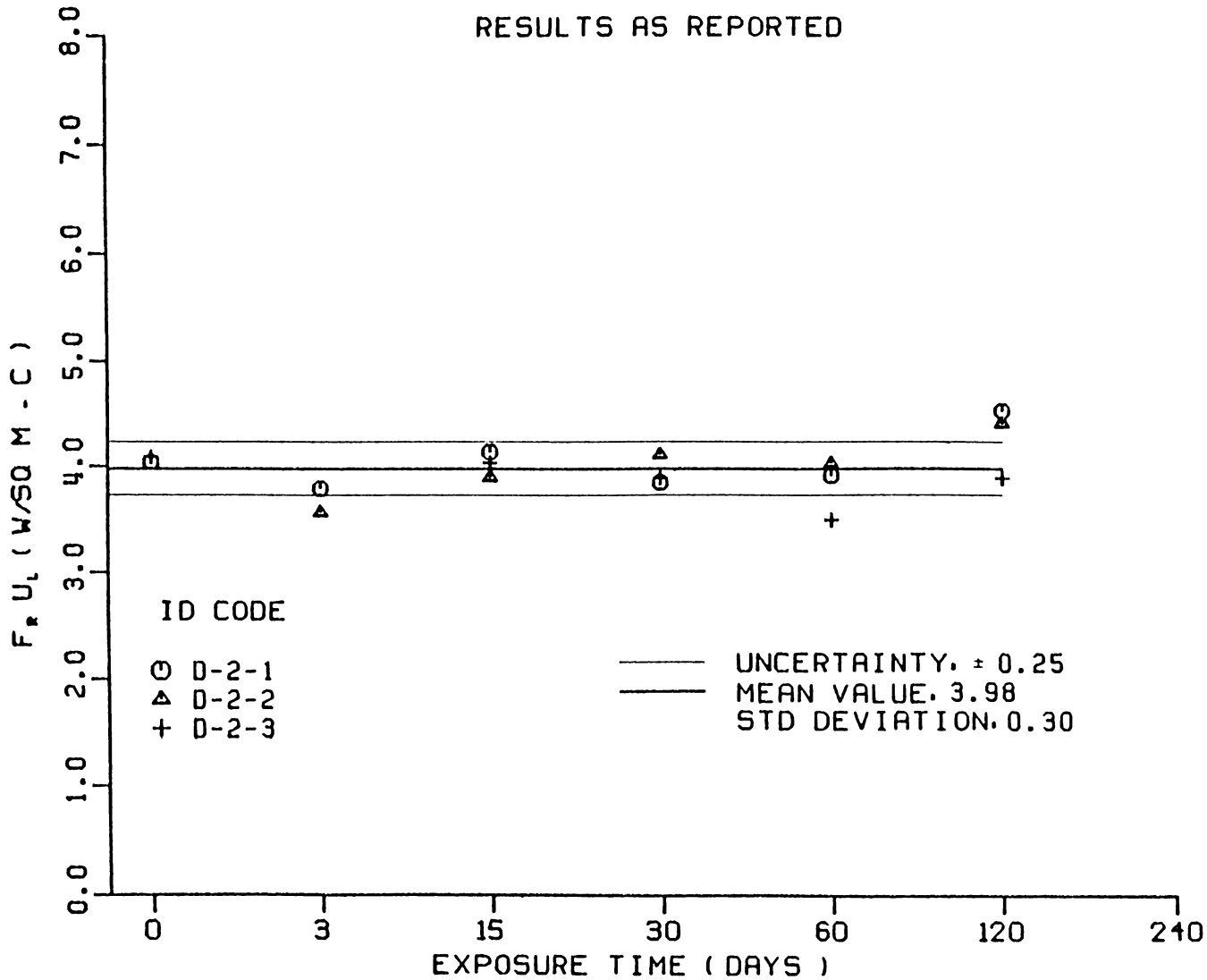

Figure B-16 $F_r U_L$ versus Exposure Time - Collector D, Test Site 2

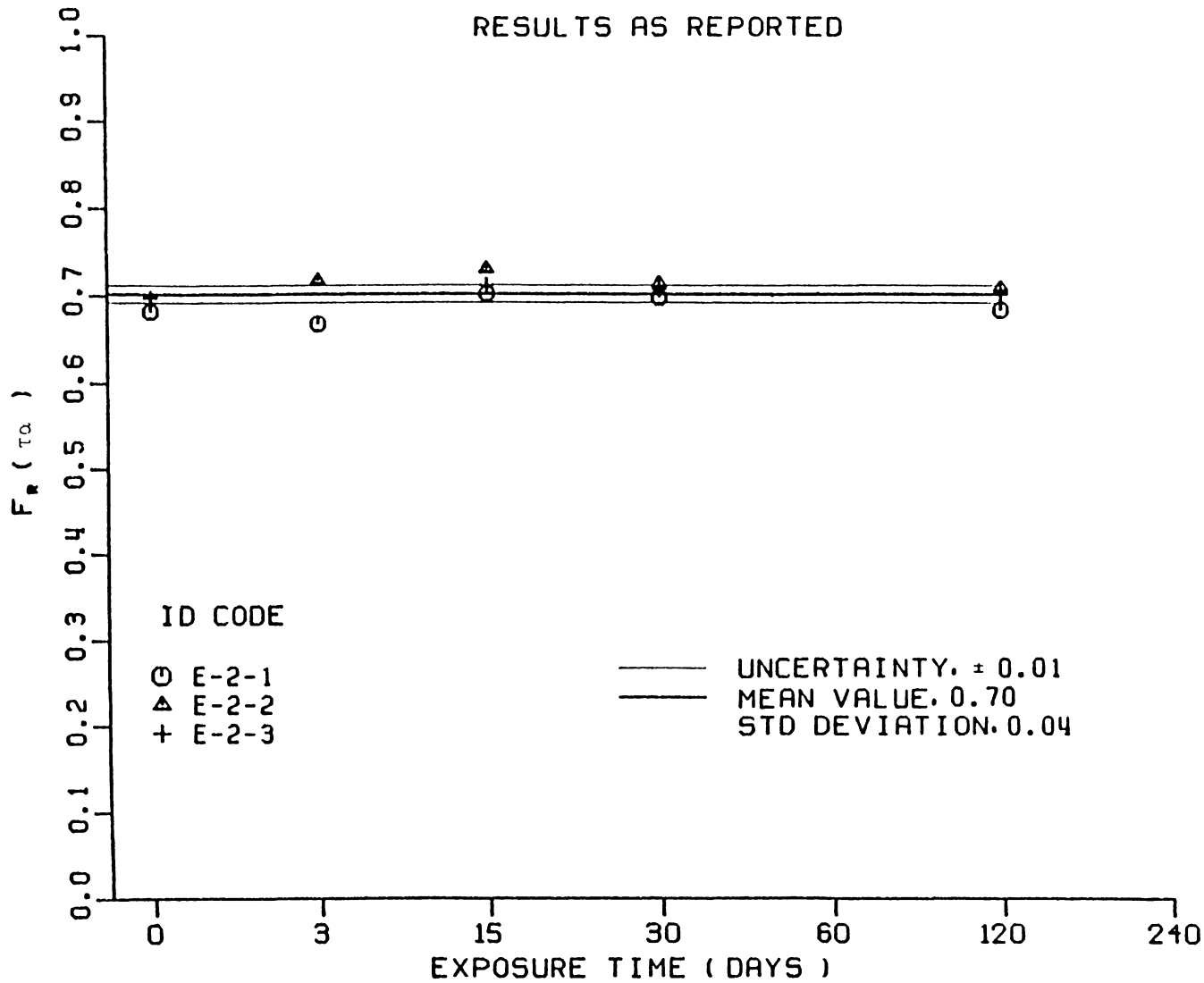

Figure B-17 $F_r(\tau\alpha)$ versus Exposure Time - Collector E, Test Site 2

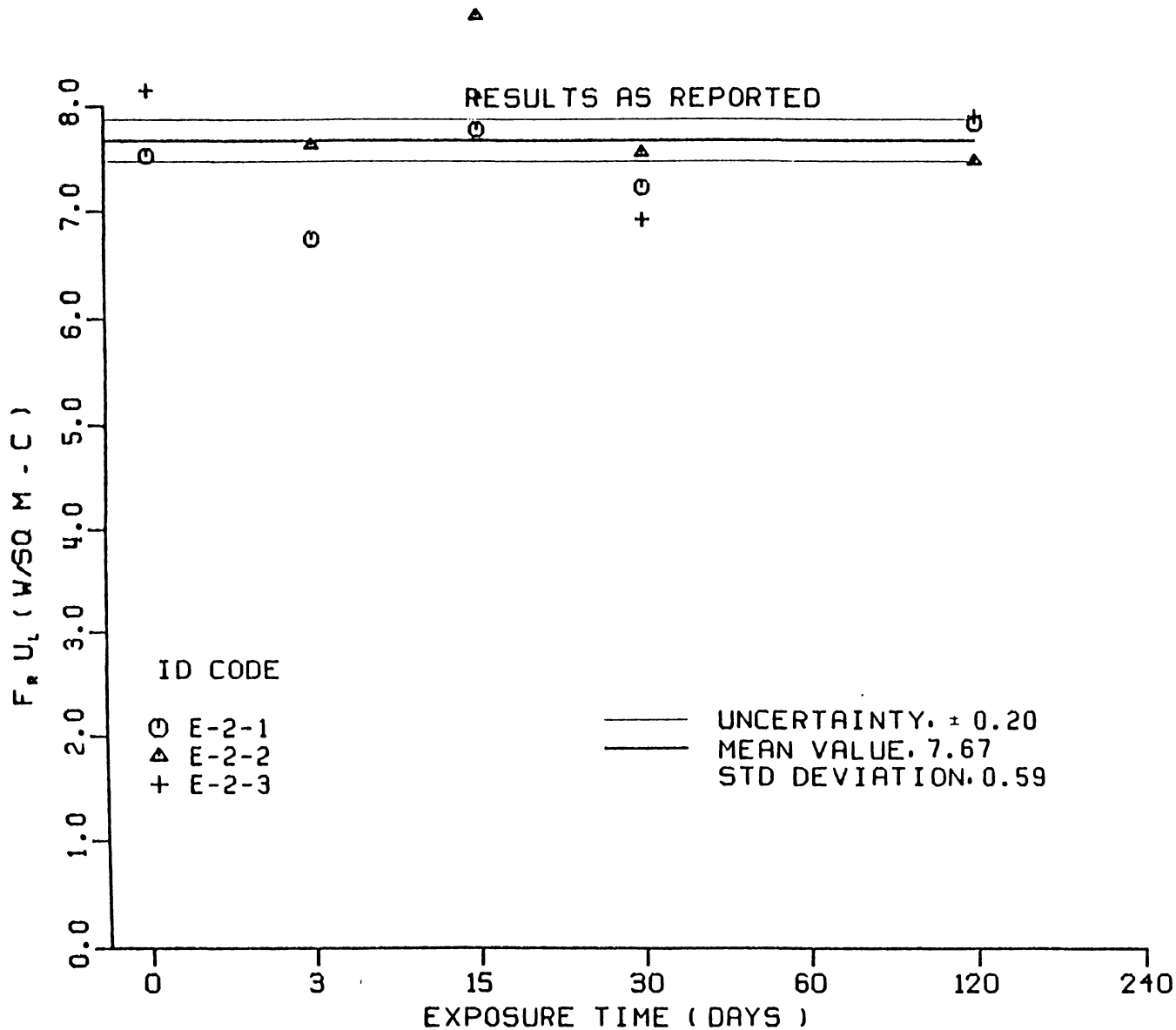

Figure B-18 $F_r U_L$ versus Exposure Time - Collector E, Test Site 2

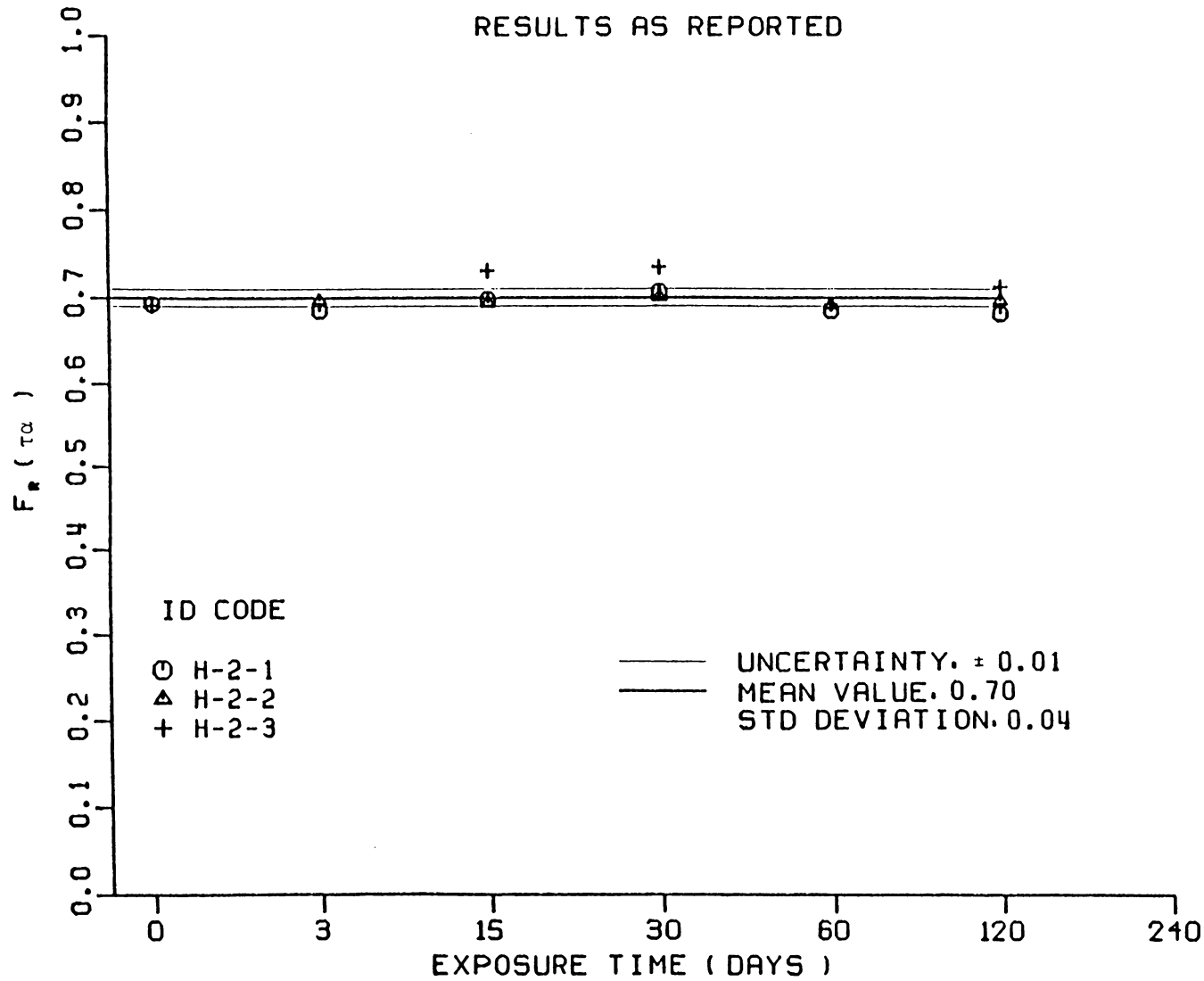

Figure B-19 $F_r(\tau\alpha)$ versus Exposure Time - Collector H, Test Site 2

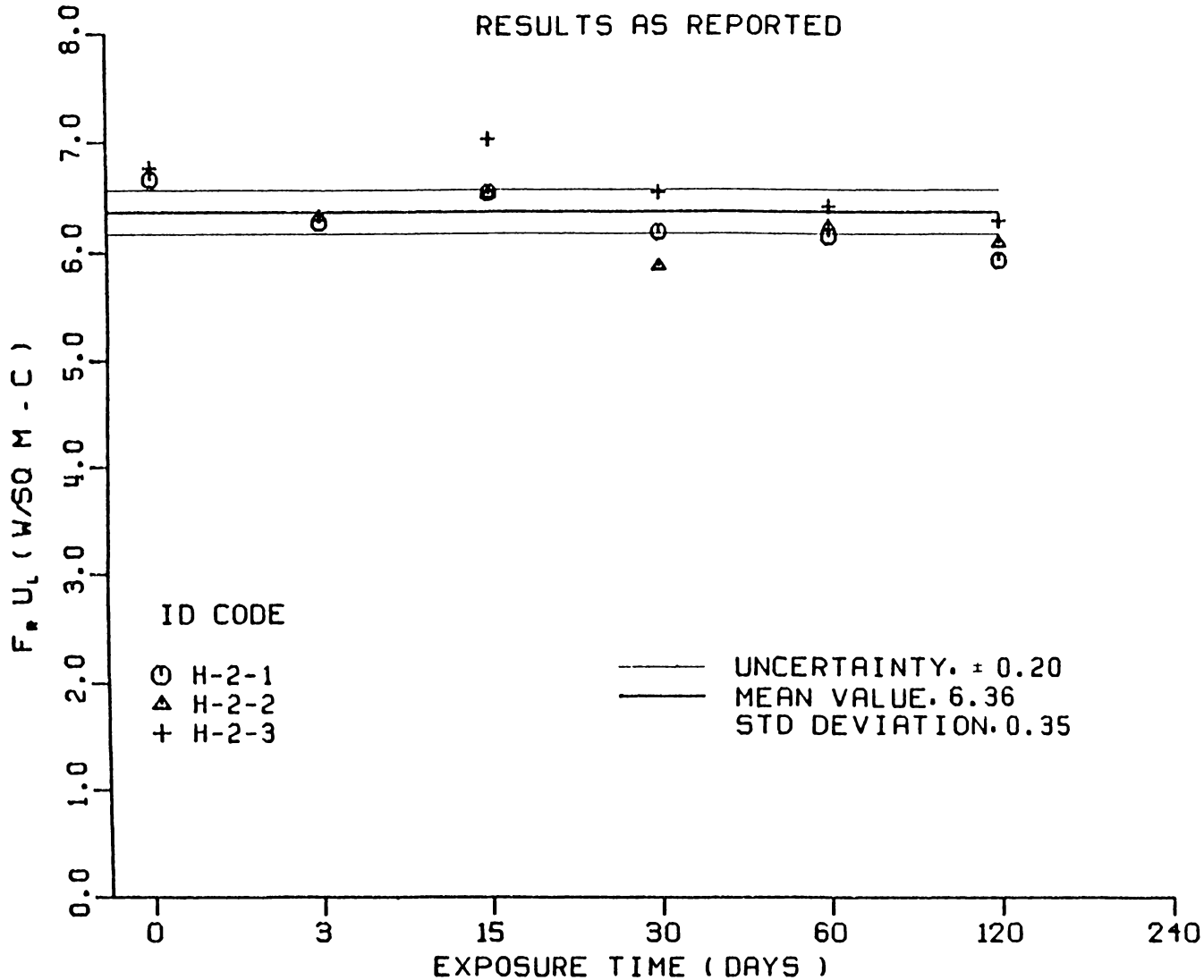

Figure B-20 $F_r U_L$ versus Exposure Time - Collector H, Test Site 2

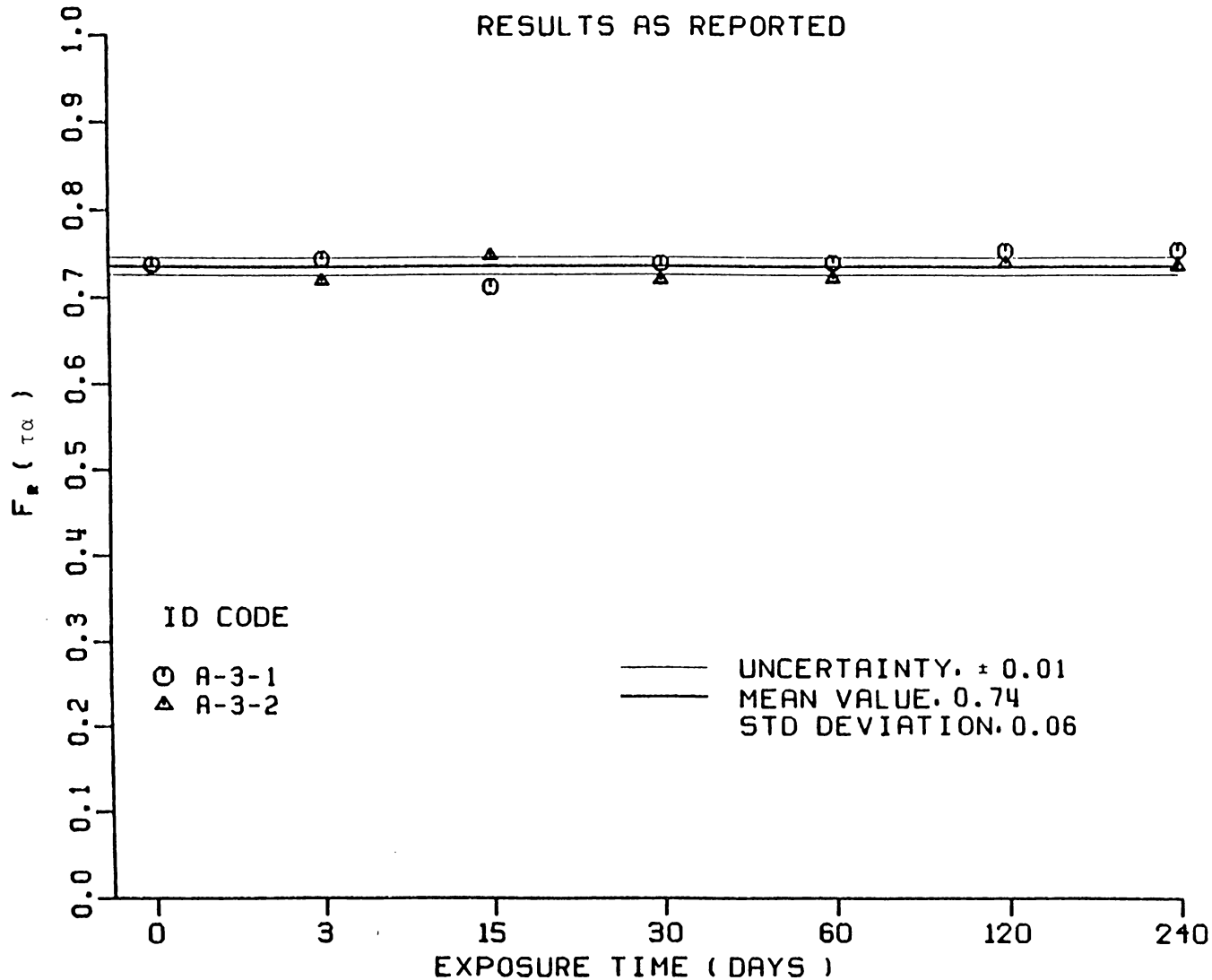

Figure B-21 $F_r(\tau\alpha)$ versus Exposure Time - Collector A, Test Site 3

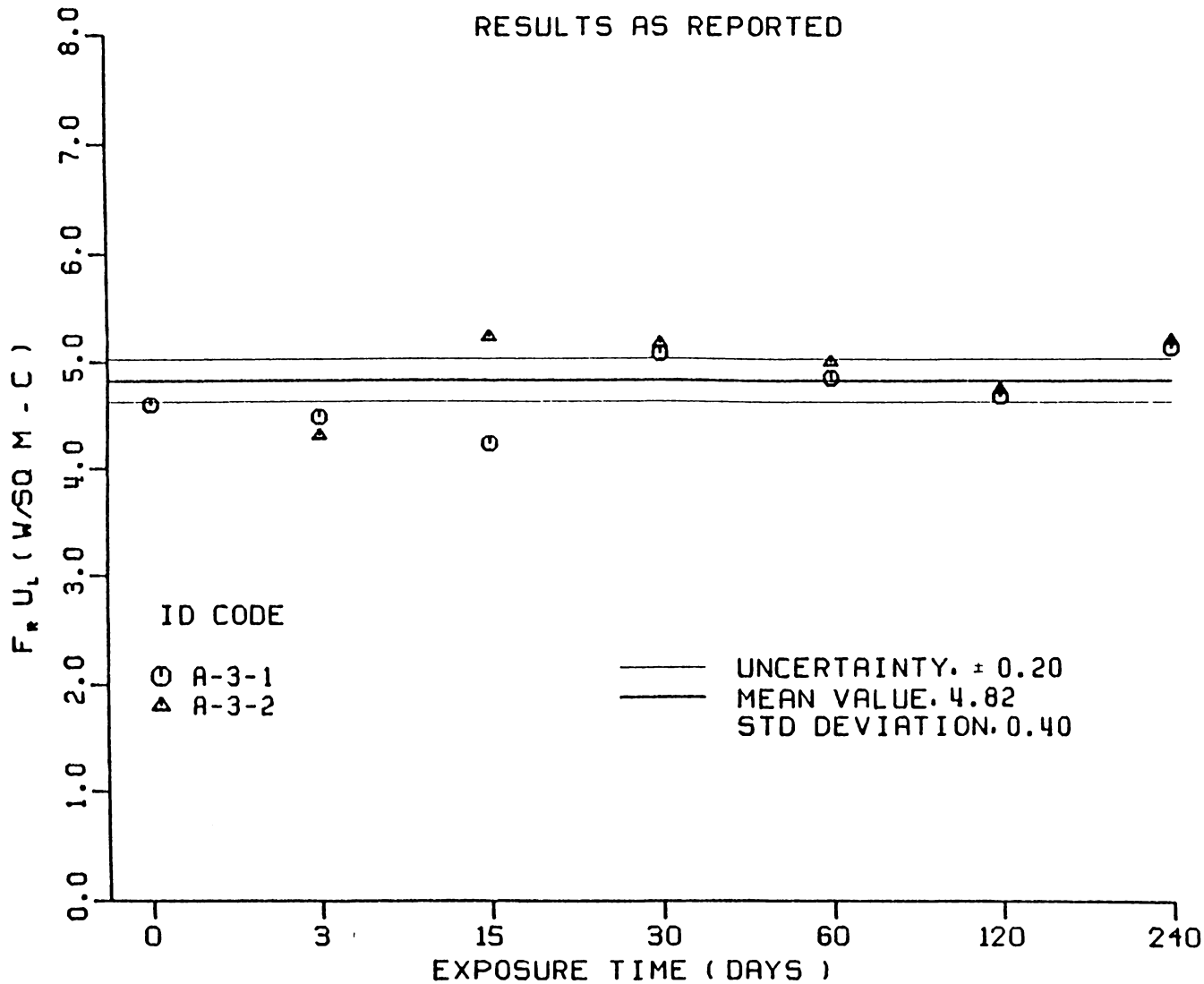

Figure B-22 $F_r U_L$ versus Exposure Time - Collector A, Test Site 3

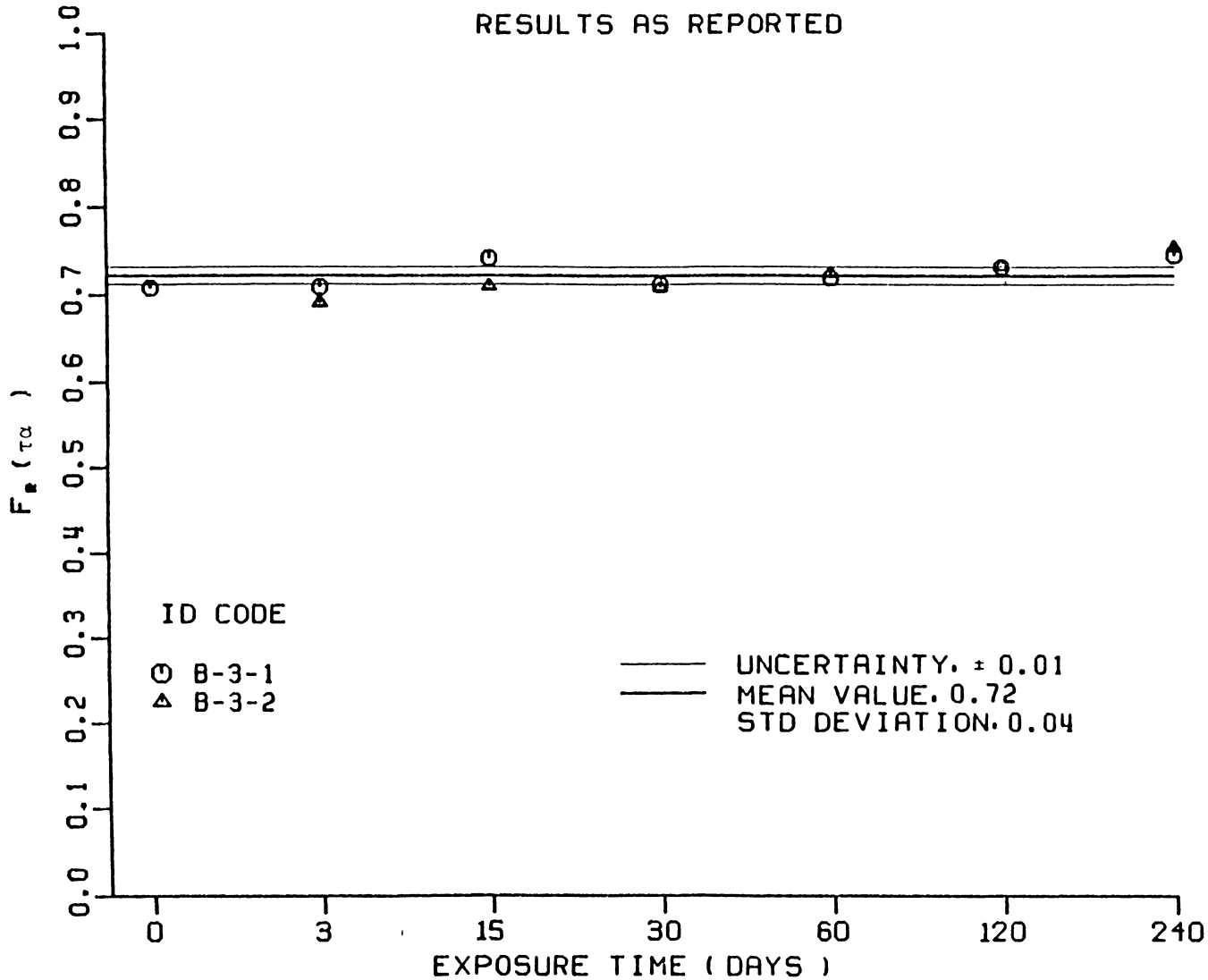

Figure B-23 $F_r(\tau\alpha)$ versus Exposure Time - Collector B, Test Site 3

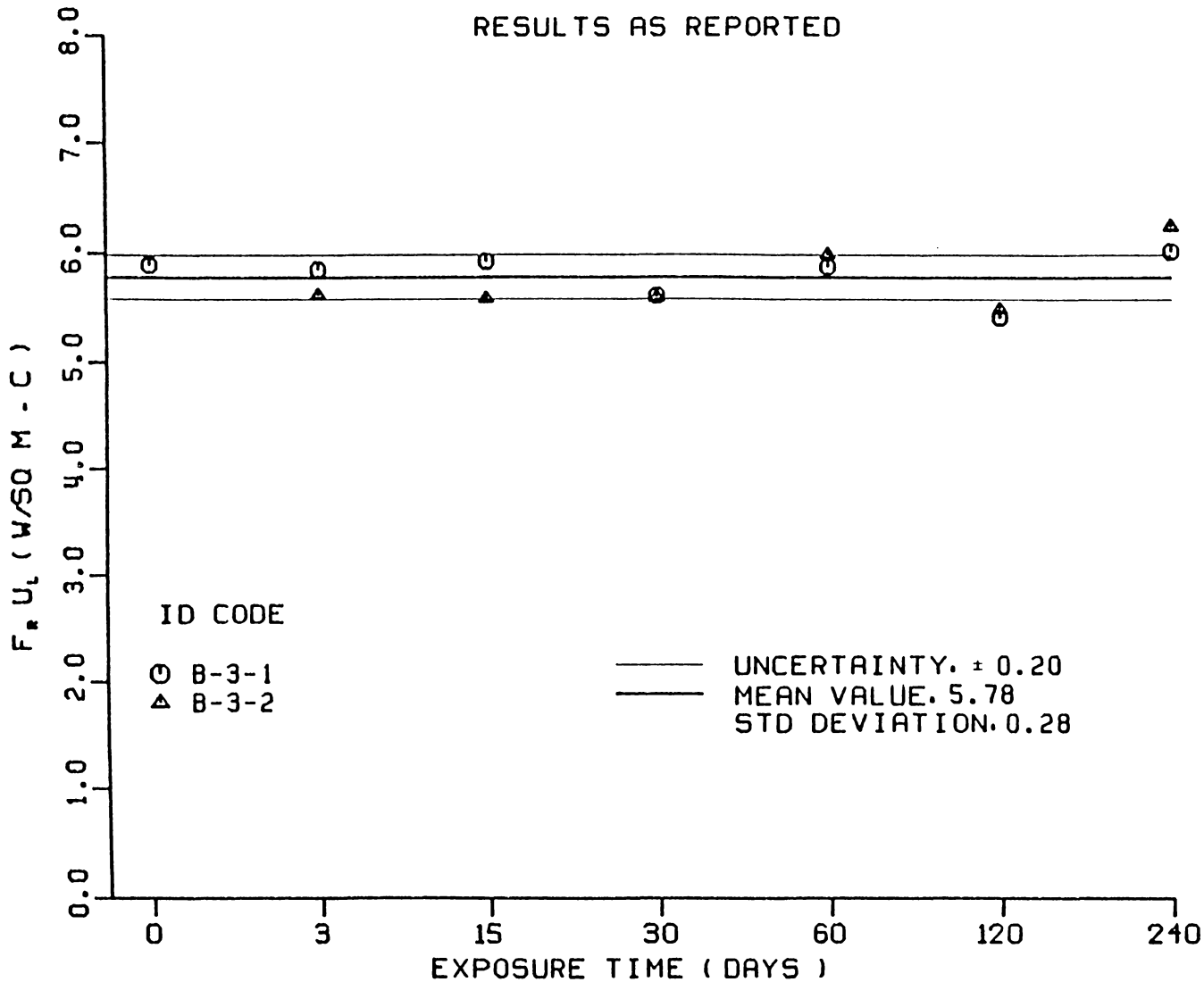

Figure B-24 $F_r U_L$ versus Exposure Time - Collector B, Test Site 3

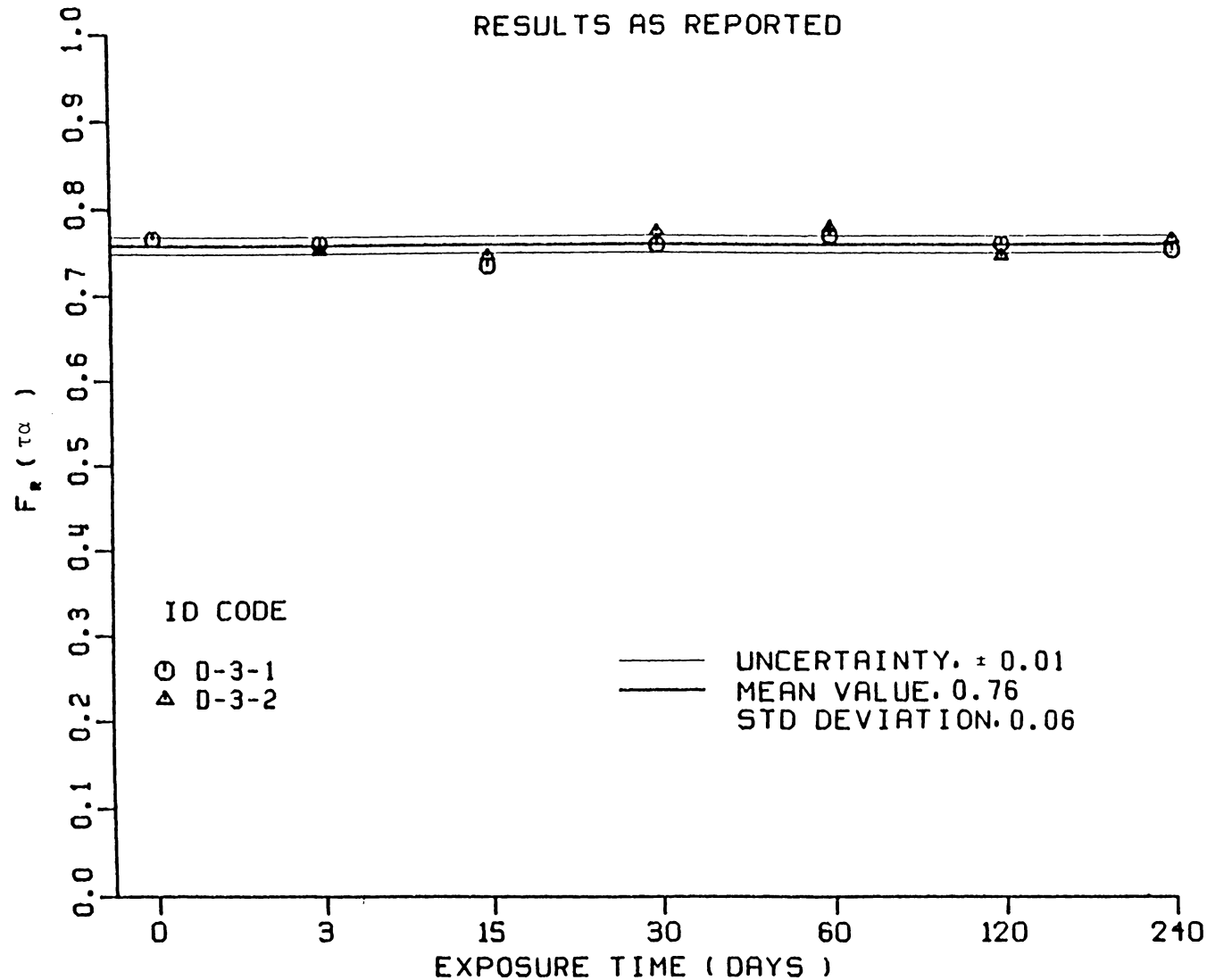

Figure B-25 $F_r(\tau\alpha)$ versus Exposure Time - Collector D, Test Site3

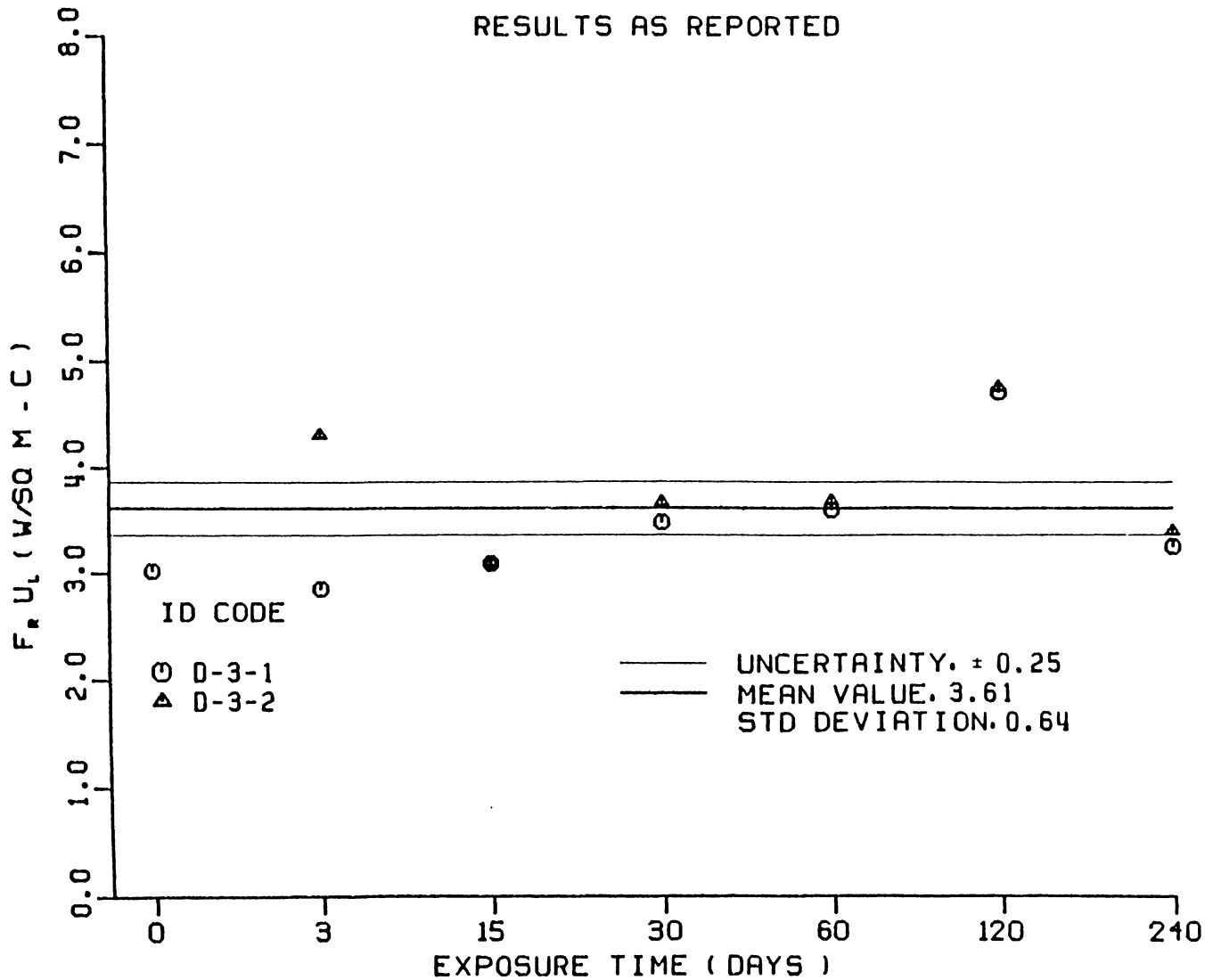

Figure B-26 $F_r U_L$ versus Exposure Time - Collector D, Test Site 3

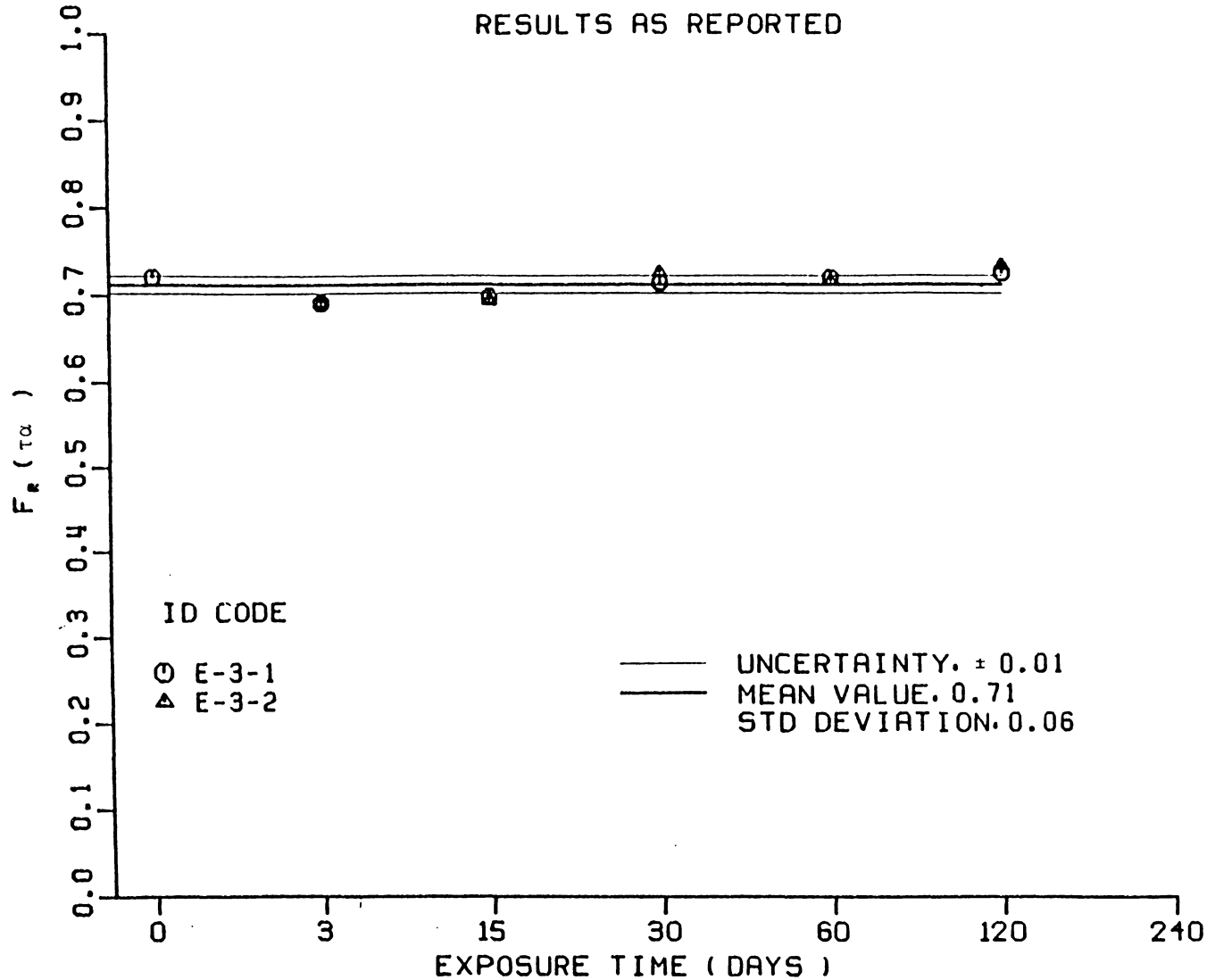

Figure B-27 $F_r(\tau\alpha)$ versus Exposure Time - Collector E, Test Site 3

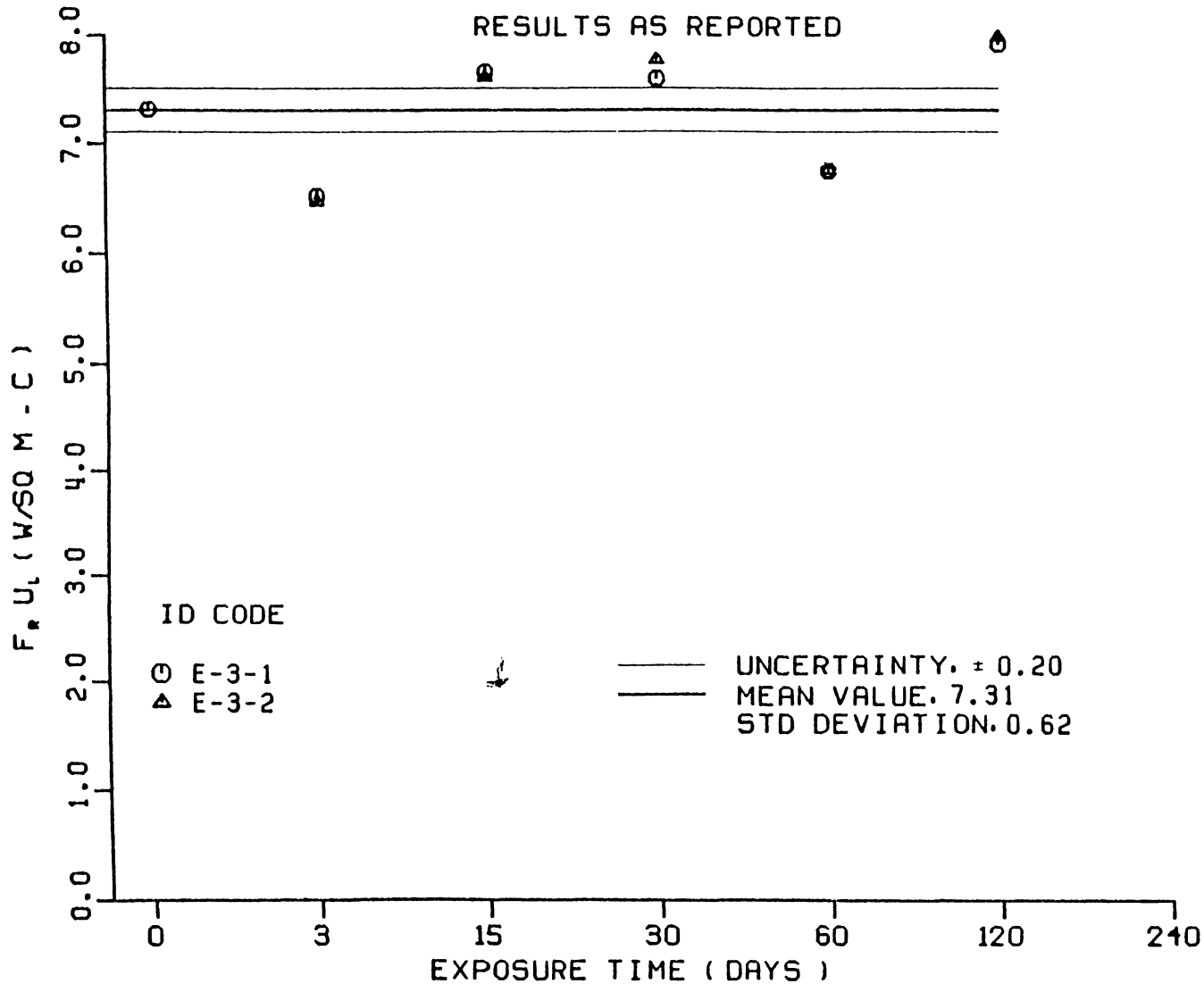

Figure B-28 $F_r U_L$ versus Exposure Time - Collector E, Test Site 3

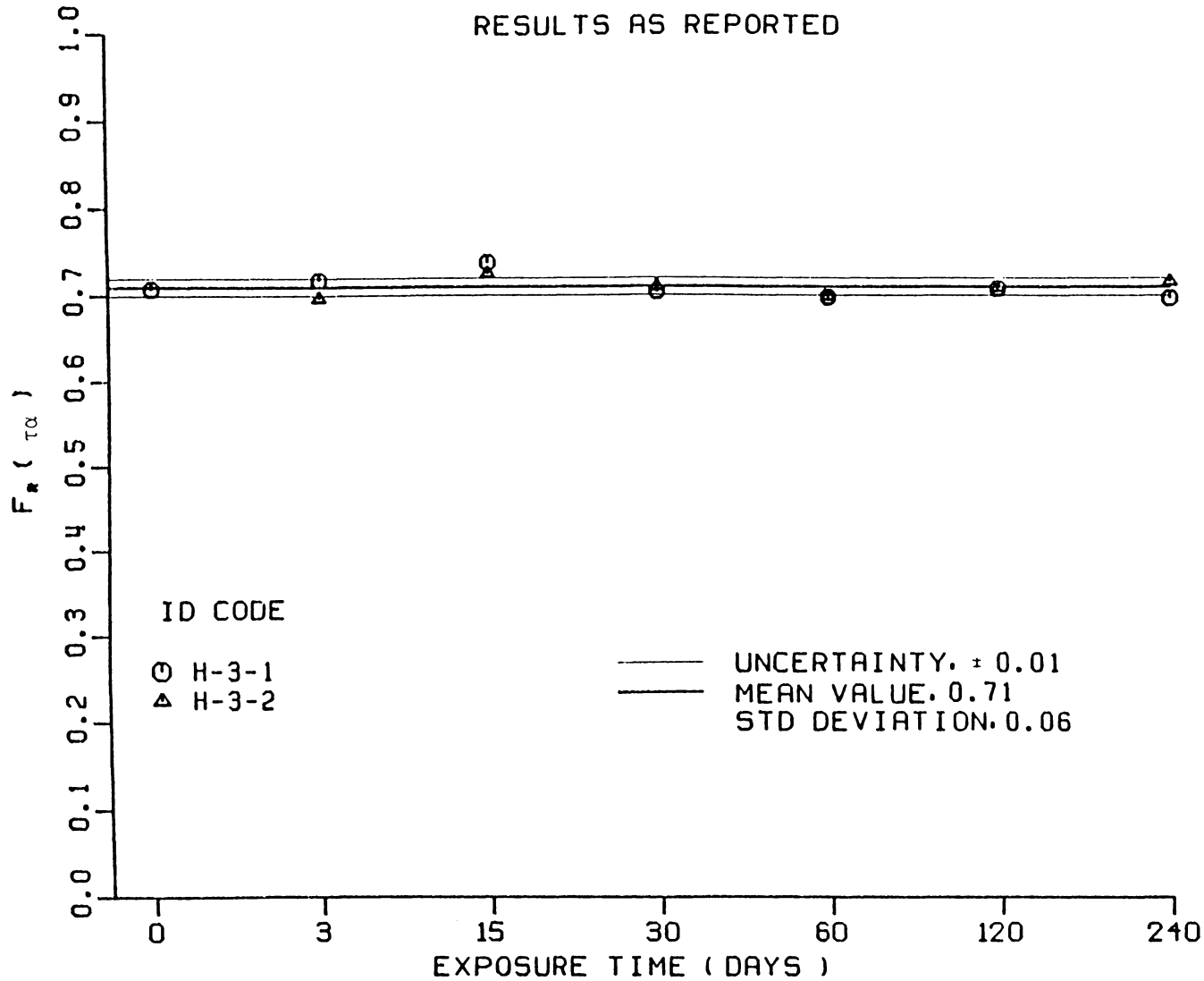

Figure B-29 $F_r(\tau\alpha)$ versus Exposure Time - Collector H, Test Site 3

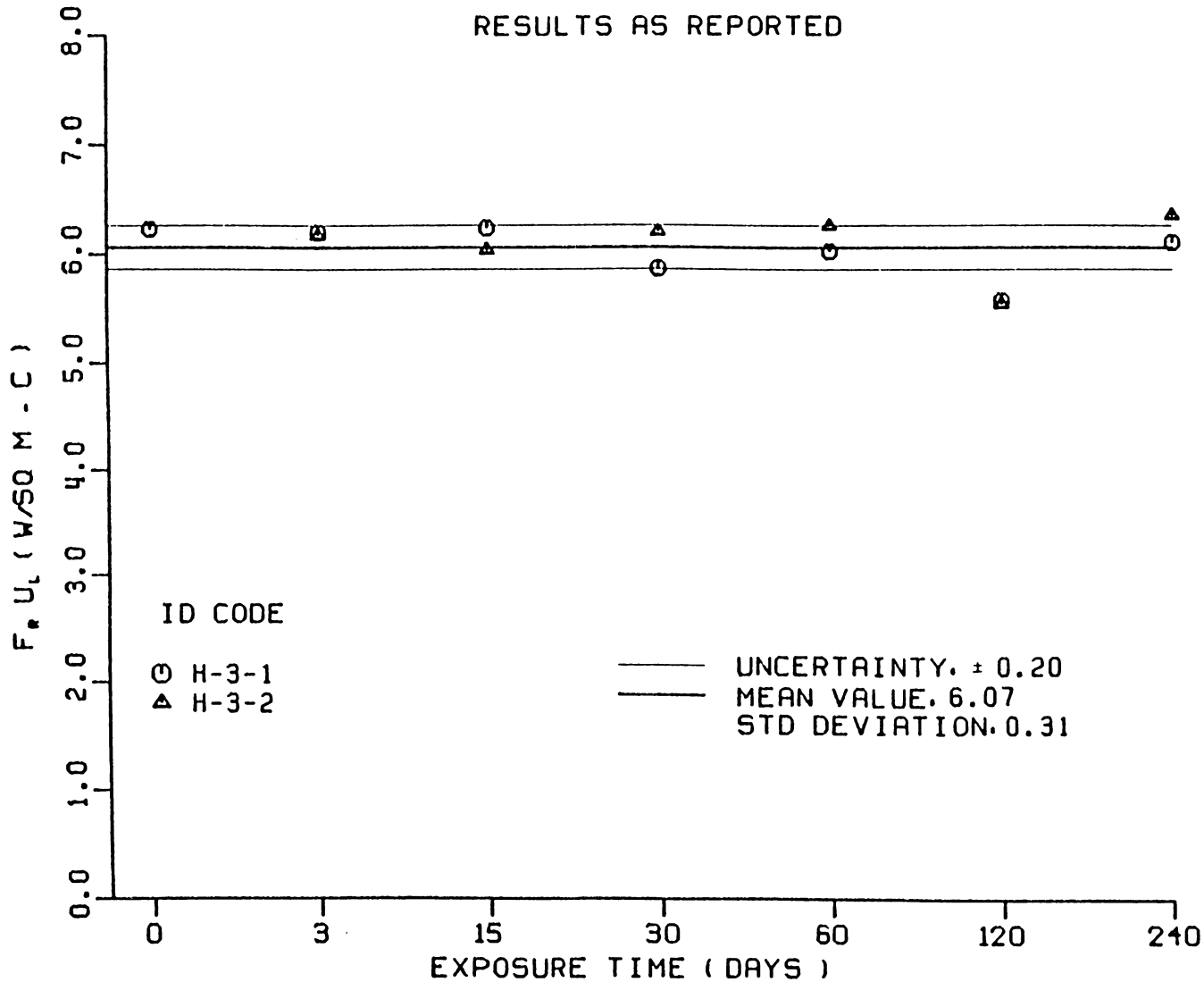

Figure B-30 $F_r U_L$ versus Exposure Time - Collector H, Test Site 3

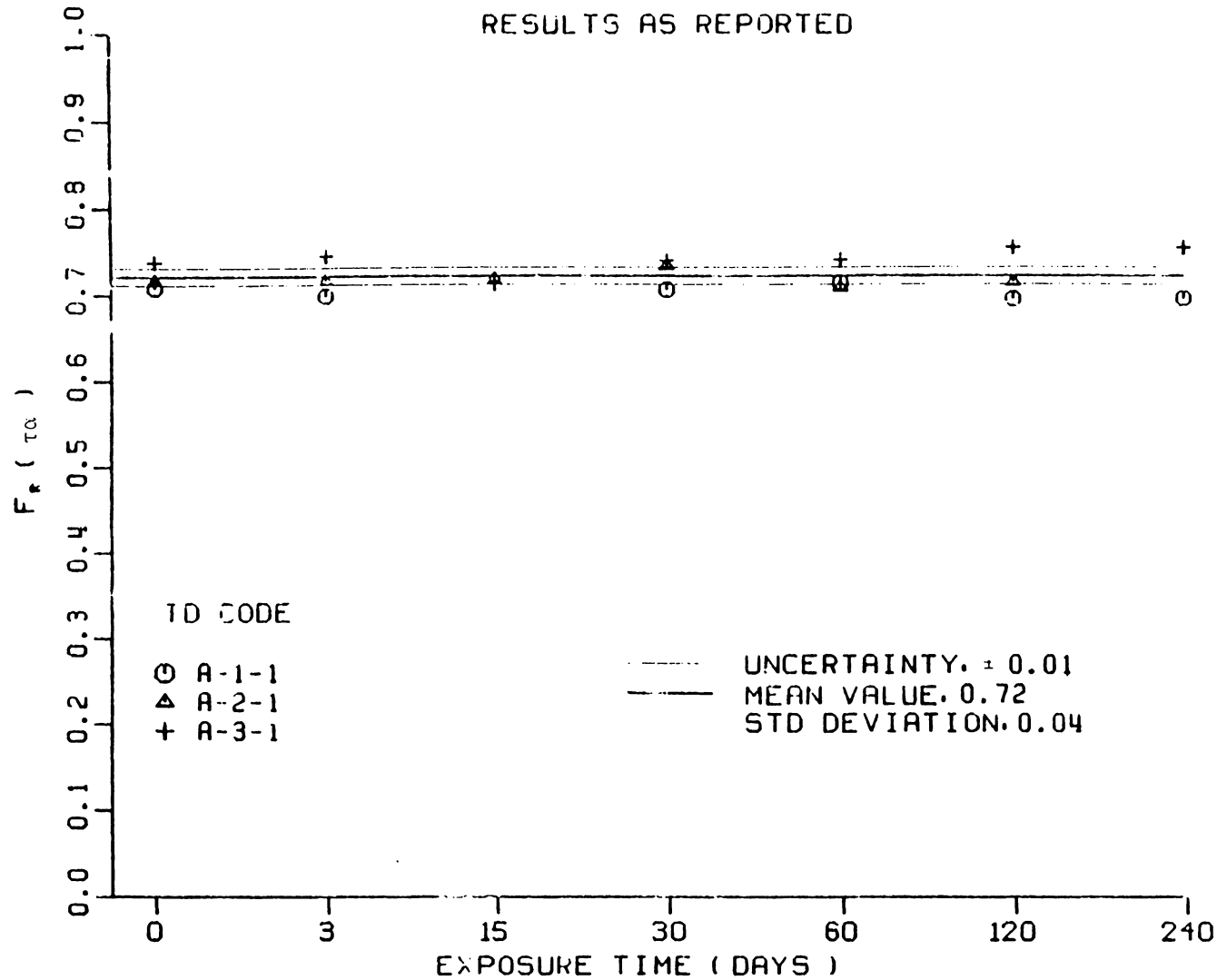

Figure B-31 $F_r(\tau\alpha)$ versus Exposure Time - Collector A, Test Series 1

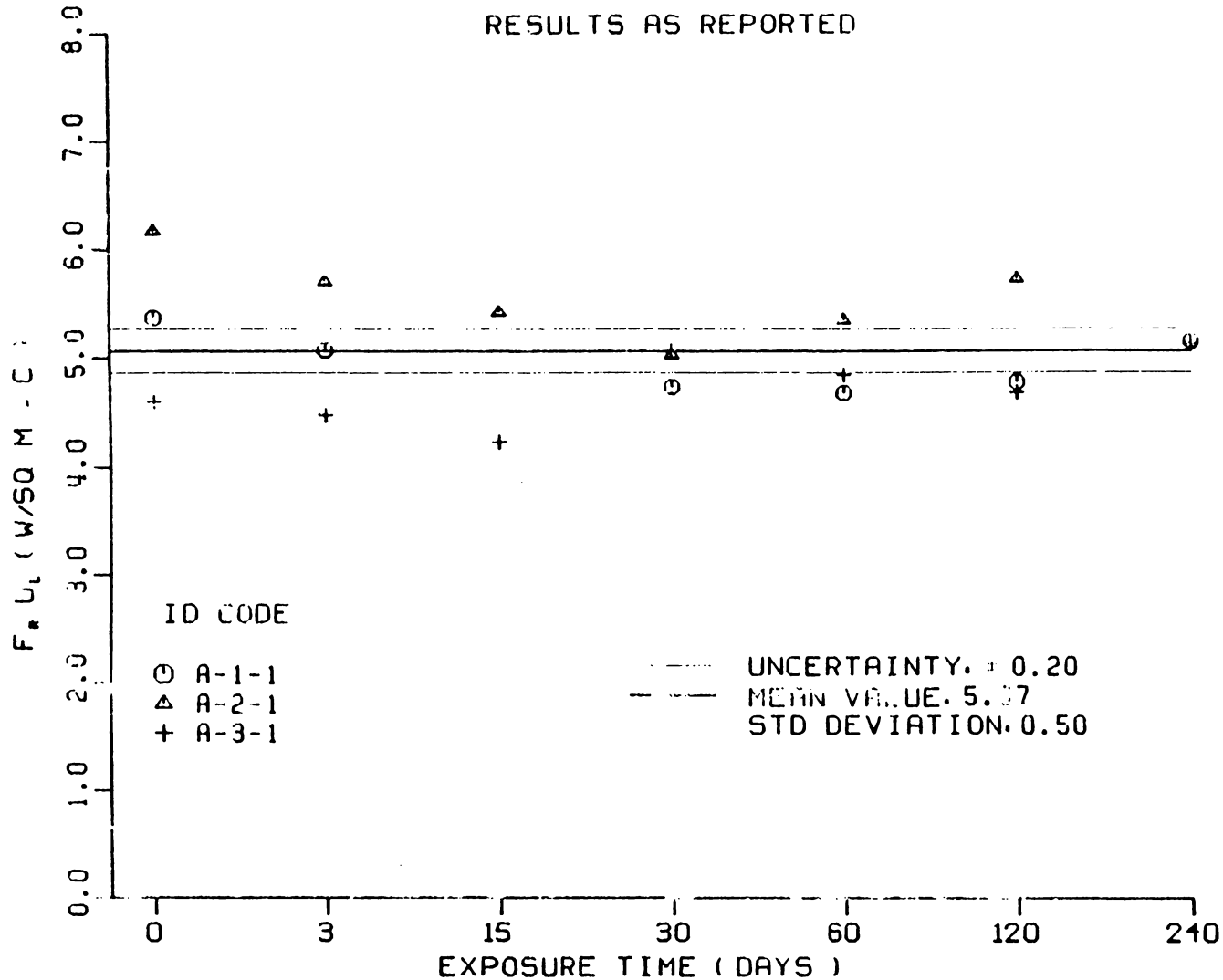

Figure B-32 $F_r U_L$ versus Exposure Time - Collector A, Test Series 1

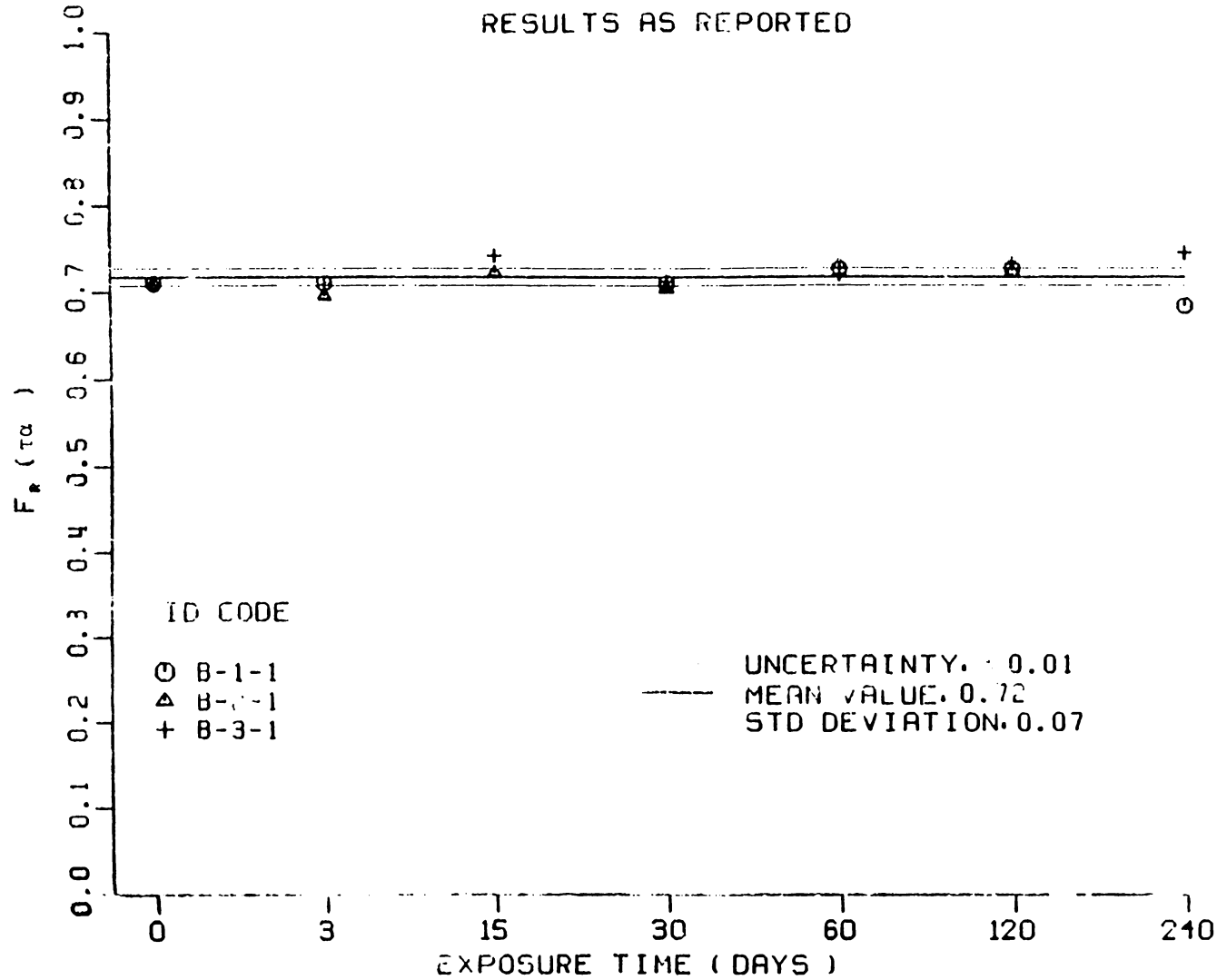

Figure B-33 $F_r(\tau\alpha)$ versus Exposure Time - Collector B, Test Series 1

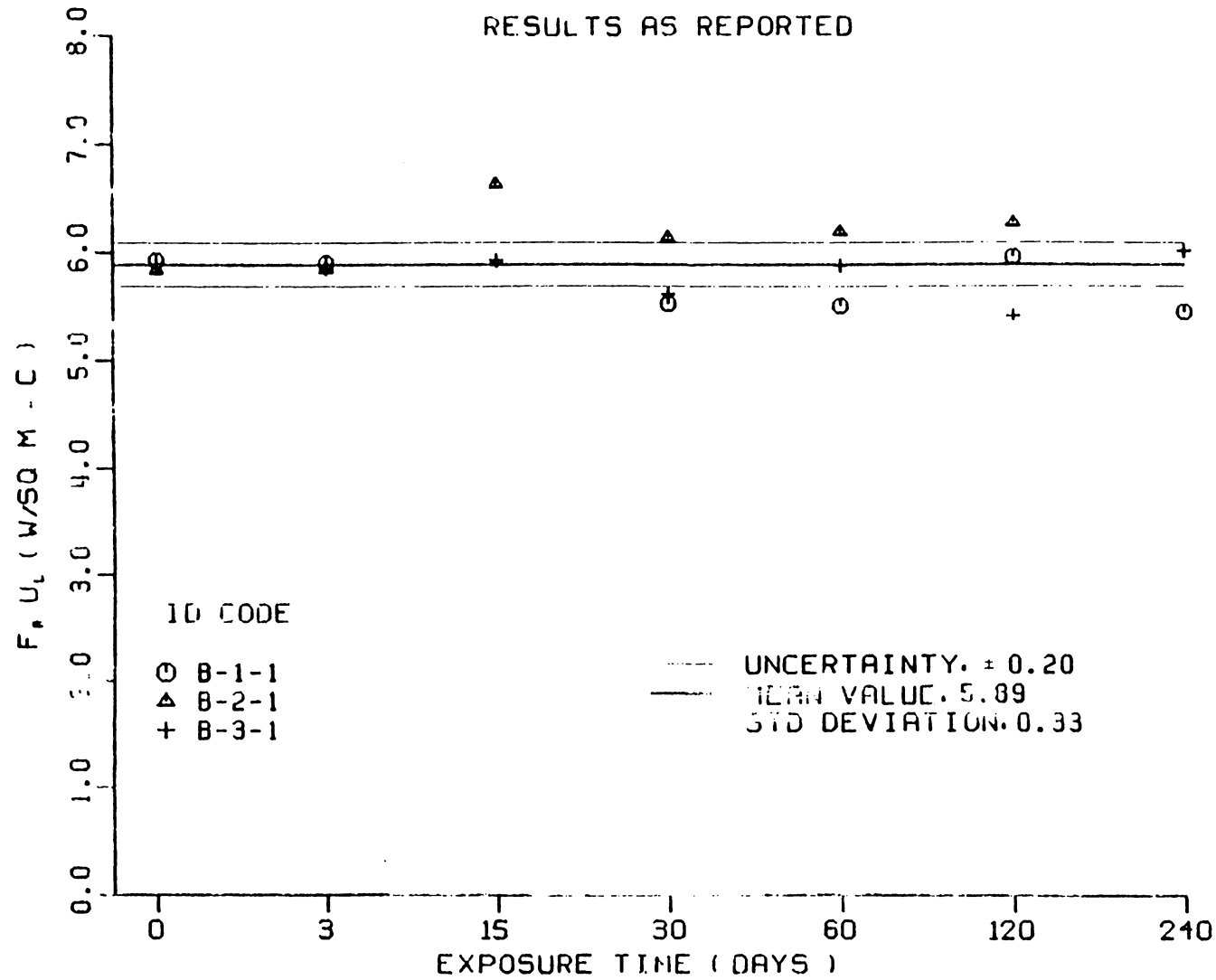

Figure B-34 $F_r U_L$ versus Exposure Time - Collector B, Test Series 1

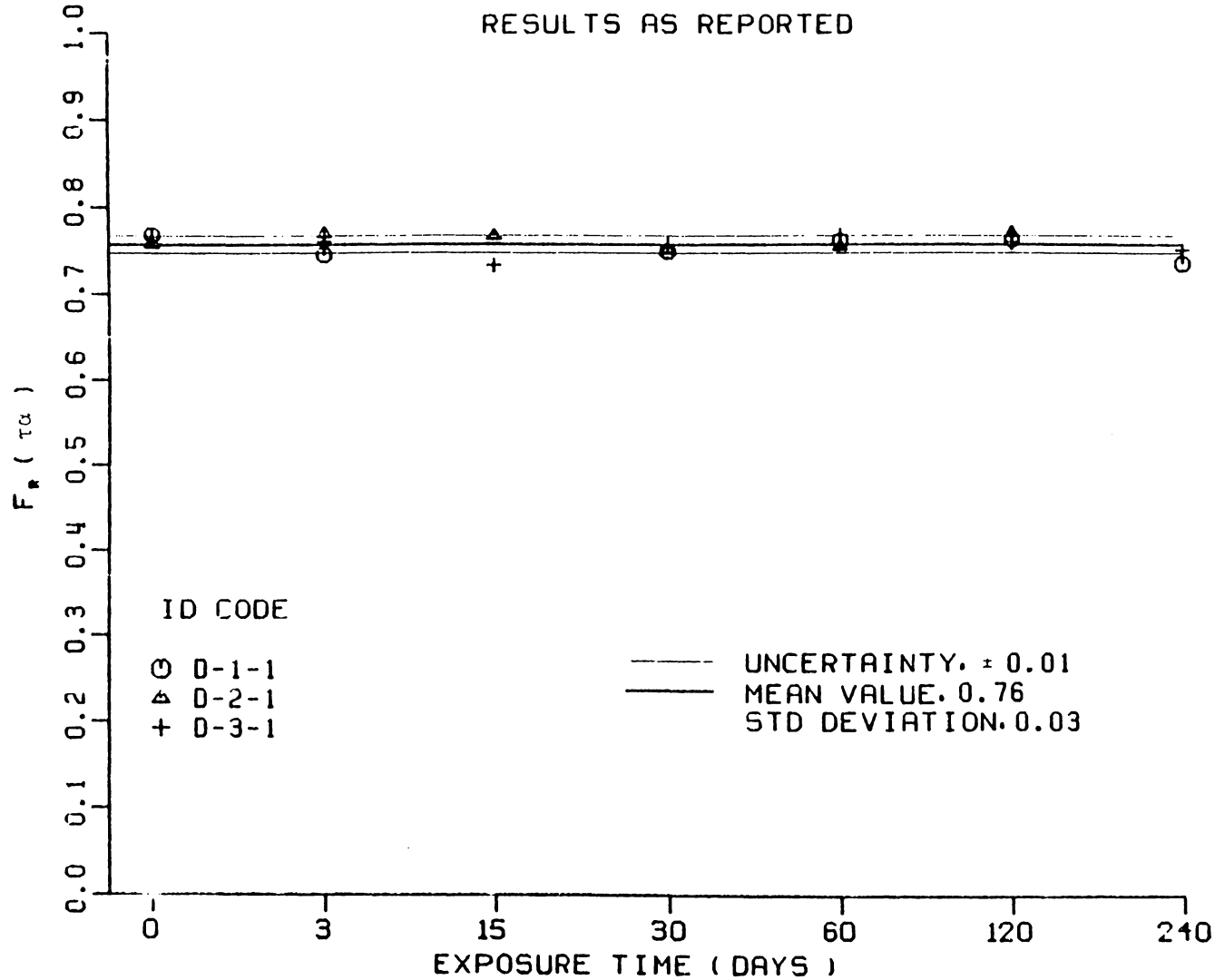

Figure B-35 $F_r(\tau\alpha)$ versus Exposure Time - Collector D, Test Series 1

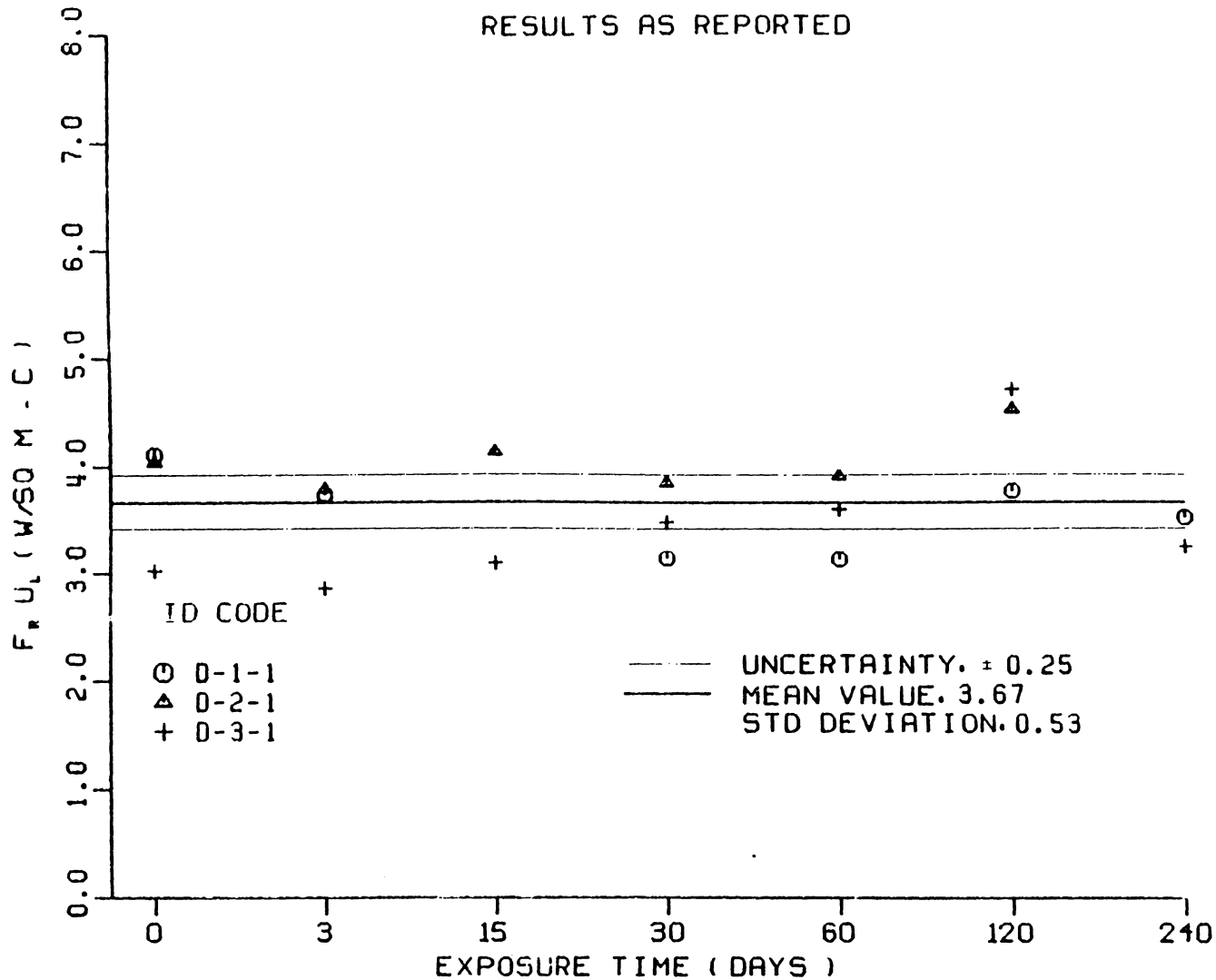

Figure B-36 $F_r U_L$ versus Exposure Time - Collector D, Test Series 1

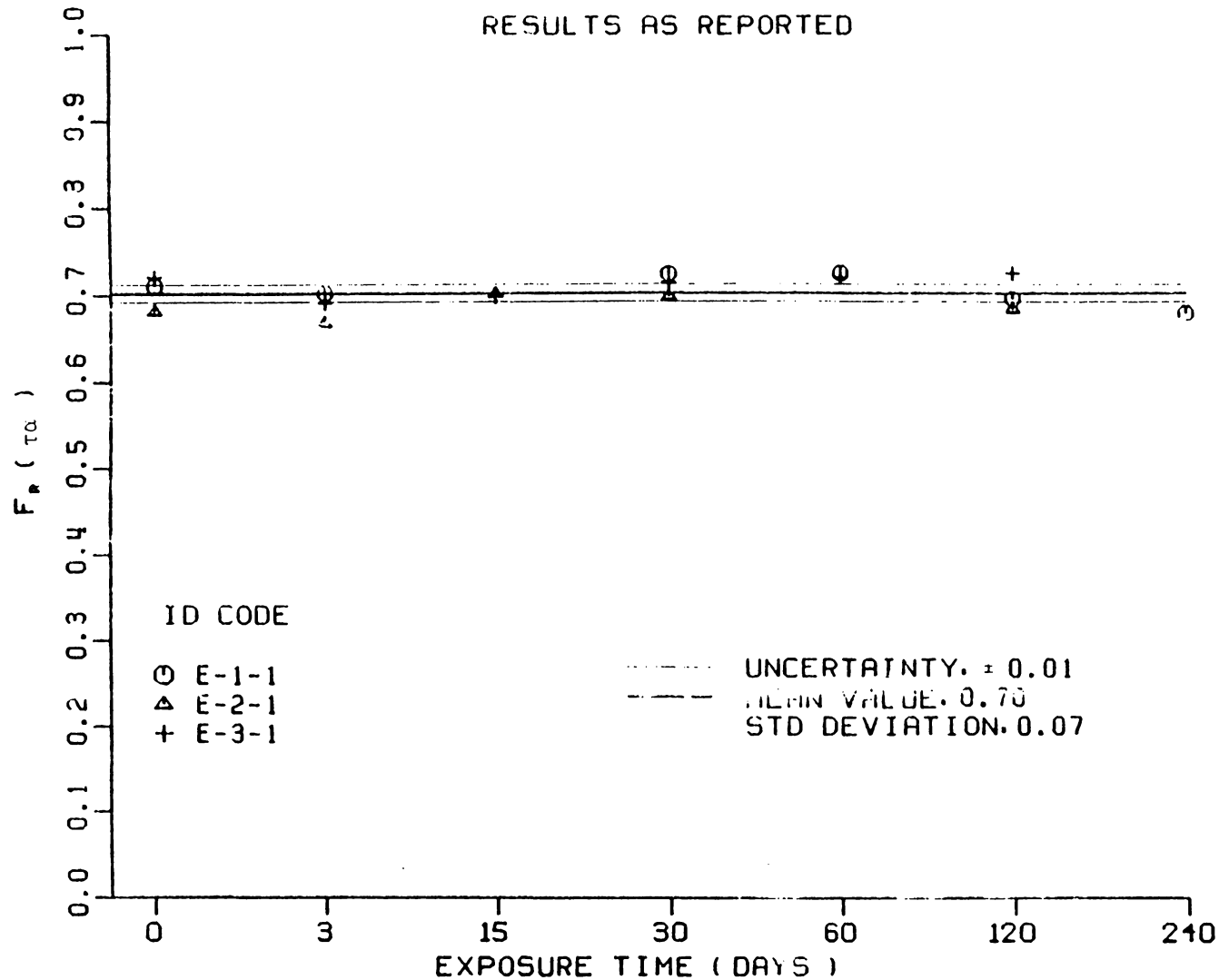

Figure B-37 $F_r(\tau\alpha)$ versus Exposure Time - Collector E, Test Series 1

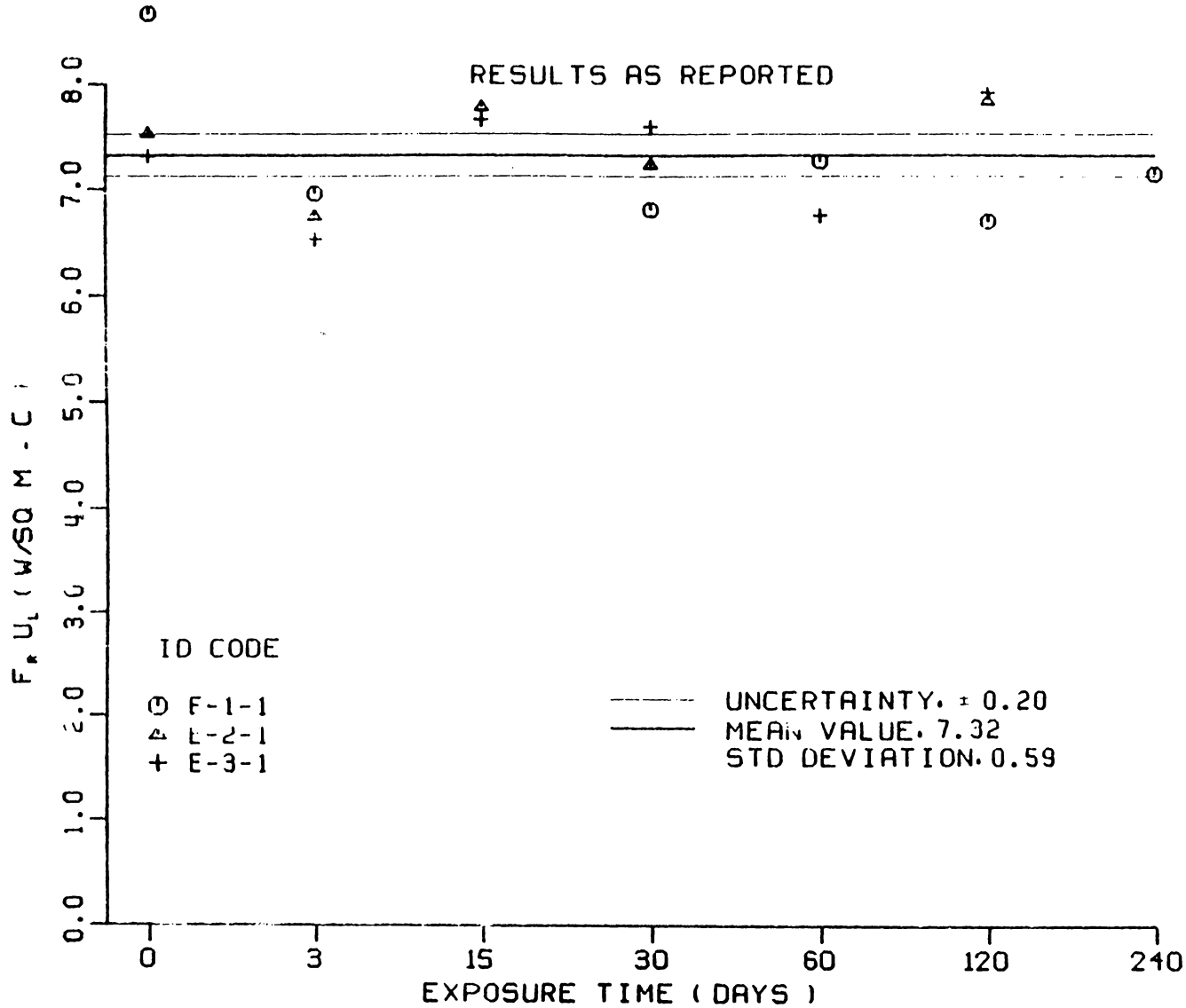

Figure B-38 $F_r U_L$ versus Exposure Time - Collector E, Test Series 1

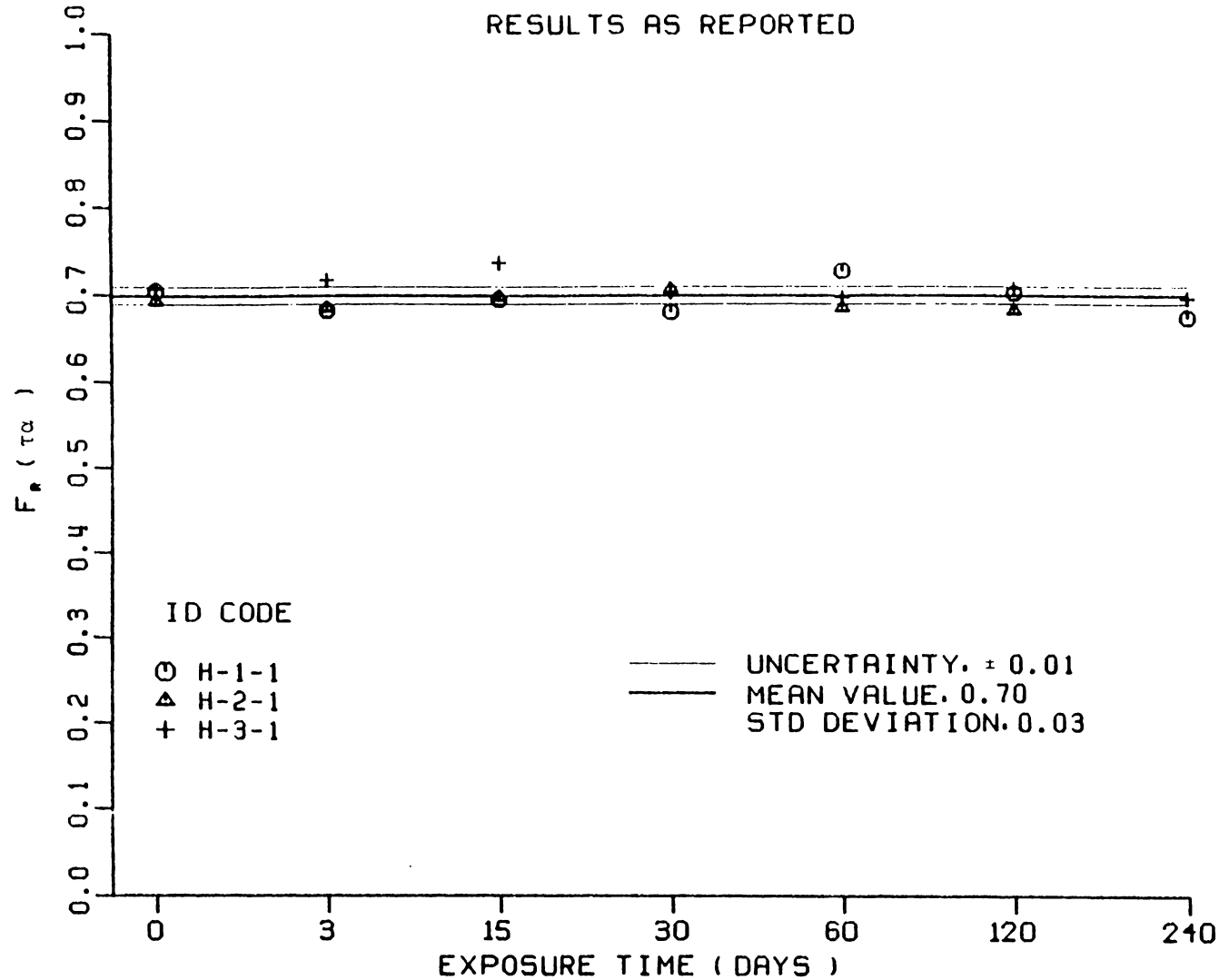

Figure B-39 $F_r(\tau\alpha)$ versus Exposure Time - Collector H, Test Series 1

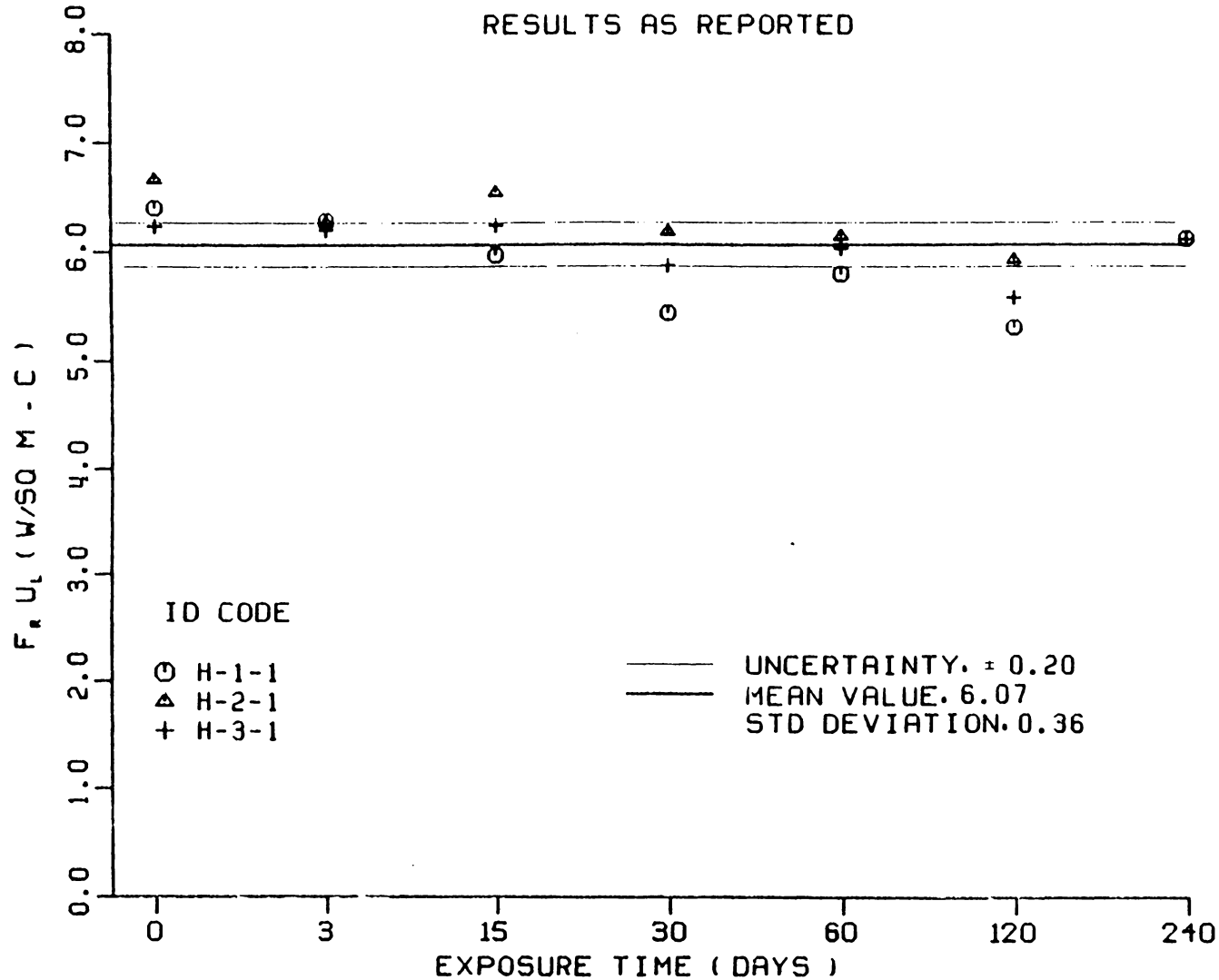

Figure B-40 $F_r U_L$ versus Exposure Time - Collector H, Test Series 1

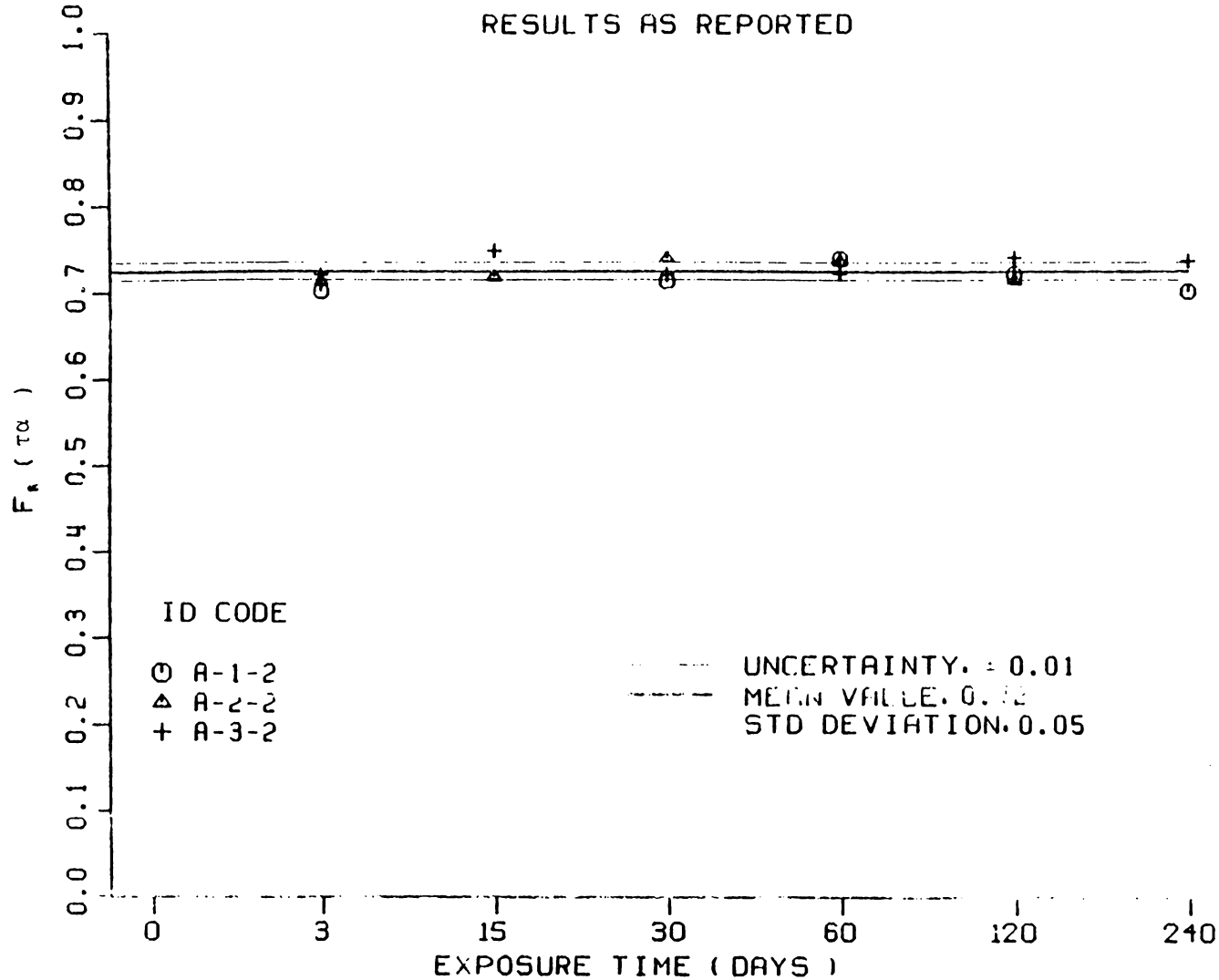

Figure B-41 $F_r(\tau\alpha)$ versus Exposure Time - Collector A, Test Series 2

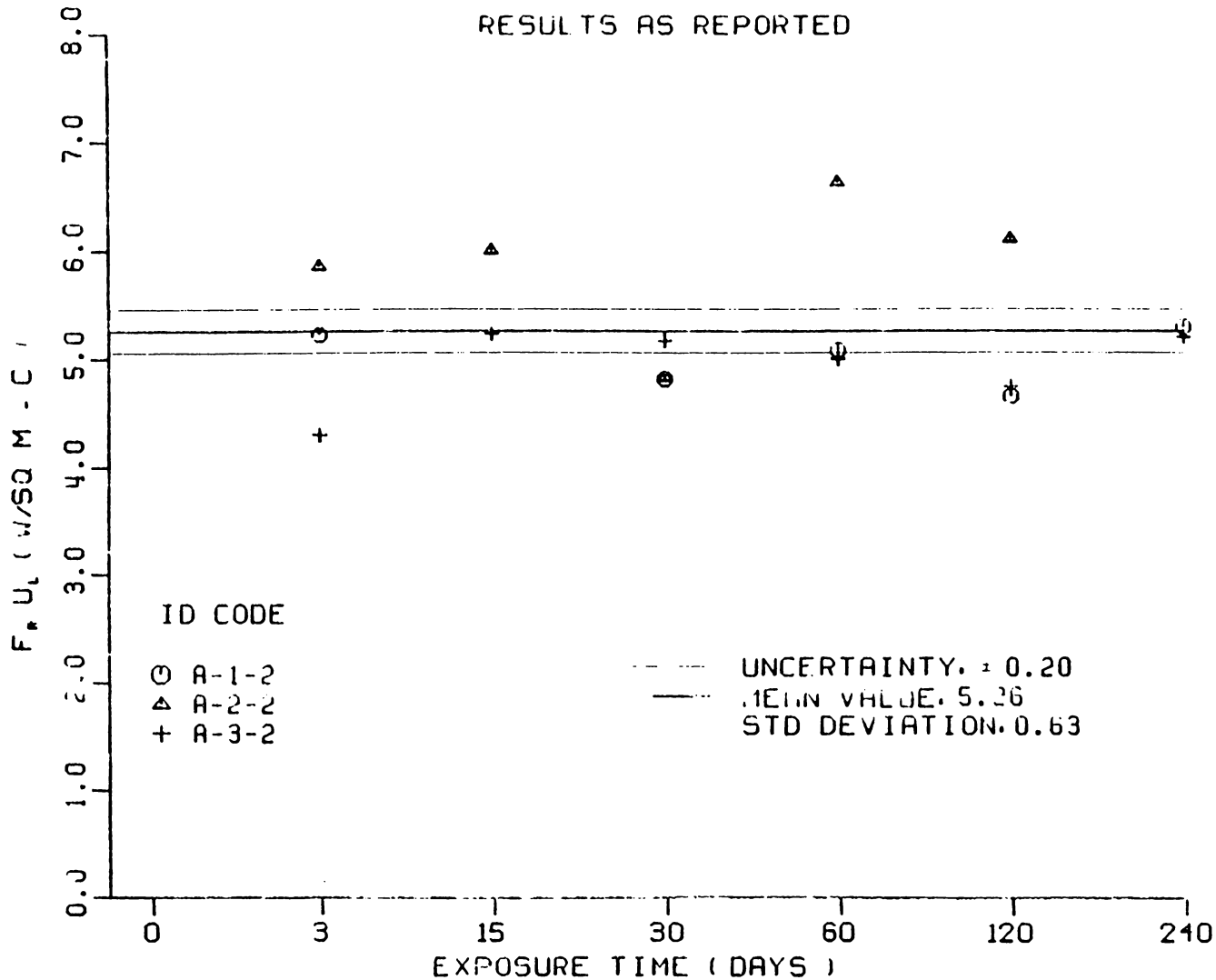

Figure B-42 $F_r U_L$ versus Exposure Time - Collector A, Test Series 2

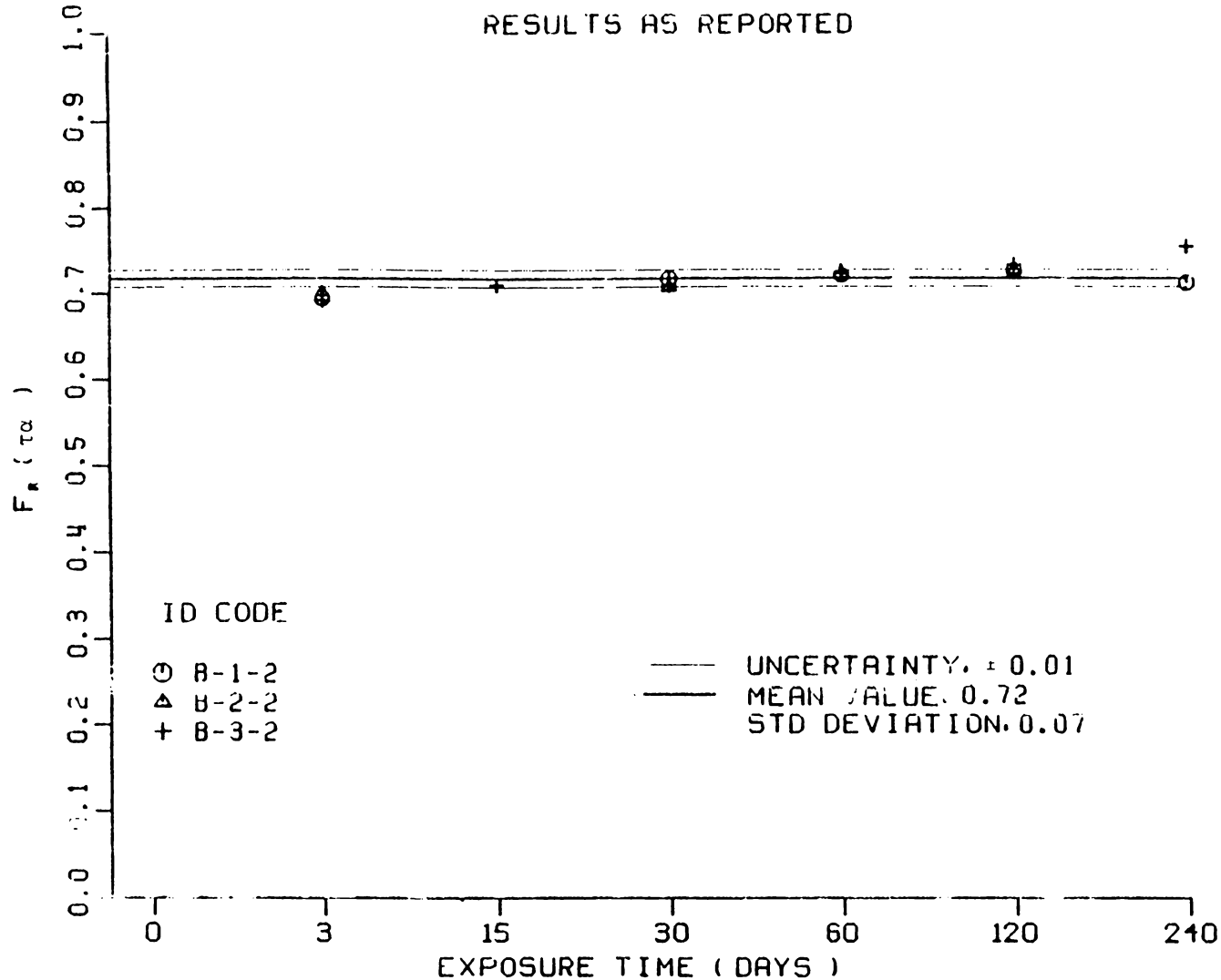

Figure B-43 $F_r(\tau\alpha)$ versus Exposure Time - Collector B, Test Series 2

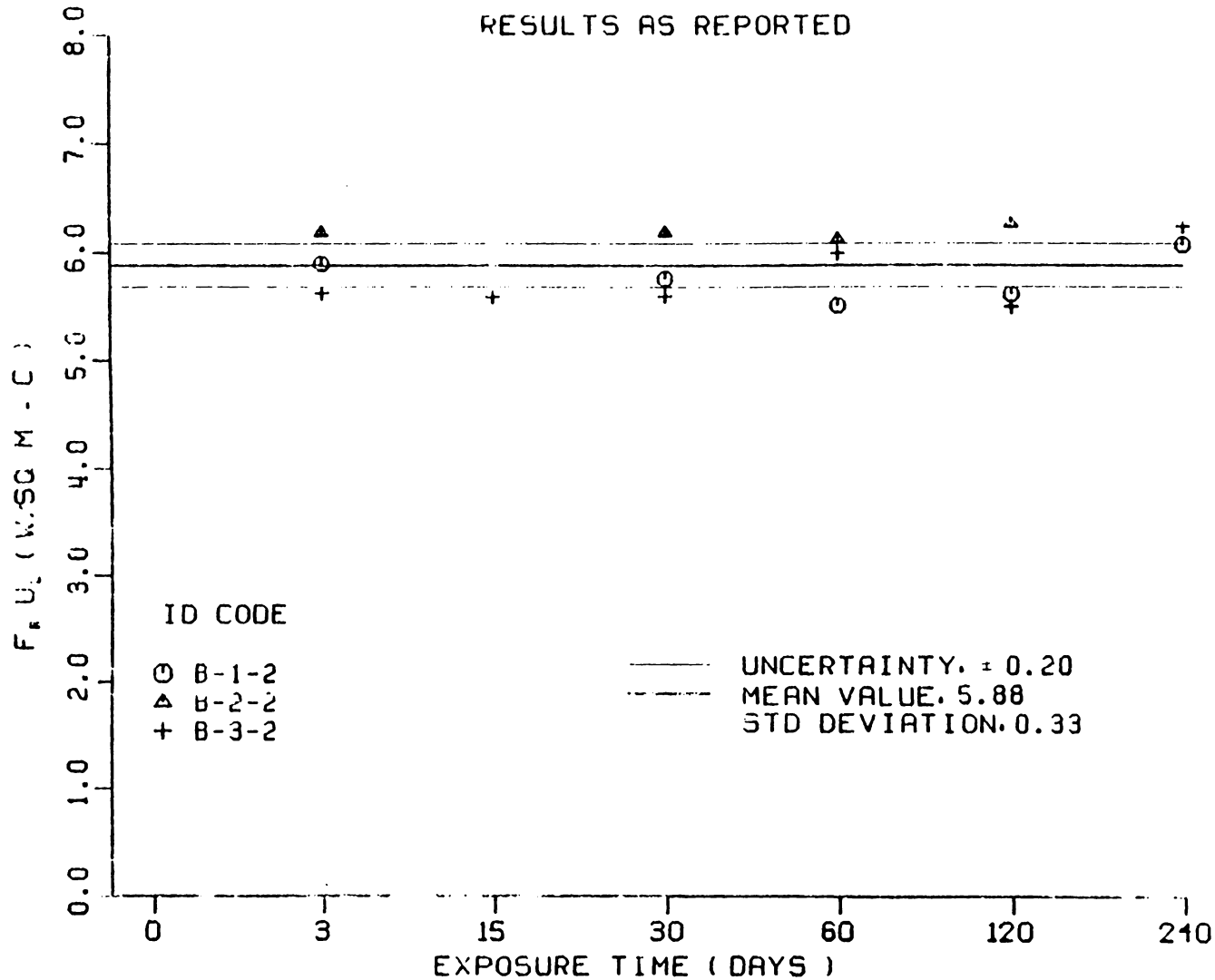

Figure B-44 $F_r U_L$ versus Exposure Time - Collector B, Test Series 2

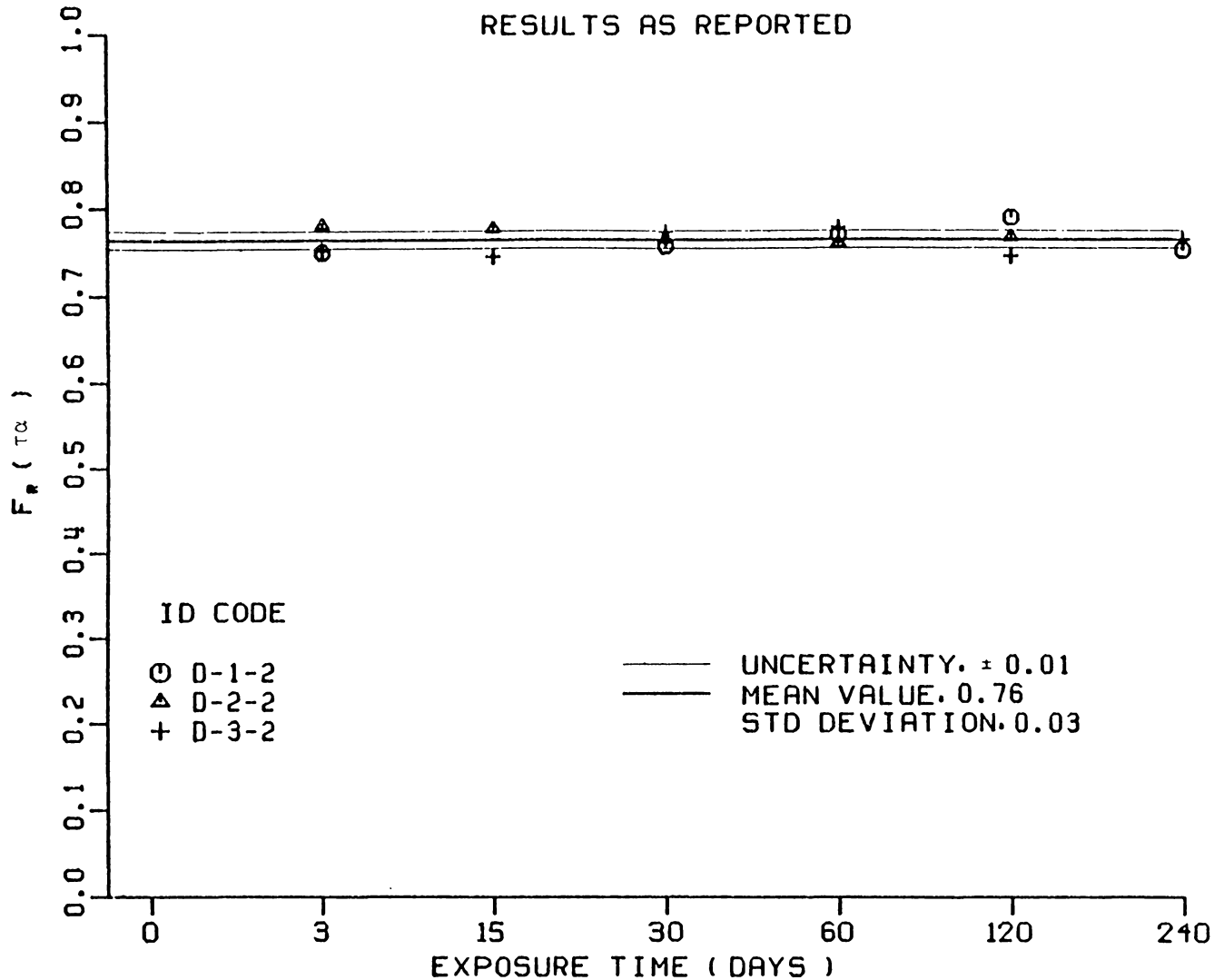

Figure B-45 $F_r(\tau\alpha)$ versus Exposure Time - Collector D, Test Series 2

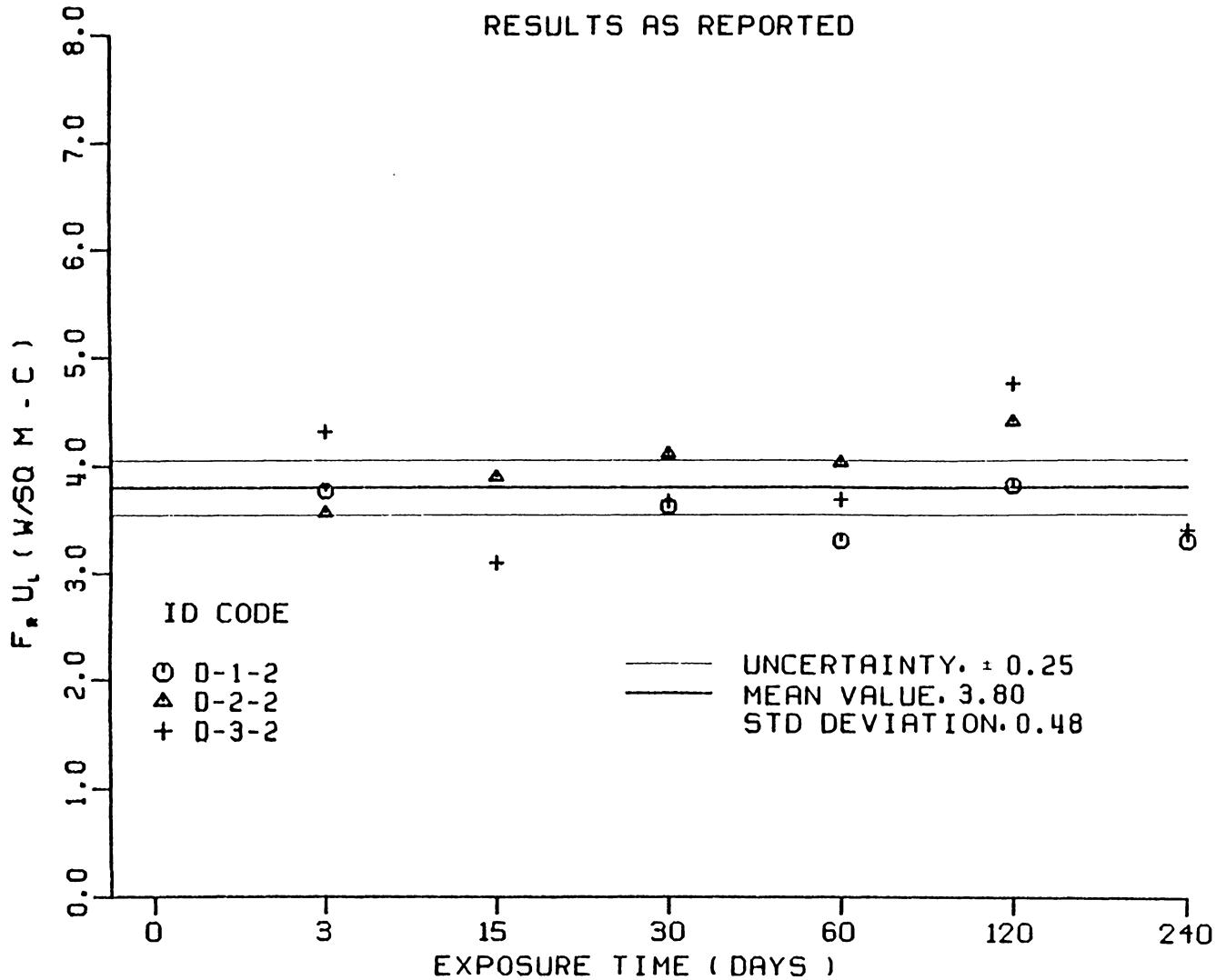

Figure B-46 $F_r U_L$ versus Exposure Time - Collector D, Test Series 2

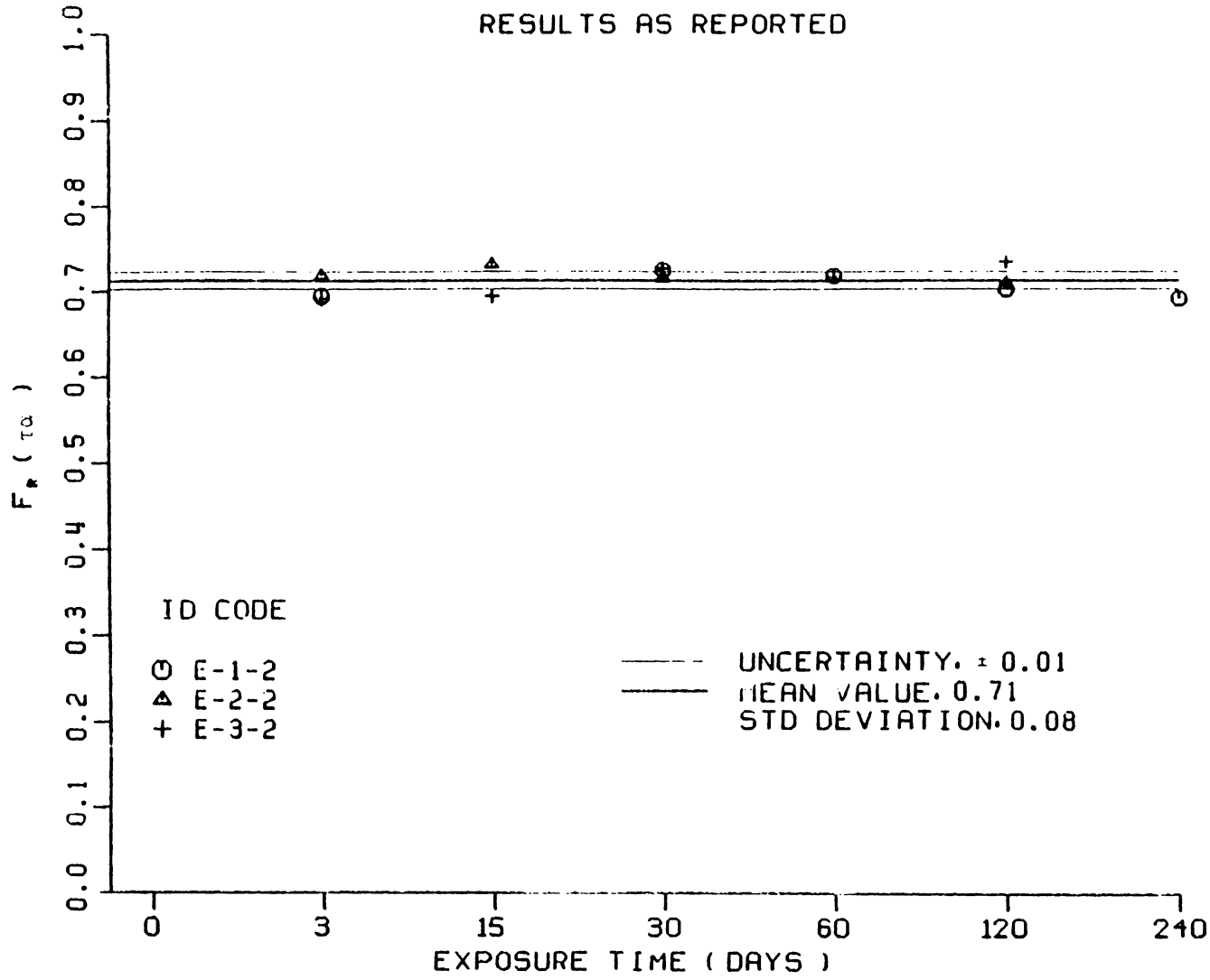

Figure B-47 $F_r(\tau\alpha)$ versus Exposure Time - Collector E, Test Series 2

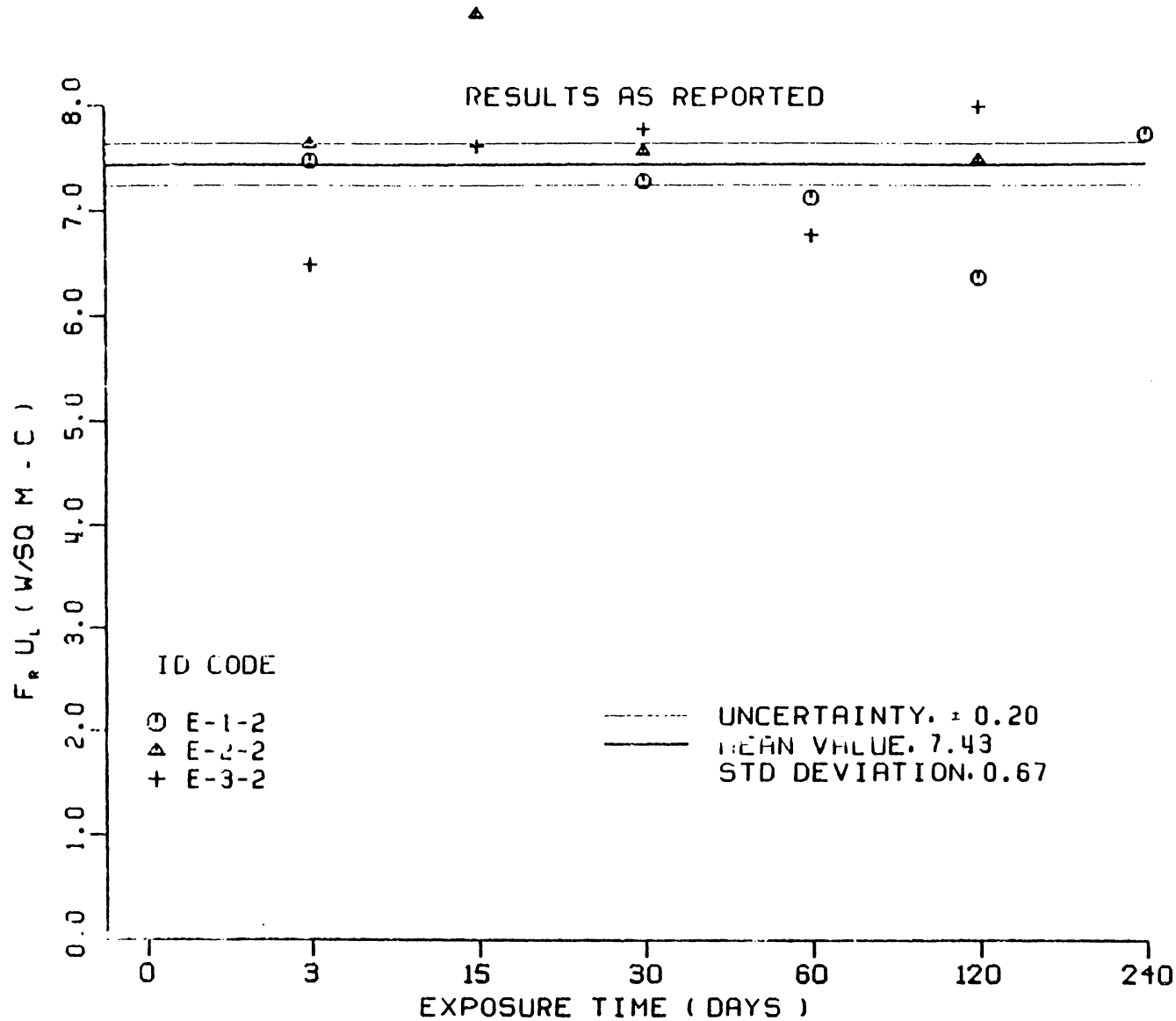

Figure B-48 $F_r U_L$ versus Exposure Time - Collector E, Test Series 2

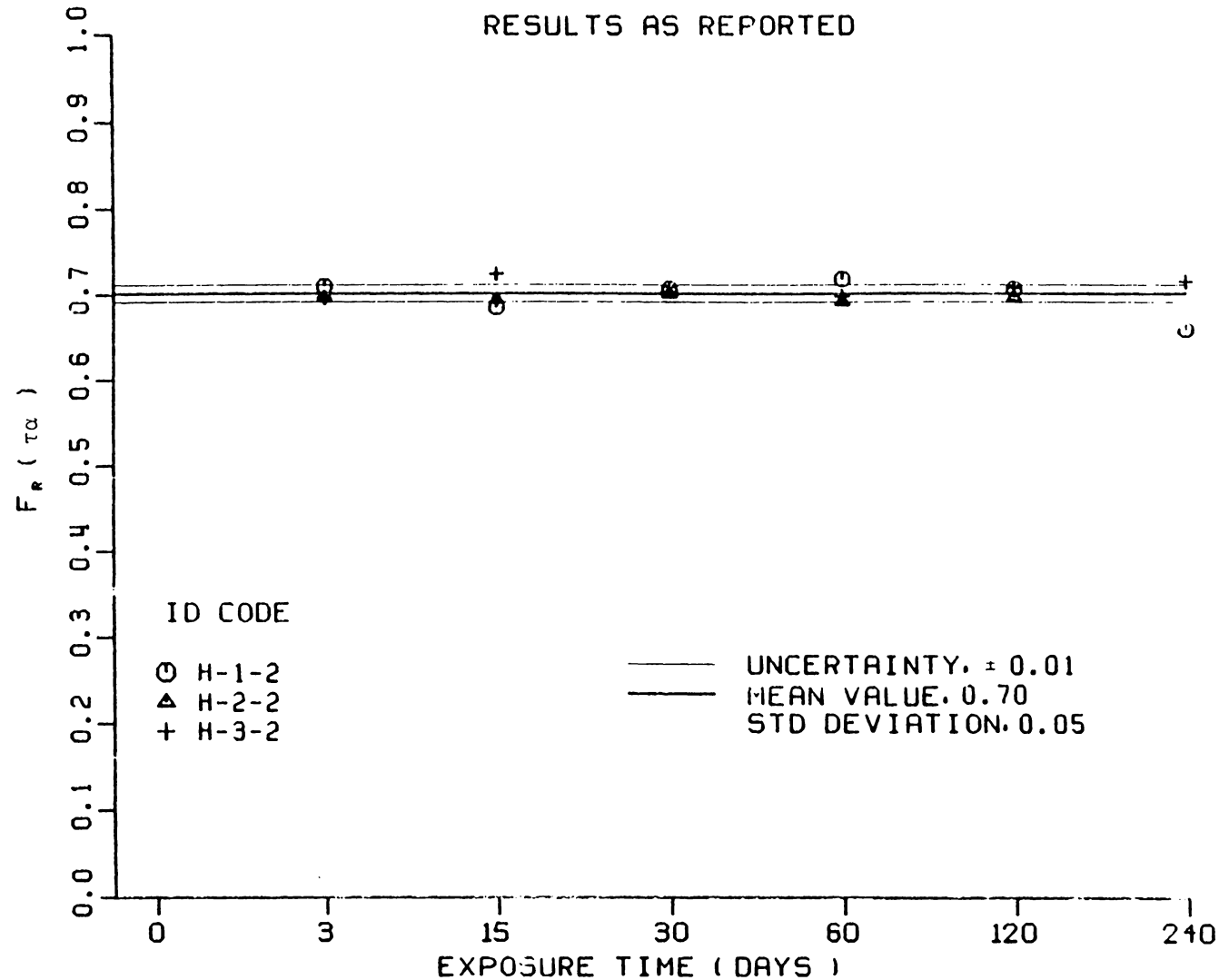

Figure B-49 $F_r(\tau\alpha)$ versus Exposure Time - Collector H, Test Series 2

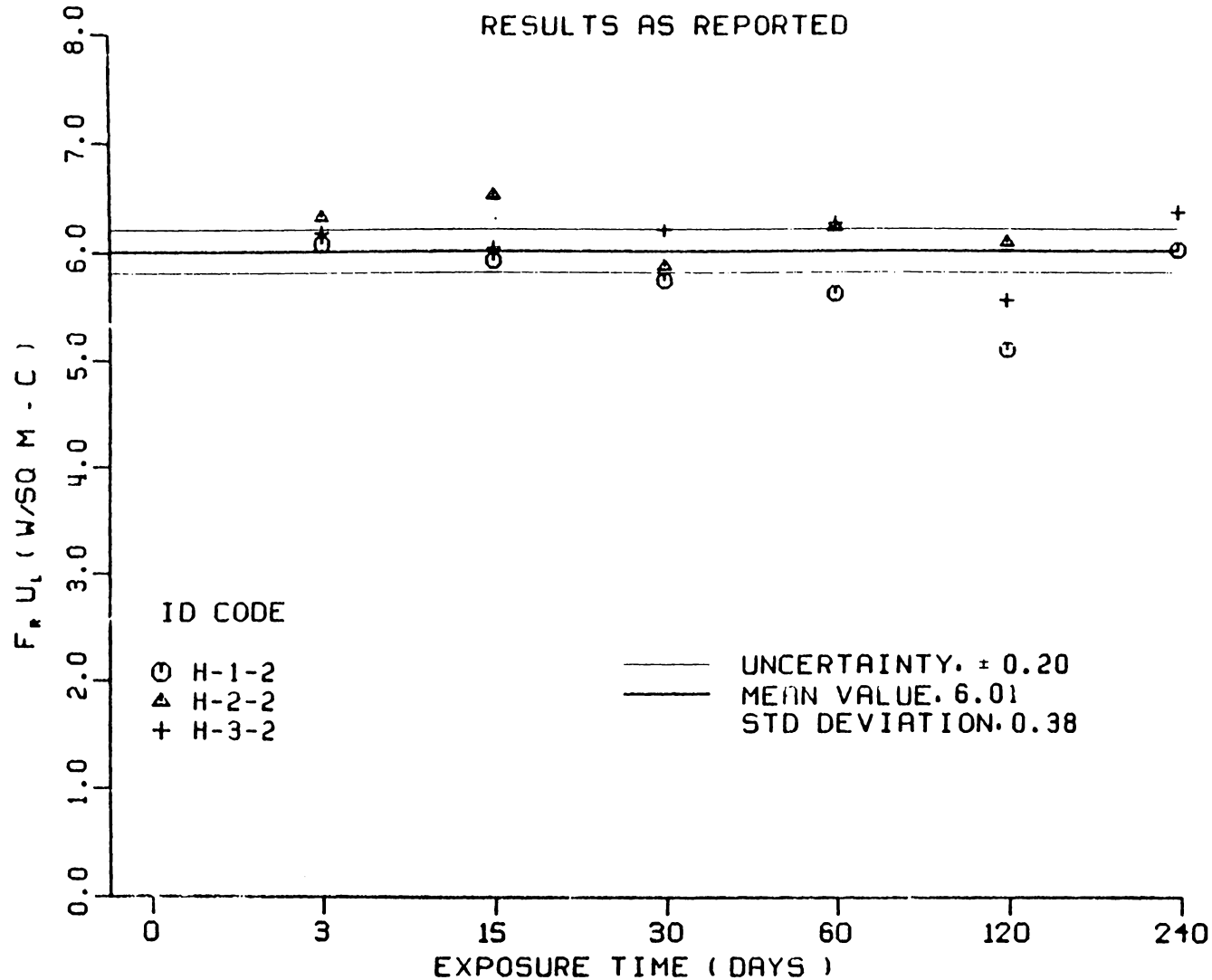

Figure B-50 $F_r U_L$ versus Exposure Time - Collector H, Test Series 2

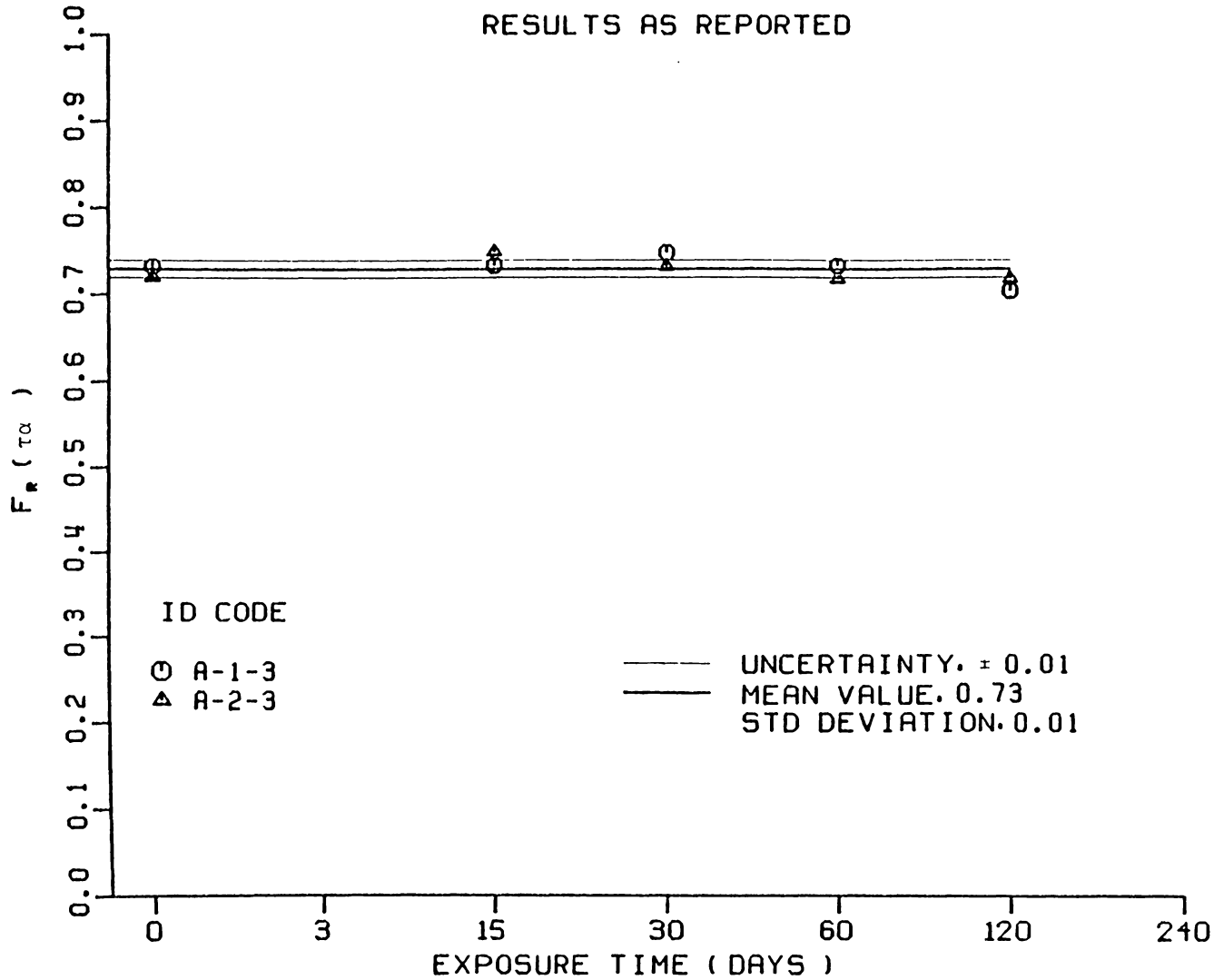

Figure B-51 $F_r(\tau\alpha)$ versus Exposure Time - Collector A, Test Series 3

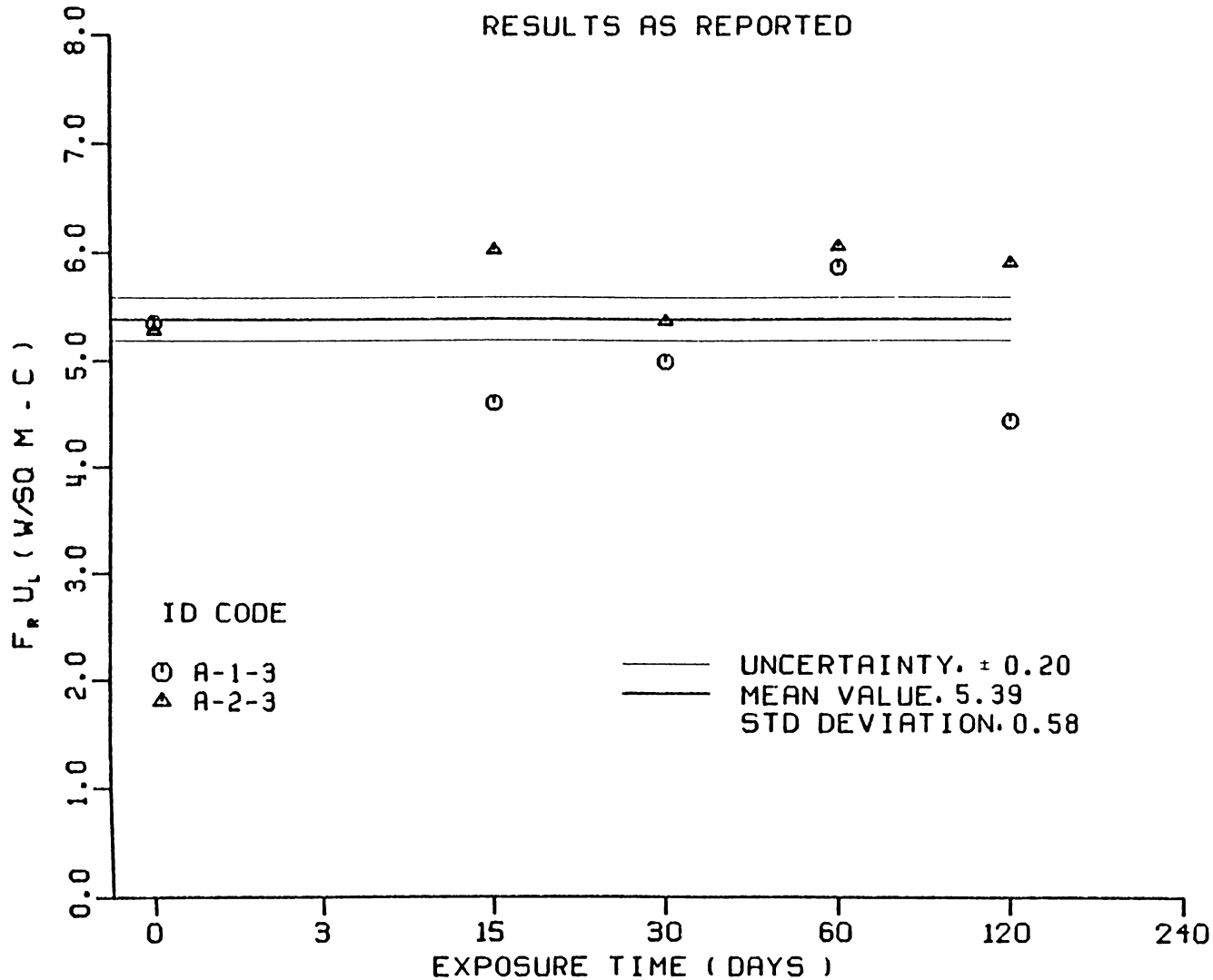

Figure B-52 $F_r U_L$ versus Exposure Time - Collector A, Test Series 3

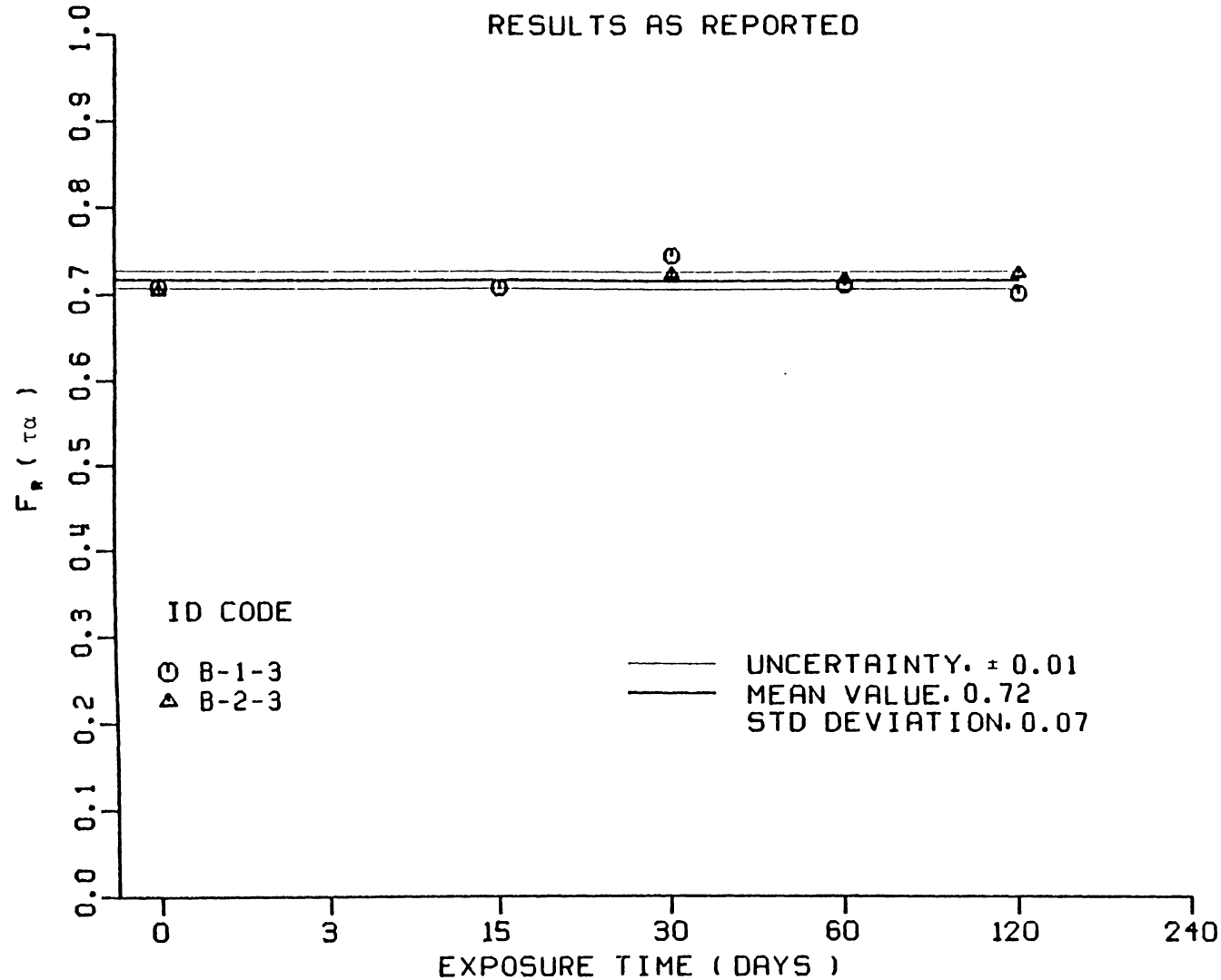

Figure B-53 $F_r(\tau\alpha)$ versus Exposure Time - Collector B, Test Series 3

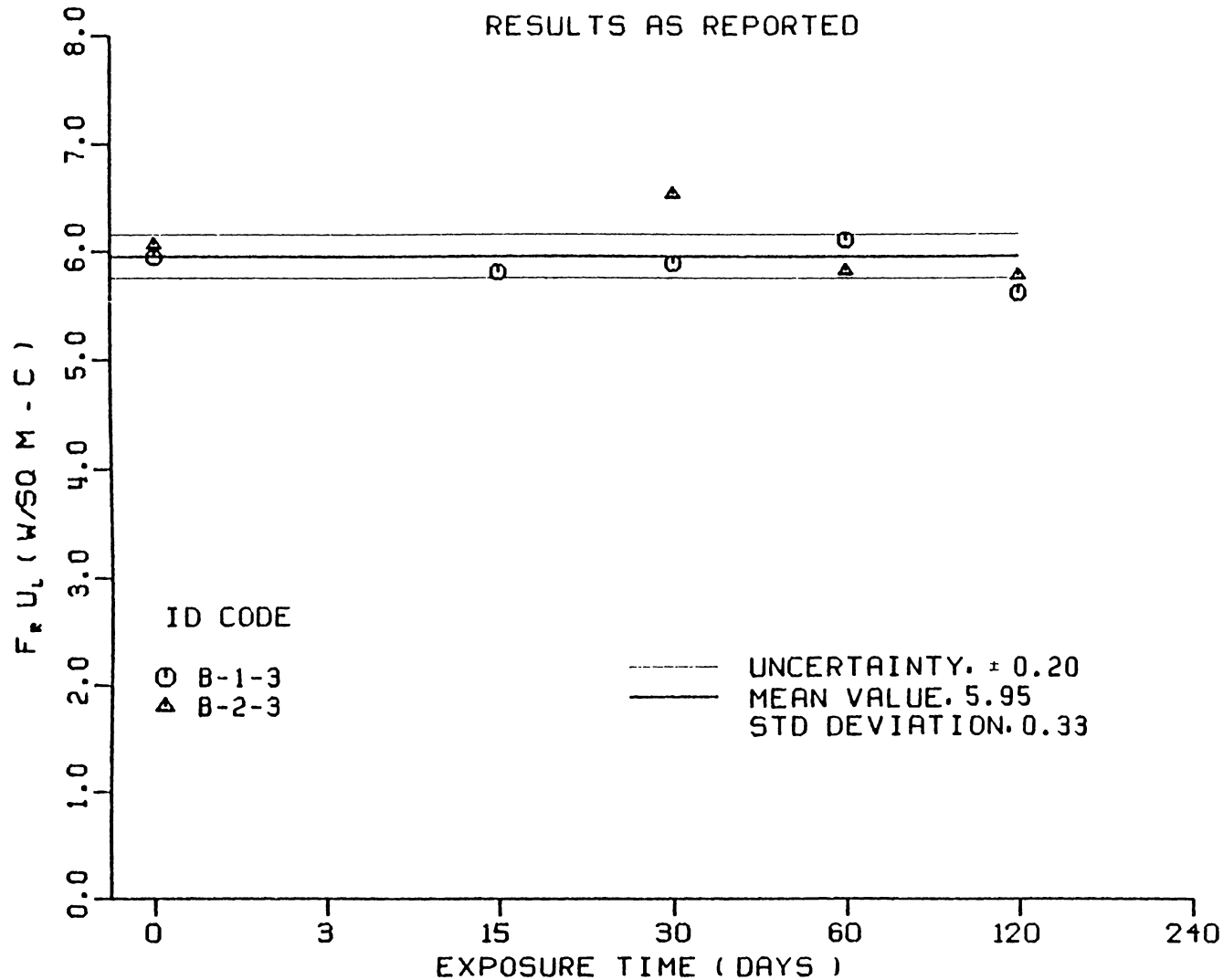

Figure B-54 $F_r U_L$ versus Exposure Time - Collector B, Test Series 3

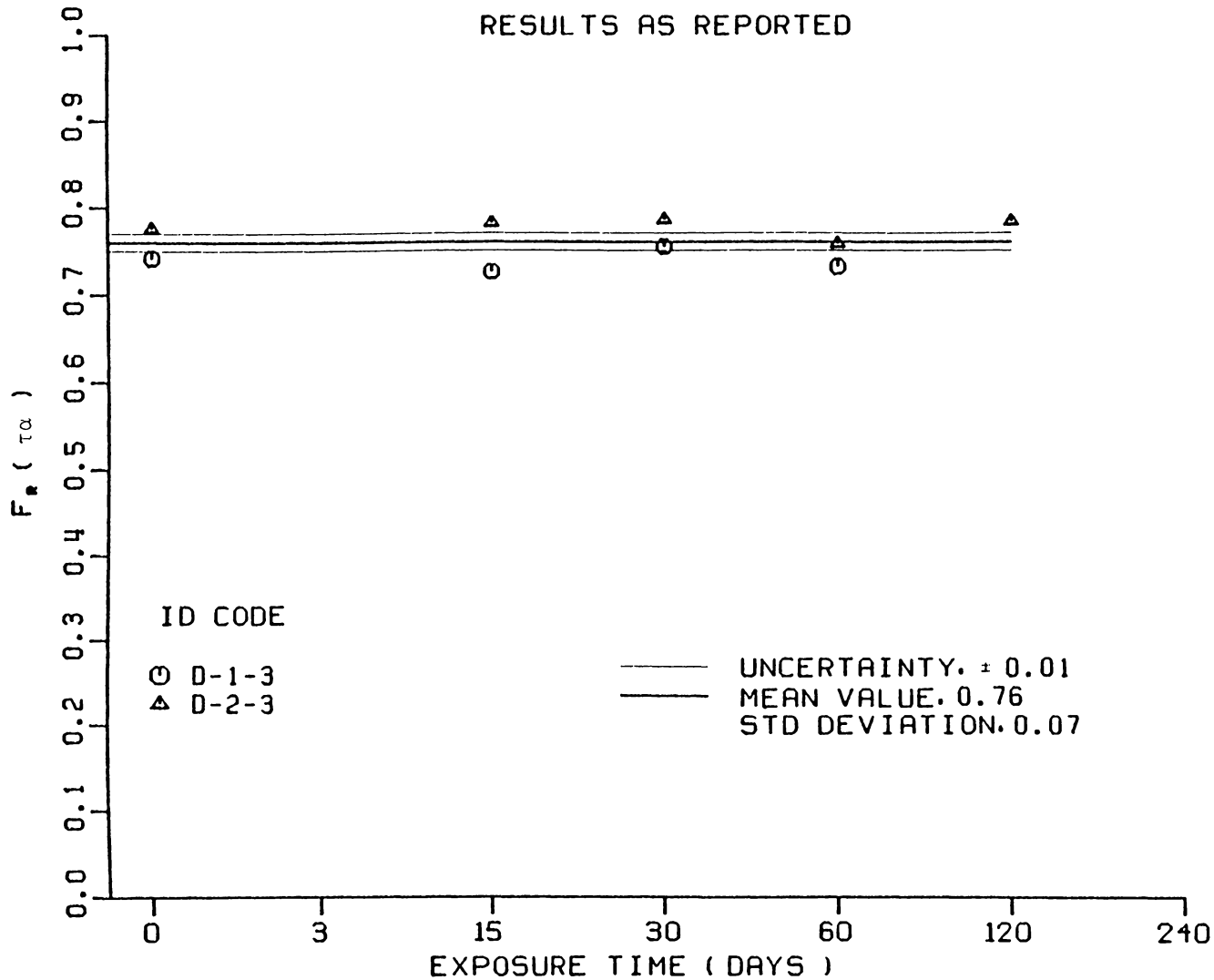

Figure B-55 $F_r(\tau\alpha)$ versus Exposure Time - Collector D, Test Series 3

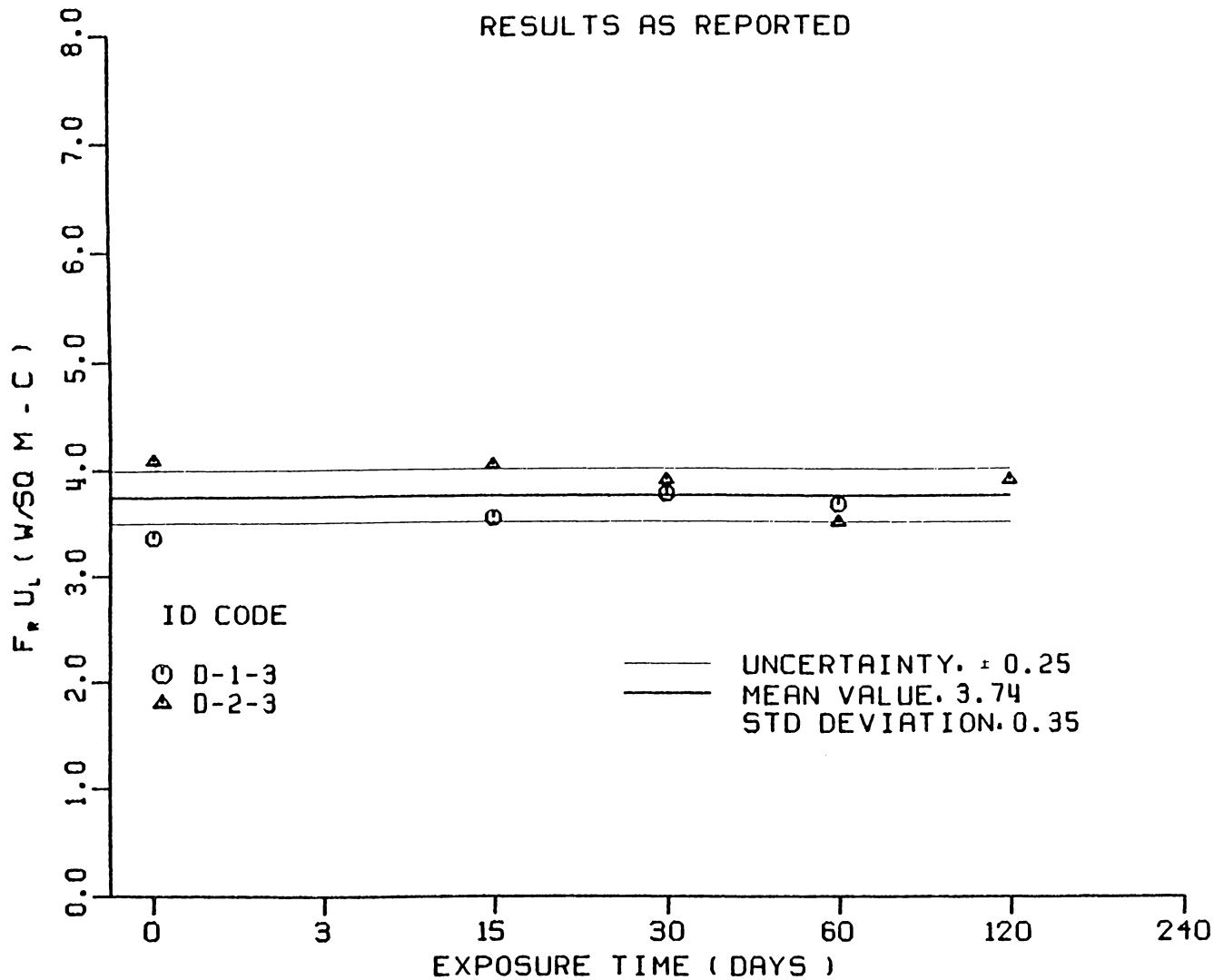

Figure B-56 $F_r U_L$ versus Exposure Time - Collector D, Test Series 3

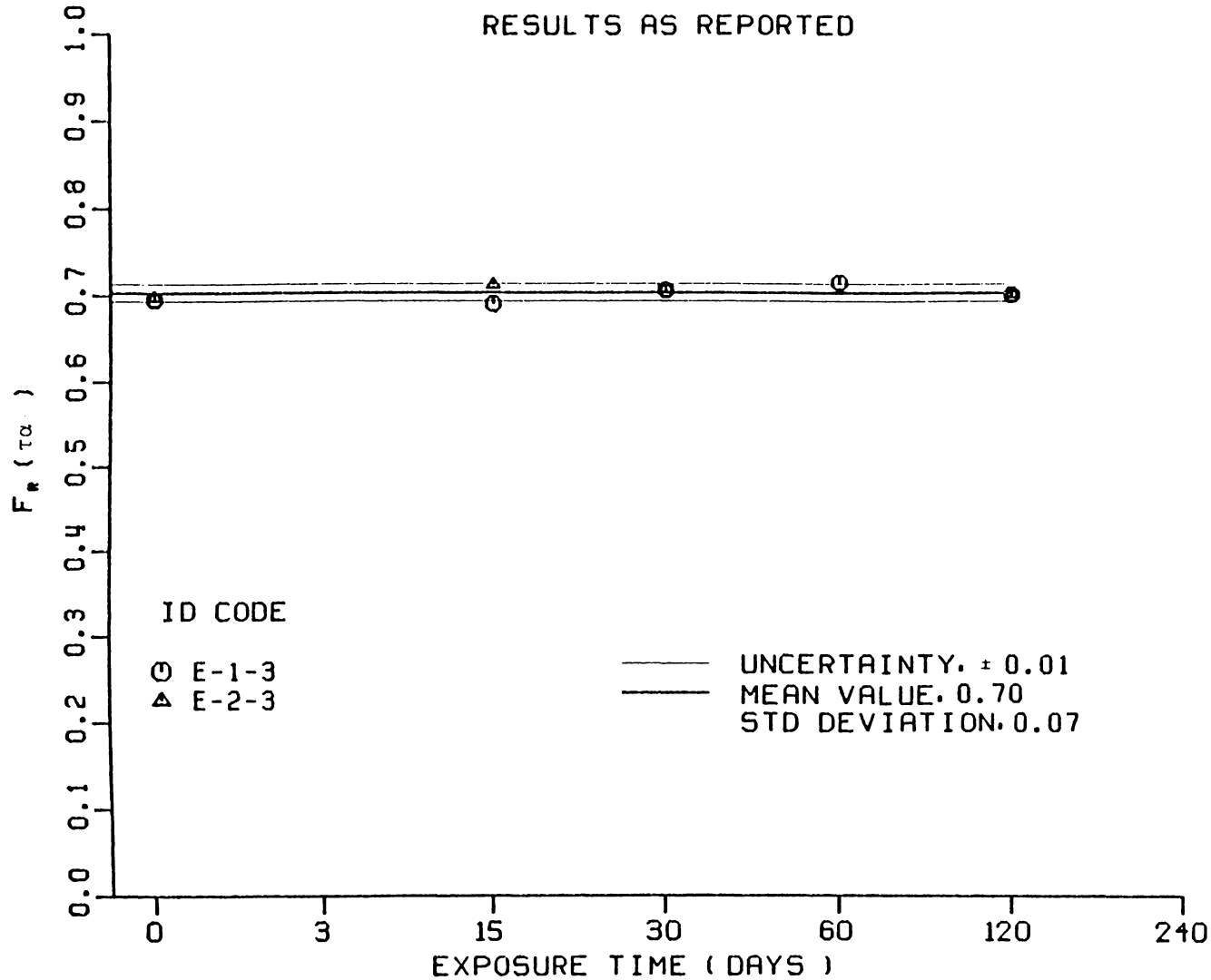

Figure B-57 $F_r(\tau\alpha)$ versus Exposure Time - Collector E, Test Series 3

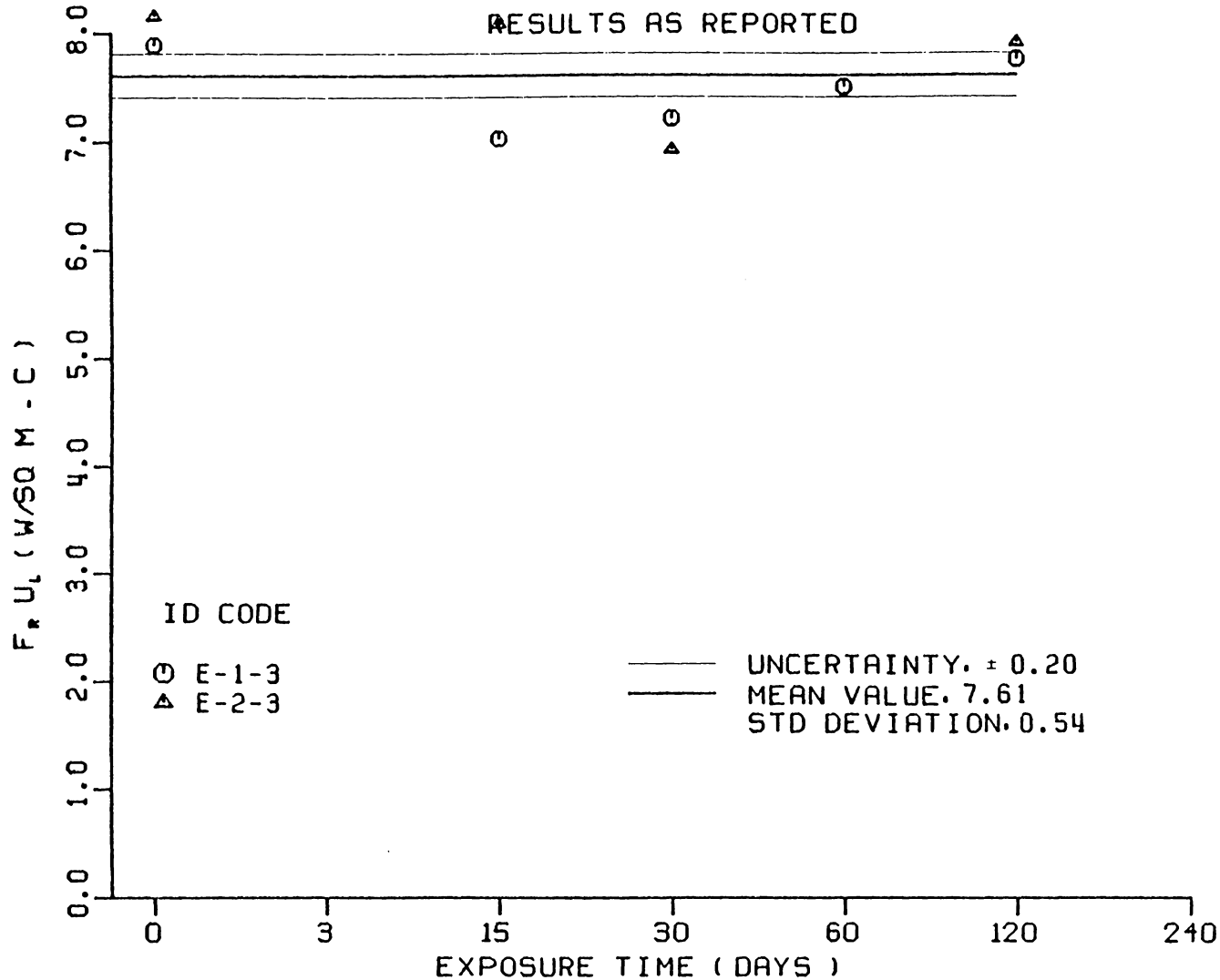

Figure B-58 $F_r U_L$ versus Exposure Time - Collector E, Test Series 3

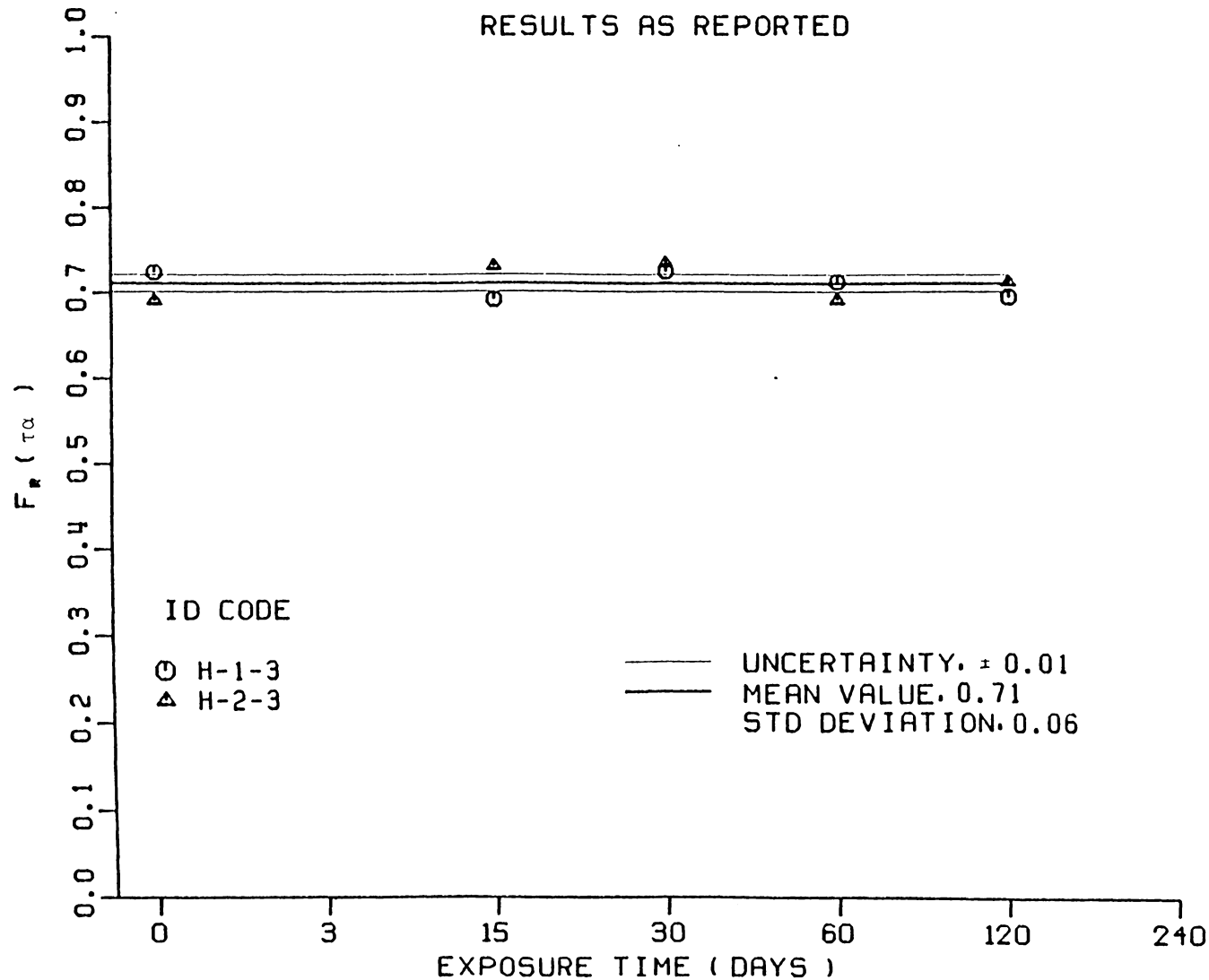

Figure B-59 $F_r(\tau\alpha)$ versus Exposure Time - Collector H, Test Series 3

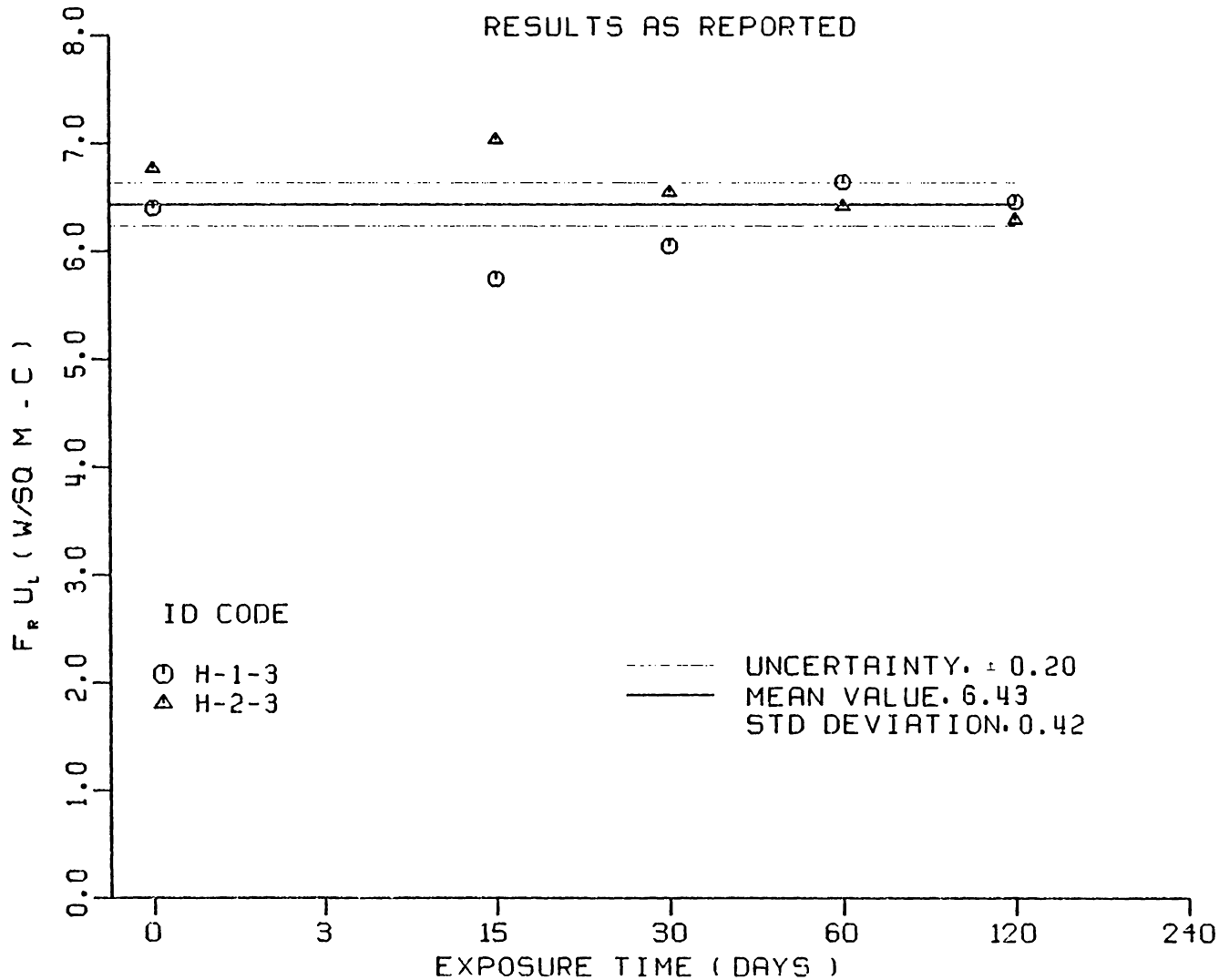

Figure B-60 $F_r U_L$ versus Exposure Time - Collector H, Test Series 3

APPENDIX C

PLOTS OF PERFORMANCE PARAMETERS AS A FUNCTION OF SEASON

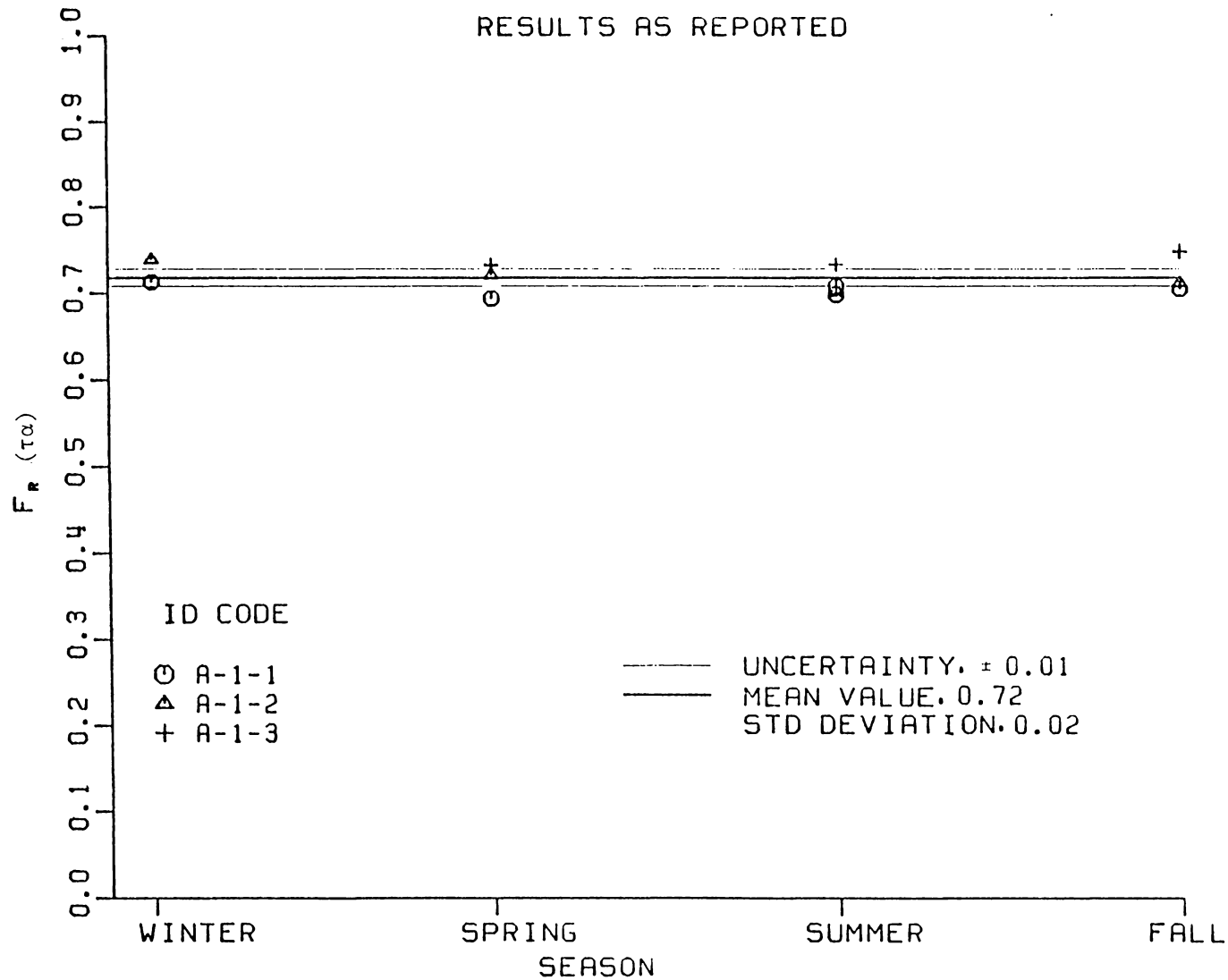

Figure C-1 $F_r(\tau\alpha)$ versus Season - Collector A, Test Site 1

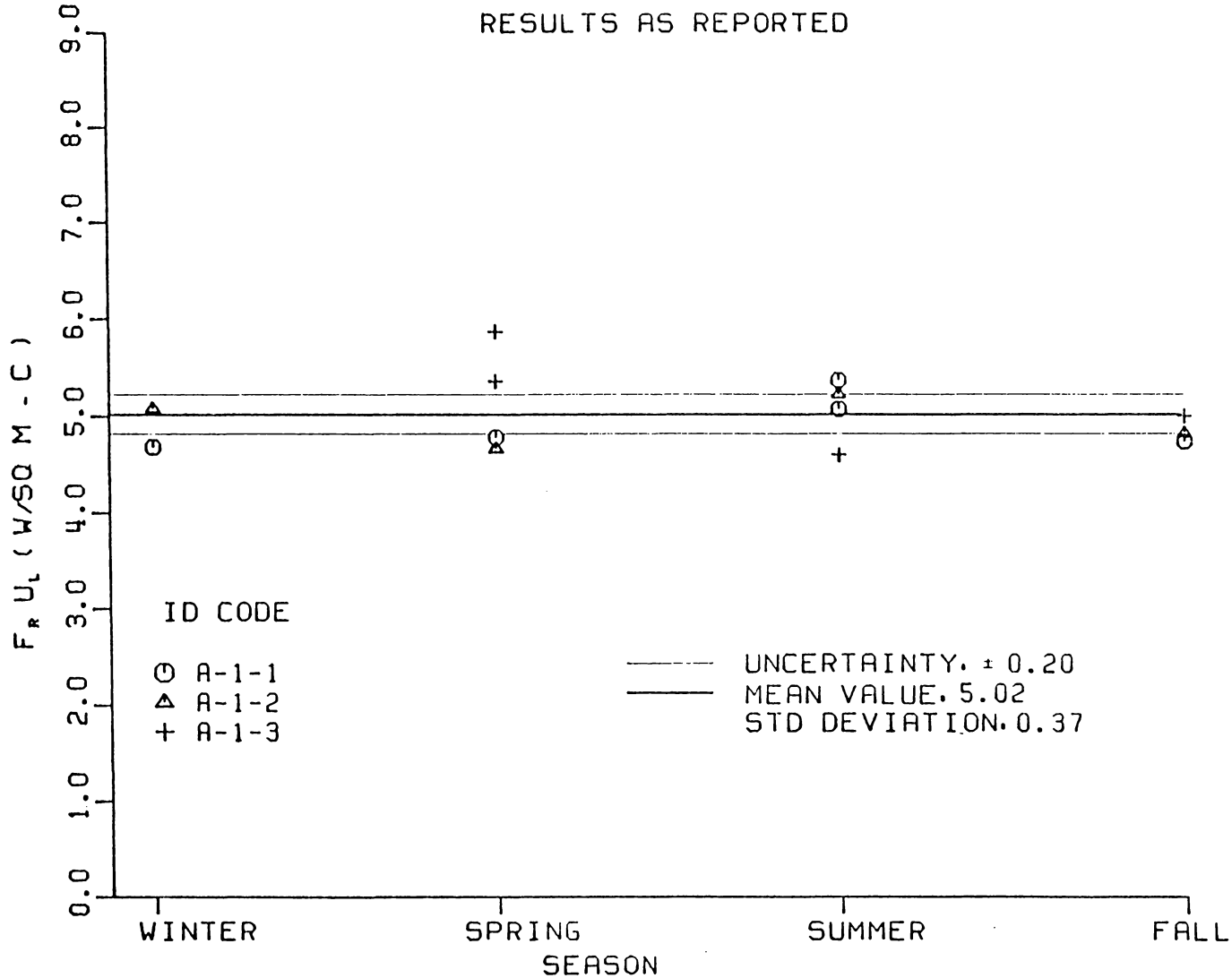

Figure C-2 $F_r U_L$ versus Season - Collector A, Test Site 1

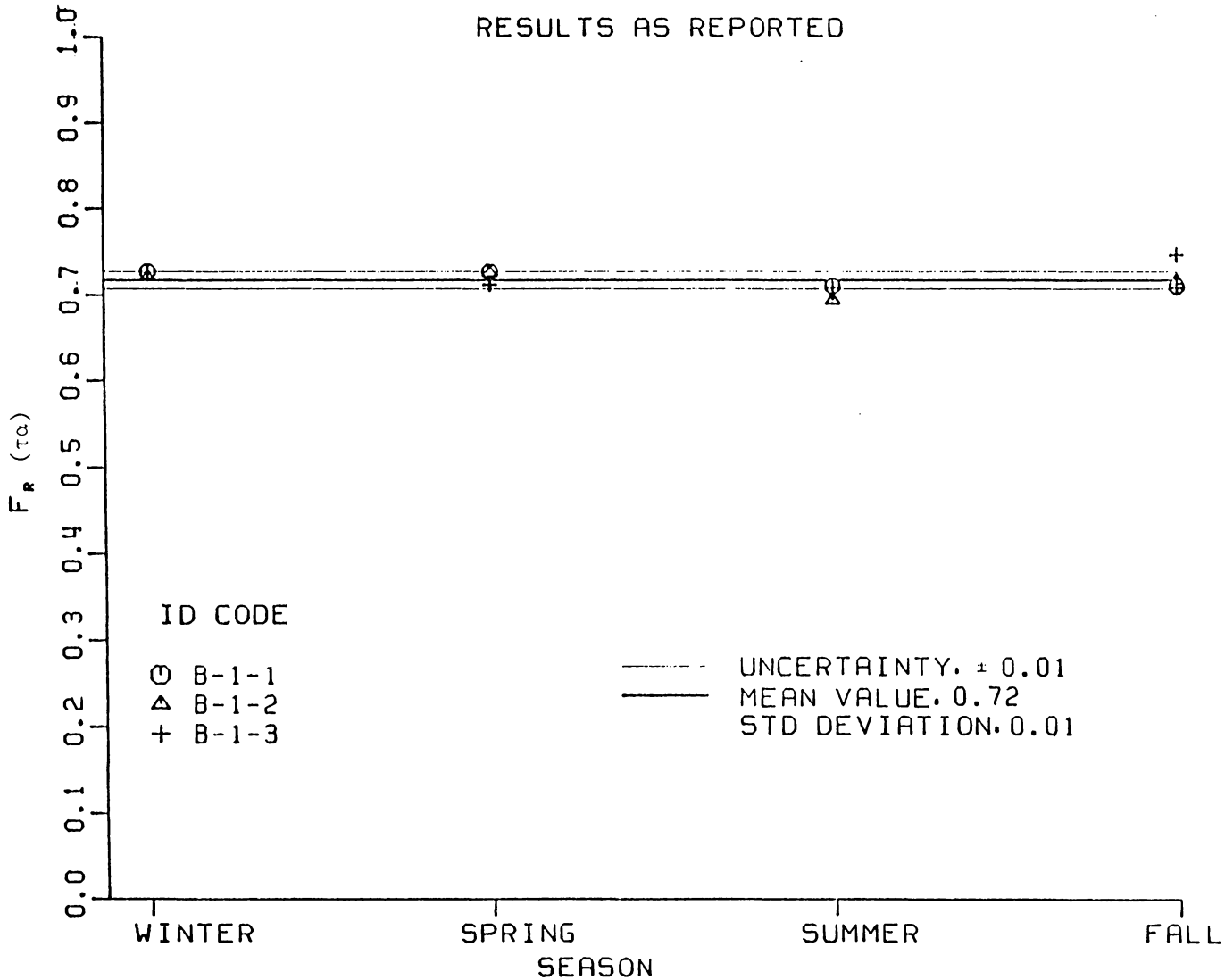

Figure C-3 $F_r(\tau\alpha)$ versus Season - Collector B, Test Site 1

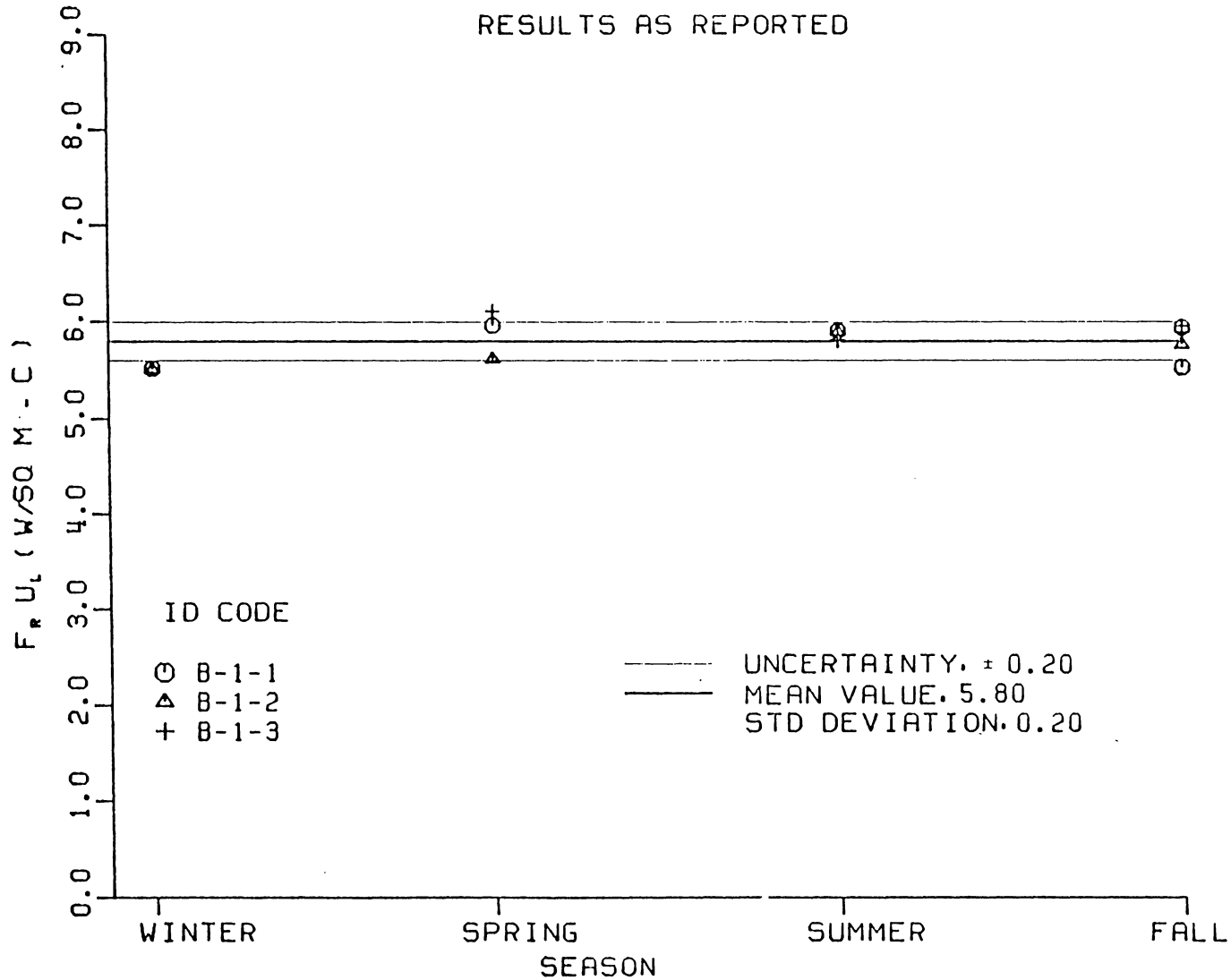

Figure C-4 $F_r U_L$ versus Season - Collector B, Test Site 1

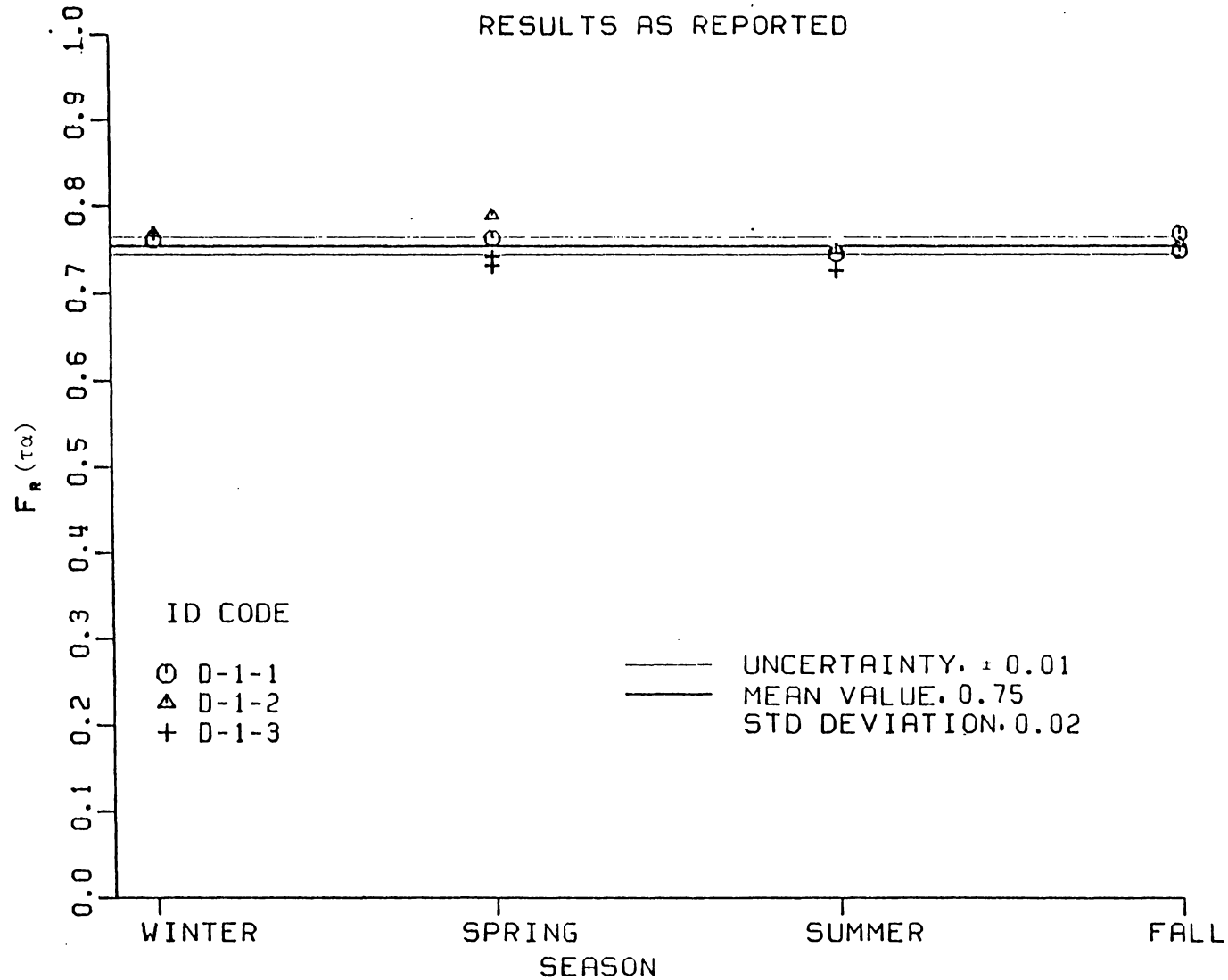

Figure C-5 $F_r(\tau\alpha)$ versus Season - Collector D, Test Site 1

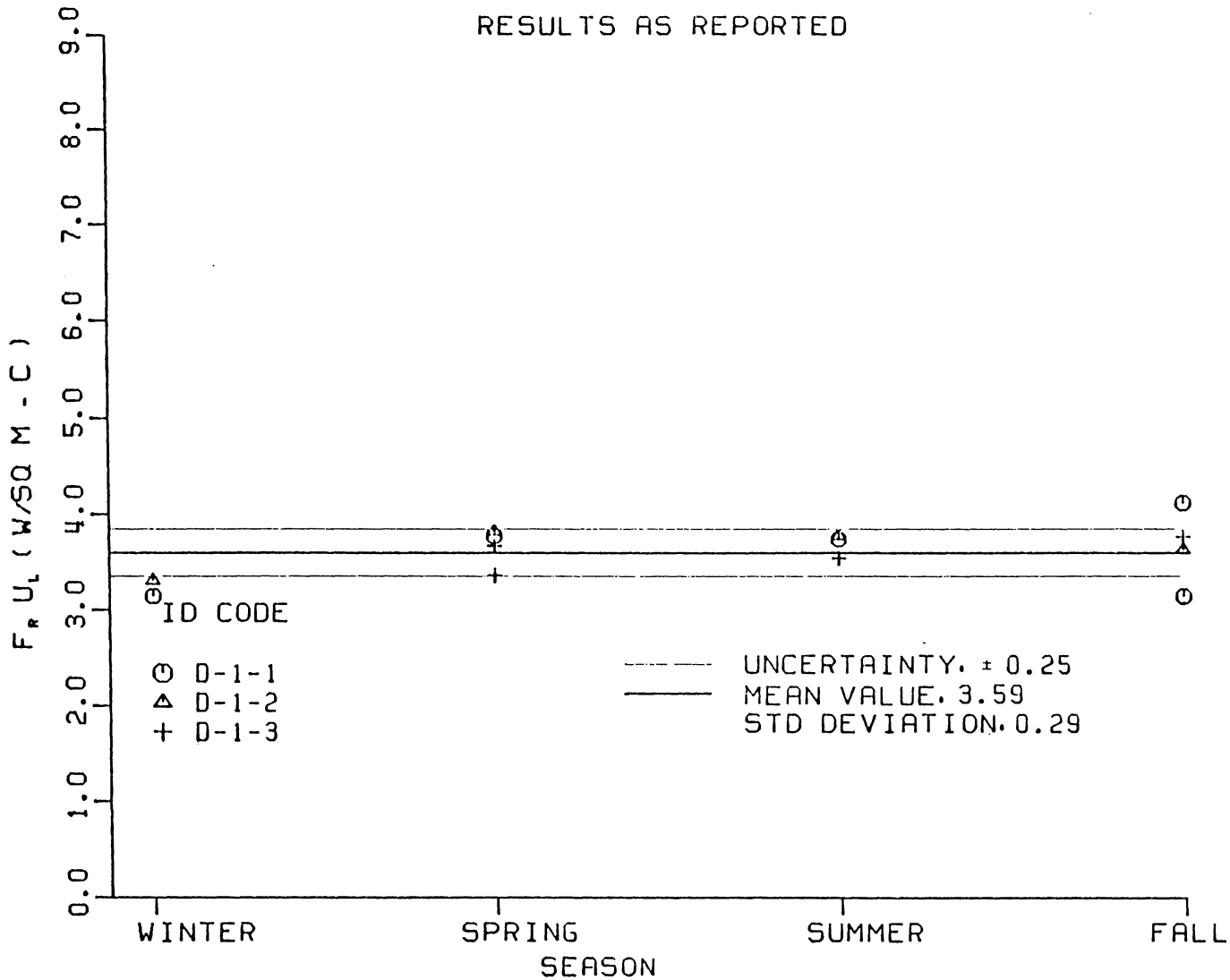

Figure C-6 $F_r U_L$ versus Season - Collector D, Test Site 1

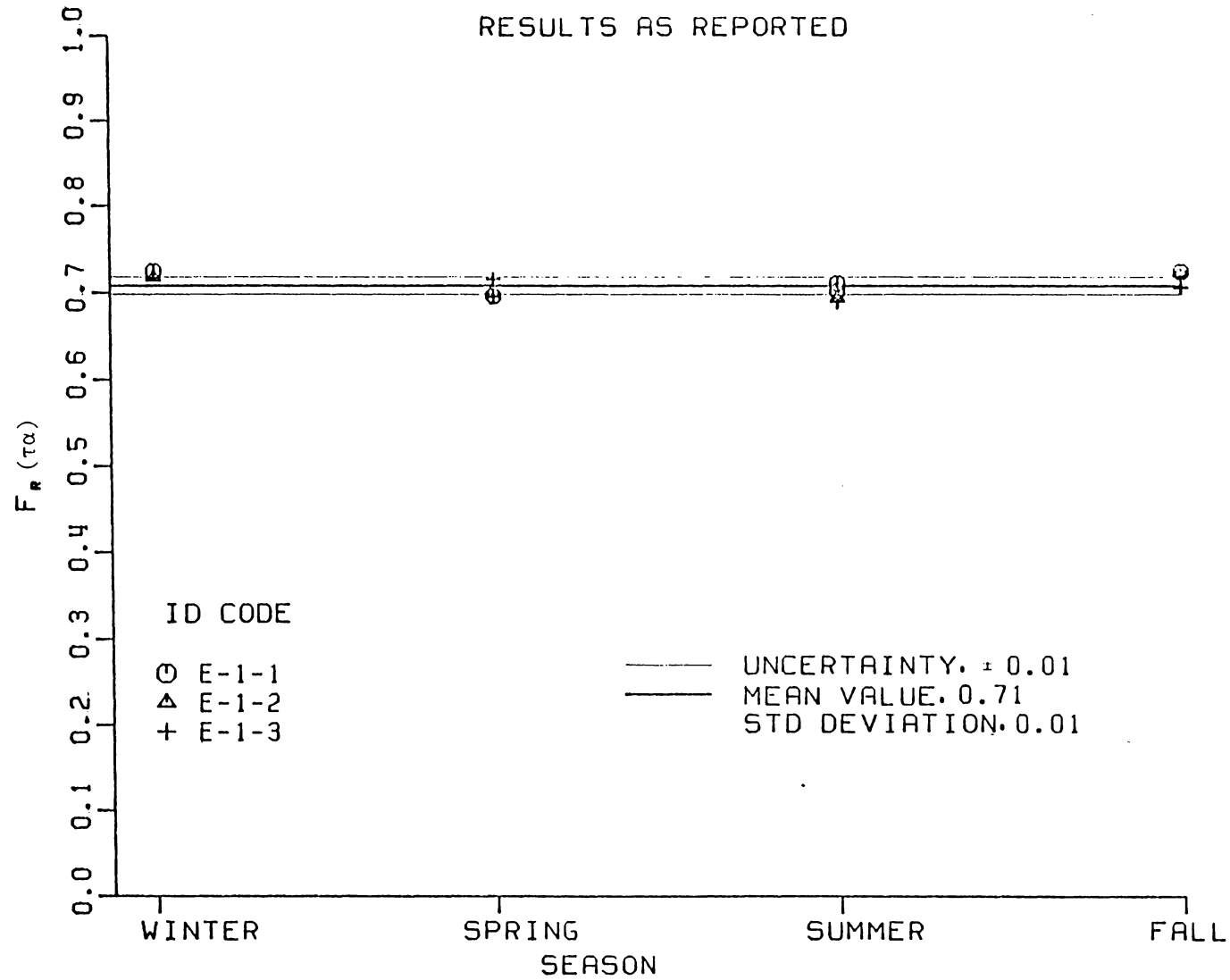

Figure C-7 $F_r(\tau\alpha)$ versus Season - Collector E, Test Site 1

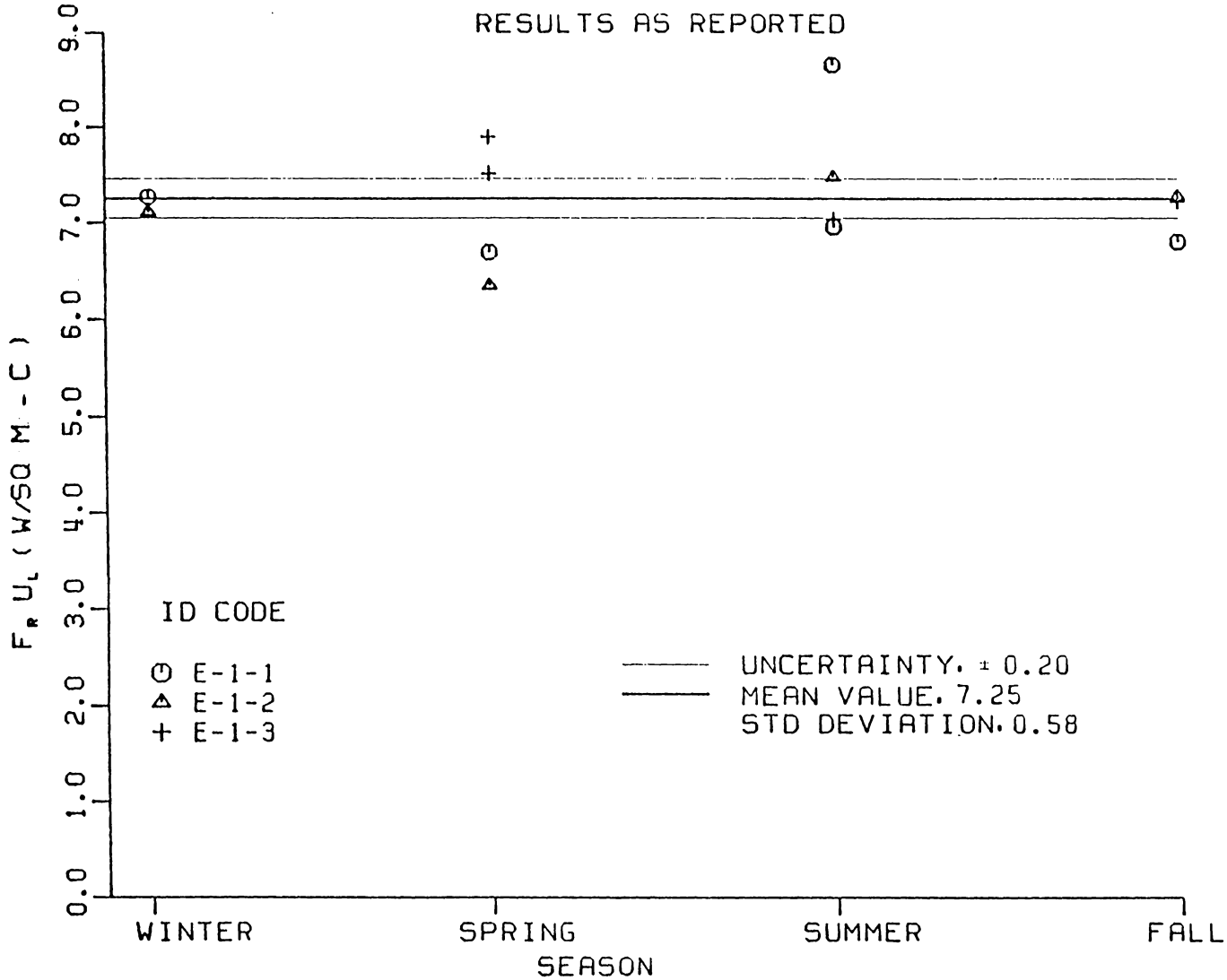

Figure C-8 $F_r U_L$ versus Season - Collector E, Test Site 1

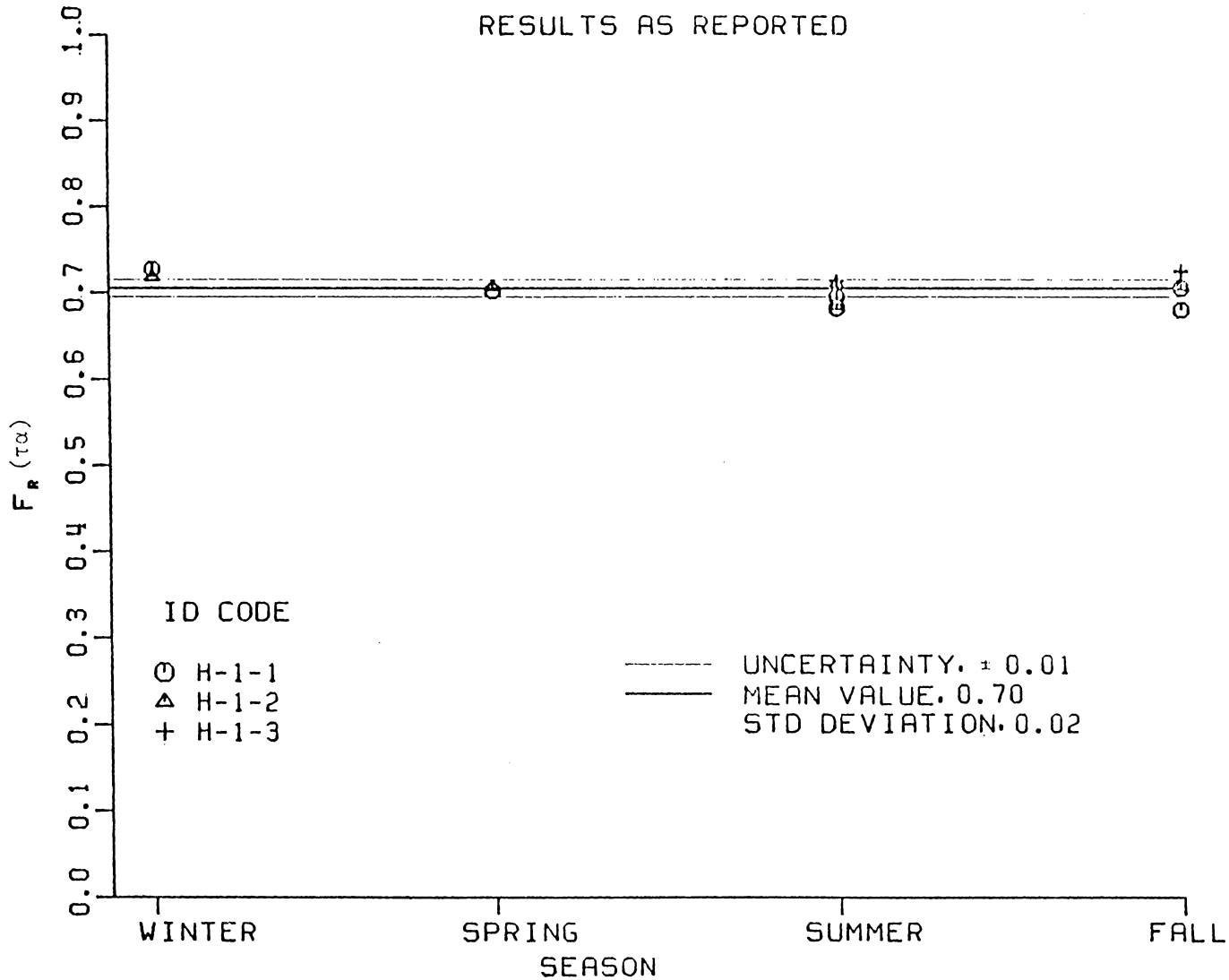

Figure C-9 $F_r(\tau\alpha)$ versus Season - Collector H, Test Site 1

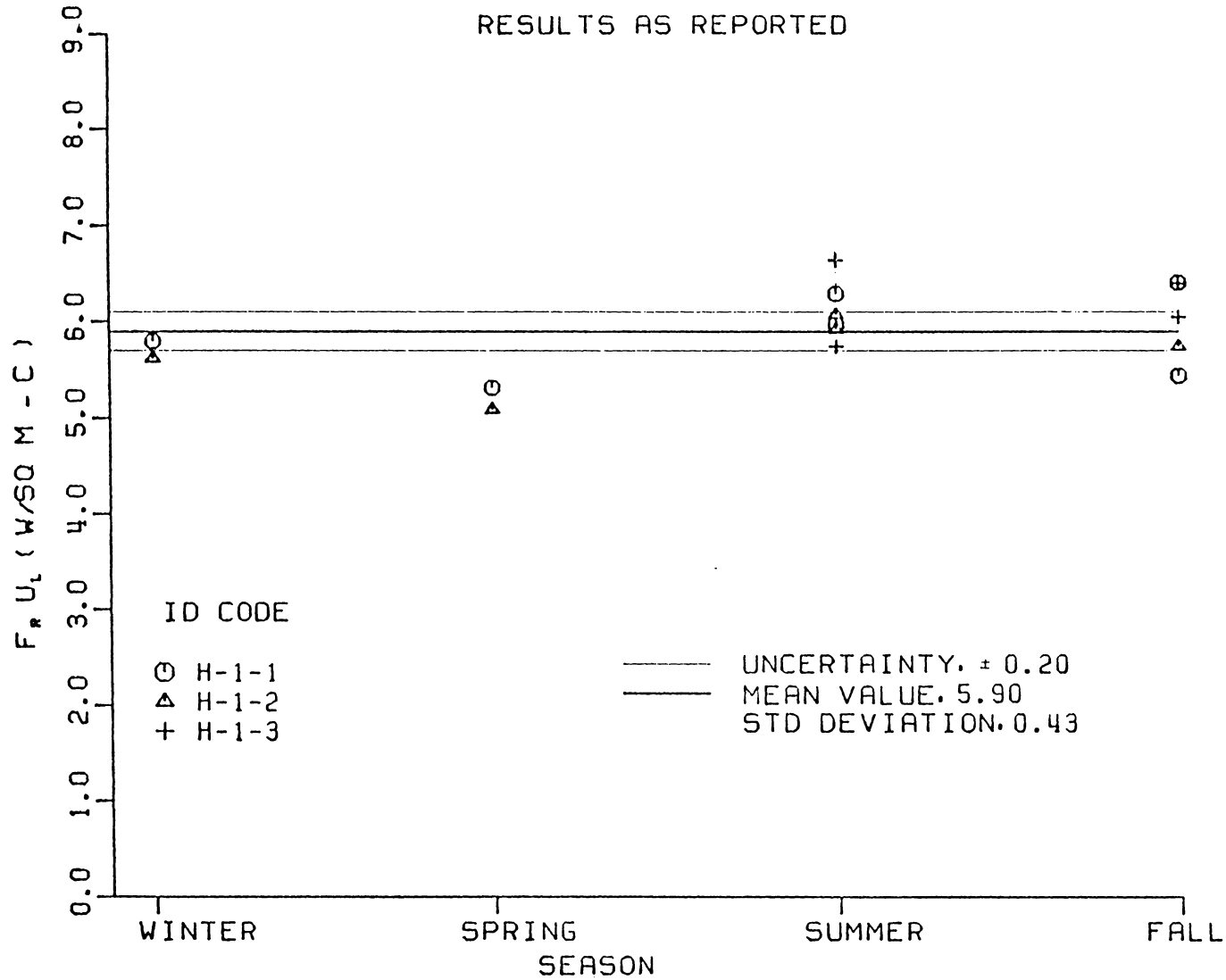

Figure C-10 $F_r U_L$ versus Season - Collector H, Test Site 1

The vita has been removed from the scanned document

ANALYSIS OF FLAT PLATE SOLAR COLLECTOR DURABILITY TEST DATA

by

Donald Sean Culkin

(ABSTRACT)

The National Bureau of Standards conducted outdoor durability tests on eight different types of commercially available flat plate solar collectors. The test results for five types of collectors are analyzed. The purpose of the test program was to investigate the feasibility of determining the durability of materials by measuring collector thermal efficiency at specified intervals. The important material properties include the solar absorptance and long wave emittance of the absorber surface, solar and long wave transmittance of the cover material and the thermal conductivity of the insulation.

Tests were conducted by three independent testing laboratories located in Phoenix, Arizona, Cape Canaveral, Florida, and Palo Alto, California. The test sites were chosen to investigate the effects of the various environmental conditions found in the United States on collector degradation. Three test series were considered to study the effect of various operating conditions on collector degradation.

The collectors were exposed to the environment for up to 240 days. The thermal performance test results did not reveal significant degradation in the performance parameters, $F_r(\tau\alpha)$ and F_rU_L, of the collectors

considered. Any degradation that may have occurred was overshadowed by experimental uncertainty.

The test results did not depend on test series, geographic location or season of the year. Referring the test results to a common set of weather conditions did not reduce the scatter in the results.